UNIVERZITA KARLOVA

Přírodovědecká fakulta

Katedra biochemie

Studijní program: Biochemie

Studijní obor: Biochemie

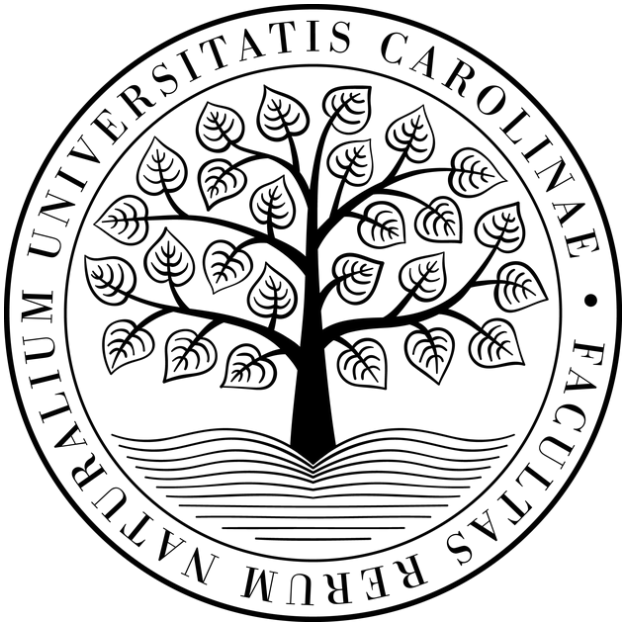

Bc. Dominik Hirko

Vakuolární aspartátová proteasa kvasinky *Candida albicans*

Vacuolar aspartic protease of *Candida albicans*

DIPLOMOVÁ PRÁCE

Školitel: Doc. RNDr. Olga Heidingsfeld, CSc.

Praha 2024

I affirm this thesis was elaborated independently under the supervision of Doc. RNDr. Olga Heidingsfeld, CSc., that all sources used were cited properly and that any part of the thesis has not been submitted for obtaining another degree.

(Prohlašuji, že jsem závěrečnou práci zpracoval samostatně a že jsem uvedl všechny použité informační zdroje a literaturu. Tato práce ani její podstatná část nebyla předložena k získání jiného nebo stejného akademického titulu.

May 17, 2024, Prague ……..

Acknowledgements

I am deeply indebted to my supervisor, Doc. RNDr. Olga Heidingsfeld, CSc., for her unwavering support and encouragement throughout my Masters. Her expertise and insightful feedback were invaluable, and her friendship made this experience truly enjoyable. I will always be grateful for the lessons learned and the opportunities she provided. I also wish to thank my lab mates – Richard, Mikuláš, Teri, Eliška, Veronika, and Zdenka – for their camaraderie and for creating a supportive atmosphere in the lab.

Tiež chcem poďakovať svojím rodičom za podporu a umožnenie ísť si za svojím cieľom. Ľúbim Vás.

Abstract

Aspartic proteases (APs) are crucial for diverse cellular processes. This thesis delves into the complexities of protein expression and characterization of vacuolar aspartic endoprotease Apr1p from *Candida albicans*, comparing it to its *Saccharomyces cerevisiae* ortholog, Pep4p.

Recombinant expression of Apr1p in *Escherichia coli* yielded the inactive proenzyme, proApr1p. Extensive refolding efforts failed to produce mature, active Apr1p, suggesting a reliance on intricate cellular machinery or specific post-translational modifications for activation. Attempts to leverage vacuolar enzymes or cell lysates for proApr1p activation were unsuccessful, potentially due to the fragility of isolated vacuoles and the complex mixture of enzymes in cell lysates.

Positive results emerged when Apr1p was expressed in *S. cerevisiae*, where fractionated cell lysates exhibited specific proteolytic activity at acidic pH after inhibiting serine and metalloproteases proteases. The eukaryotic system can probably produce active Apr1p. However, after preliminary small-scale experiments, upscaling of Apr1p expression in *S. cerevisiae* will be necessary in order to obtain sufficient amount of protein for further characterization.

A reciprocal gene swap experiment, exchanging *PEP4* in *S. cerevisiae* with *APR1* and vice versa, revealed surprisingly similar growth patterns and stress tolerance between swapped and wild-type strains. This suggests potential functional complementation between these orthologs under our chosen laboratory conditions. However, differences in nitrogen source utilization emerged, hinting at potential subtle distinctions in metabolic regulation.

Overall, this thesis contributes to our understanding of Apr1p protease expression, maturation, and function. It emphasizes the challenges in replicating complex biological processes *in vitro* and highlights the importance of exploring alternative protease activation and purification strategies. Additionally, the gene swap experiment underscores the potential for subtle functional divergence between orthologous proteases, warranting further investigation into their specific roles in cellular physiology and adaptation.

Keywords: *Candida albicans*, *Saccharomyces cerevisiae*, vacuole, peptidase, protease

Abstrakt

Aspartátové proteázy (AP) mají zásadní význam pro různé buněčné procesy. Tato diplomová práce se zabývá problematikou exprese a charakterizace vakuolární aspartátové endoproteasy Apr1p z *Candida albicans* a srovnává ji s jejím orthologem Pep4p ze *Saccharomyces cerevisiae*.

Rekombinantní exprese Apr1p v *Escherichia coli* poskytla neaktivní proenzym, proApr1p. Rozsáhlé snahy o aktivaci nevedly k maturaci Apr1p, což naznačuje závislost aktivace na posttranslačních modifikacích, jako je glykosylace a specifické interakce s jinými proteázami podobně jako u Pep4p. Pokusy o využití vakuolárních enzymů nebo buněčných lyzátů k aktivaci proApr1p byly také neúspěšné, což může být způsobeno křehkostí izolovaných vakuol a komplexní směsí enzymů v buněčných lyzátech ztěžjucií analýzu aktivace. Tyto problémy podtrhují složitou povahu aktivace proteas kdy ani různe *in vitro* techniky nedokážou simulovat *in vivo* aktivaci proteas.

Slibné výsledky se však objevily u heterologní exprese proApr1p v *Saccharomyces cerevisiae*, kde frakcionovaný buněčný lyzát vykazovaly specifickou proteolytickou aktivitu při kyselém pH po inhibici jiných proteáz. To by mohlo naznačovat, že Apr1p může být produkován v aktivní formě v rámci eukaryotického systému, nicméně je třeba dále zkoumat jeho purifikaci.

Experiment s reciproční výměnou genů, při kterém byl gen *PEP4* v *S. cerevisiae* nahrazen genem *APR1* a naopak, odhalil překvapivě podobné růstové vzorce a toleranci vůči stresu mezi vyměněnými a divokými kmeny. To naznačuje možnou funkční komplementaci mezi těmito orthology, přinejmenším za námi zvolených laboratorních podmínek. Objevily se však rozdíly ve využití zdrojů dusíku, což naznačuje možné jemné rozdíly v regulaci metabolismu.

Celkově tato práce přispívá k našemu poznání exprese, aktivaci a funkce aspartátových proteáz. Zdůrazňuje problémy při replikaci složitých biologických procesů *in vitro* a zdůrazňuje význam zkoumání alternativních strategií aktivace a purifikace proteinů. Experiment s výměnou genů navíc podtrhuje možnost malých funkčních rozdílů mezi orthologickými proteázami, což je důvodem pro další zkoumání jejich specifických rolí v buněčné fyziologii a adaptaci.

Klíčová slova: *Candida albicans*, *Saccharomyces cerevisiae*, vakuola, peptidasa, proteasa

Table of Contents

List of abbreviations

AA	Amino acid
AIDS	Acquired Immune Deficiency Syndrome
ALS	Agglutinin-like sequence
AP	Aspartic protease
APR1	Vacuolar aspartic protease (*C. albicans*)
CA	*Candida albicans*
CPS	carboxypeptidase S
CYP	carboxypeptidase Y
CYP450	Cytochrome P450
ECE1	Extent of Cell elongation (Candidialysin)
ER	Endoplasmic reticulum
ERG11	Lanosterol 14-alpha-demethylase
FTR1	High-affinity iron permease
GA	Golgi apparatus
GPI	Glycosylphosphatidylinositol
GTT	Germ-tube test
HIV	Human immunodeficiency virus
IA3	Protease A inhibitor 3
ICU	Intensive care unit
IDP	Intrinsically disordered protein
MALDI-TOF	Matrix-assisted laser desorption/ionization-Time of flight
MLEE	Multi-locus enzyme electrophoresis
MS	Mass spectrometry
NAS	Non-*albicans* species
NCBI	National Center for Biotechnology Information
NTS	N-terminal sequence
PAPs	pepsin-like aspartic proteases
PCR	Polymerase chain reaction
PEP4	Protease A/Vacuolar aspartic protease (*S. cerevisiae*)
PFGE	Pulse-field gel electrophoresis
PolyPi	Polyphosphate
PRA1	pH-regulated antigen 1
RC	Reaction centre
ROS	Reactive oxygen species
SAP	Secreted aspartic protease
SC	*Saccharomyces cerevisiae*
UPC	Ubiquitin proteasome complex
VTC	Vacuolar transport chaperone
WHO	World Health Organisation
WT	Wild type

1. Introduction

1.1.Fungal taxonomy and taxonomy of genus *Candida*

Due to wide variation of fungal species their taxonomy proves to be particularly difficult to make sense of. Some use phenotype-based identification, however its practice tends to be laborious and not applicable in fungi that are nonculturable. With the rise of MALDI-TOF spectrometry, profile identification based on biomarkers, like metabolites and proteins comes as a massive aid, yet once again has similar drawbacks with unculturable fungi. These two examples, among many others, prove that fungal taxonomy is a dynamic field with many obstacles however to simplify it, most species can be divided into three groups – yeasts, moulds, and mushrooms. Scientists presume that there is over 1 million species of unrecognized fungi in existence, where only about 30,000 have been identified.[1]

According to National Center for Biotechnology Information (NCBI) genus *Candida* is classified as following:[2]

Domain:	*Eukaryota*
Kingdom:	*Fungi*
Phylum:	*Ascomycota*
Class:	*Saccharomycetes*
Order:	*Saccharomycetales*
Family:	*Debaryomycetaceae*
Genus:	*Candida*

1.2.Characteristics of the genus *Candida*

The genus *Candida* encompasses a diverse array of over 200 microorganisms that have a large number of uses. Examples include the use of *C. utilis* in biotechnology and pharmaceuticals to obtain β-glucans, through food industry like *C. krusei* and their use in cocoa fermentation to commensally found species like *C. albicans* and *C. parapsilosis.*[3–5]

Genus *Candida* has gained its name from the pale-white colony morphology, (*candidus* meaning white) due to lack of carotenoid dye production. Under physiological conditions unicellular yeasts *Candida* reproduce asexually by budding and form oval or elliptical cells with a size range of 1-8 × 1-6 μm. Their primary aerobic metabolism produces low-to-no levels of alcohol, under ideal environmental conditions of 25 to 30°C (with exceptions) and pH range of 4-6. This genus is also characterized by inability to utilize nitrite as its nitrogen

source (except *C. utilis*), with preference for ammonium cation as a preferred nitrogen source.[3,6]

1.2.1. Characteristics and morphology of *Candida albicans*

Candida albicans is a diploid opportunistic fungal pathogen capable of undergoing polymorphic changes, each conferring different advantages to its adaptation and pathogenesis. It is an early post-partum colonizer, and inhabits the skin, gastrointestinal tract, and reproductive organs. Although commonly considered a human commensal, immunocompromised individual are under the risk of developing fungal infections – candidiasis. These infections range from common benign infections of the skin and mucosal membranes, however, in certain instances, they can progress to systemic infections with high mortality rates.[7] *C. albicans* under physiological conditions exhibits itself as an oval cell, which under stress or in host invasion, can form pseudohyphae to true hyphae (*Figure 1*). This switching implies the ability to remodel its cell wall depending on the host's niche. The main covalent components of the cell wall (*Figure 2*) are β-glucan and chitin. β-glucan is a glucose polymer that when linked through β-1,3 glycosidic bond, creates the primary cell wall structure. To this, β-1,6-glucan, and chitin are bound using their reducing ends. In addition, the N-acetyl group moiety of chitin can form a large amount of antiparallel hydrogen bonds, leading to high cell wall insolubility.[8] The very outer layer consists mainly of polysaccharides and glycoprotein, which play a role in cell wall remodelling and host-cell recognition.[9]

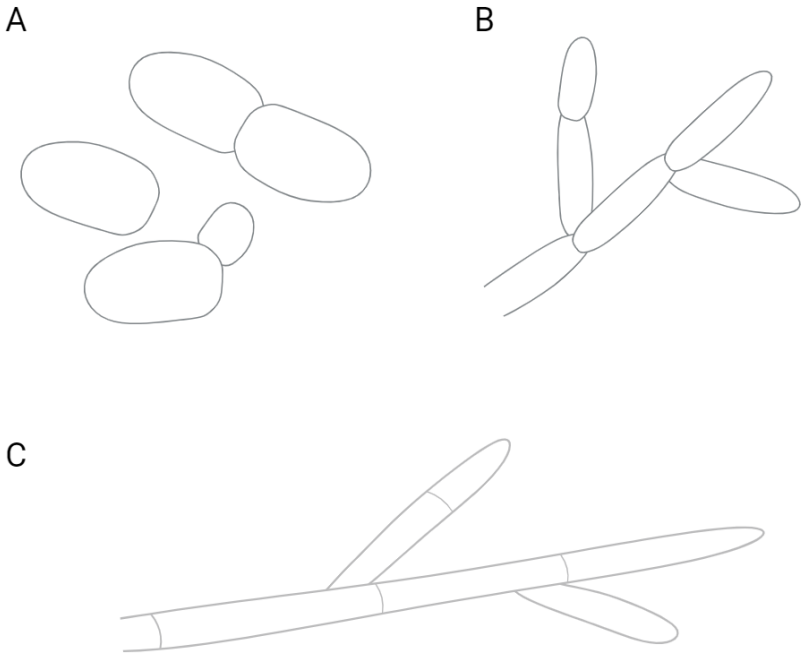

Figure 1: C. albicans is a polymorphic yeast, which means that it can take one of these morphologies - blastospores or oval yeast cells (A), pseudohyphae (B) or true hyphae (C).

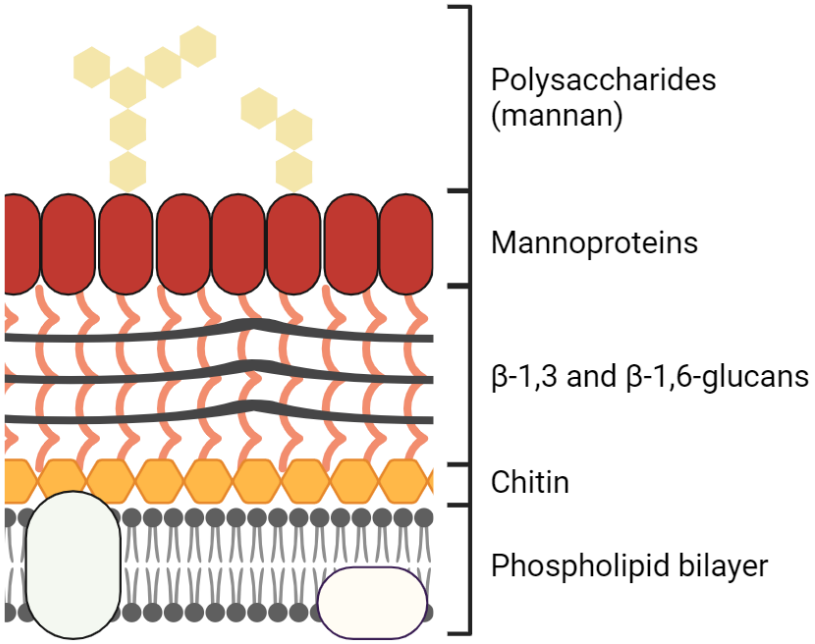

Figure 2: Illustration of a fungal cell wall found in C. albicans.

1.3. Epidemiology, pathogenesis, and its mechanisms

Despite fungi being such a diverse group of microorganisms, only about 0.001% are considered pathogenic among the already described fungi. Systemic candidiasis accounts for up to 400,000 cases globally per year, with mortality as high as 40%. [10,11] *C. albicans,* being the most common human fungal pathogen accounts for 70% of all fungal infections globally, hence why in the late 2022, World Health Organisation (WHO) has published a report called "WHO fungal priority pathogens list to guide research, development and public health action", proposing actions and strategies for all aspects of public health officials. Half of the species mentioned in the "Critical Priority Group" belong to the genus *Candida*, as well as mentioning other *Candida* species in the categories of "lower" priority.[12] In addition, most global epidemiological studies of *Candida* infections are outdated, and the more recent ones are highly localized. This is especially important since there is an obvious trend in rising fungal resistance.[13]

In terms of epidemiology, global landscape can be divided into three trends. In North America and Europe, an increasing trend of non-*albicans* species (NAS) has been observed – in the USA, *C. albicans* accounts for less than half of all *Candida* infections, *C. glabrata* accounting for one-third of them, followed by *C. parapsilosis.* Second trend occurs in Latin America and Africa, where *C. albicans* still remains the dominant species, followed by *C. parapsilosis* and *C. tropicalis* respectively. This species distribution changes in Asia, where *C. albicans* remains dominant, but is closely followed by *C. tropicalis.*[14]

1.4.Pathogenesis, and its mechanisms

As previously mentioned, *C. albicans* belongs to the natural microbiome of humans, however this commensal relationship relies on the delicate balance of the host-pathogen interaction. *C. albicans* is capable of modulating the gut microbiome through the inhibition of other species of microorganism, as well as stimulating the production of immunoglobulins which are linked to candidemia protection.[15] *C. albicans* is a pathobiont, which means that it is a symbiont of natural human microbiome but has the potential for pathogenesis. This equilibrium of interactions can be disrupted by disbalance in the microbiome, by antibiotics, immunosuppression (post-transplantation immunosuppressants) or disease-related immunosuppression (e.g. AIDS). Other risk factor includes catheters, surgery, and others.[16]

1.4.1. Morphological switching

A prominent virulence factor is the ability of *C. albicans* to undergo morphological switching between (yeast-like) oval cells, deemed avirulent, and filamentous hyphal form, considered virulent, capable of penetrating the protective mucosal membranes. These forms are dependent on environmental stimuli by the host like nutrient acquisition, quorum sensing and the overall host's niche. What is also important to note is that not all virulent strains of the genus *Candida* rely on this mechanism. Species like *C. auris* and *C. glabrata* do not undergo filamentation, but are still successful in pathogenesis, suggesting that phenotypic switching is may not a key prerequisite for virulence and each species has developed their own virulence strategy. Experiments had also shown that engineered hyper-filamenting strains showed reduced virulence in *in vivo* experiments, suggesting the importance of switching itself more, rather than the final form.[17] The dependence of *C. albicans* on the host's niche is also highlighted by studies where organs specific infections show different filamentation profiles.[18]

1.4.2. Adhesion and cell invasion

C. albicans showcases its well-developed machinery to adhere through to both biotic (e.g. skin) and abiotic surfaces (e.g. central venous catheter). During pathogenesis, adhered yeast cell, can triggers phenotypic switching and precedes to host penetration facilitated by adhesins and invasins, of the agglutinin-like sequence (ALS) and hyphal wall protein families. This can lead to two modes of membrane invasion, one in which proteins like Als3 induce endocytosis by biding to proteins like cadherin (or epidermal growth factor receptor 2) to protrude into the cell, or secondly by the act of active cell penetration using the hyphal tip and the secretion of extracellular hydrolases.[19,20]

1.4.3. Secreted hydrolases

When further penetrating the host, yeast cells use three groups of enzymes – proteases, phospholipases, and lipases. All these enzymes primarily work towards two aims – further host invasion and nutrient assimilation. *C. albicans* uses 10 secreted aspartic proteases (SAP) – Sap1-8 are secreted extracellularly, and Sap9-10 are membrane-anchored GPI proteins. The discussion on whether SAPs are key to virulence varies. Some studies suggest that they might not be essential, however most of them are actively expressed, implying role in nutrient acquisition, immunity evasion, tissue damage during infections.[21,22] The role of phospholipase is quite straightforward as it aids in host membrane disruption.[23] The role of lipases is still not fully understood but, lipases can manipulate hosts immune response and aid in pathogen's virulence.[24]

1.4.4. Candidialysin

Candidialysin is a hyphae-associated cytotoxic peptide encoded by the gene *ECE1*. This peptide has two amyloidogenic regions and can effectively lead to lysis of membranes, or form holes in them, functioning as a cytolytic agent. It is also effective in triggering of immune response, linked to Type 17 immunity (associated with IL-17), leading to amplified inflammation and further tissue damage.

1.4.5. Nutrients and adaptation

It is known that the most preferred carbon source for *C. albicans* is glucose, however under physiological condition and the natural environment its presence is sparse and in low concentrations, where the yeast cell competes in glucose sequestration with the host. Under such conditions cells shift their metabolism to utilization of alternative sources such as N-acetylglucosamine, lactate and amino acids (AA), which proves to be especially useful in conditions like those present within phagosome. What is also interesting is how presence of different carbon sources results in certain advantages – lactate increases osmotic resistance, N-acetylglucosamine promotes resistance to caspofungin and oxidative stress, while presence of all three different carbon sources heightens resistance to fluconazole.[25]

In cases of micronutrients like zinc or iron, *C. albicans* uses specific binding proteins. In case of zinc – Pra1p (pH-regulated antigen 1) is produced and serves as a "zincophore", competing with the host. It also blocks the C3 complement, granting yeast another option of immunity evasion.[26] Zinc limitation results in hyper-adherent cells (Goliath cells).[27] In case of iron, *C. albicans* promotes its iron uptake through overexpression of the *FTR1* gene encoding

permease with high affinity for iron, capable of sequestering iron from ferritin and transferrin complexes.

Due to high pH variation within the host, *C. albicans* must be able to adapt. To do so cell wall remodelling is employed , where under low pH more chitin is used in the cell wall.[28] However more important is the ability of *C. albicans* to manipulate its amino acid metabolism and generate ammonia, to neutralize the acidic pH of phagosome as well as autoinducing hyphal growth.[29] In addition to ammonia production, *C. albicans* is also capable of producing superoxide dismutases (SOD), leading to reactive oxygen species (ROS) neutralization.

1.4.6. Biofilms

The formation of biofilms provides various advantages in comparison to their planktonic counterparts. Biofilms comprises a community of organisms of one or more kind, where they irreversibly attach to a biotic or abiotic surface and form a polysaccharide matrix within which they reside. These communities show slower growth rates, but better resistance to outer negative stimuli, like heightened resistance to antimicrobial agents. In the USA about 80% of candidiasis are associated with biofilm formation. This process begins with a non-specific adherence of blastospores, upon which proliferation of filamentous cells can take place on. This can lead to maturation of a biofilm and a subsequent dispersal/dissemination of planktonic cells, potentially leading to further spread of pathogens. Biofilms offer a structure that is less susceptible to antifungal's permeation, based on the complex architecture of the biofilm. In terms of immunomodulation, *C. albicans* is capable of disguising and protect itself by presenting polysaccharides absent in the cell wall, therefore avoiding the recognition by immune cells like neutrophils. immune response.[30,31]

1.5. Candidiasis

Overall, every microorganism has the potential for pathogenesis, in the case of the genus *Candida* some are considered pathobionts – symbiotic microorganisms with potential for pathogenesis. In order for fungi to become a successful pathogen they must abide by four main principles – they must be able to grow at or above 37°C, they must be able to utilize nutrient sources found within the host, they must be able to evade the host's immune system and be able to colonize tissue associated with location of pathogensis.[32] Candidiasis can present itself from benign localized infections of mucous membranes to highly delocalized systemic infections, with high mortality rates. Groups that are at the highest risk of these

infections involve mostly immunosuppressed individuals, like those with HIV/AIDS, undergoing chemotherapy or postoperative patients. Around 1.8 million people die of candidiasis annually, with 80% of those being nosocomially transmitted.[33] This emergence of candidiasis has also been highlighted during COVID-19, where prolonged stays at the intensive care unit (ICU) have led to increase in incidence.[33]

1.5.1. Diagnostics

Since clinical treatment of candidiasis can highly depend on the species, due factors like variance in antifungal agent susceptibility and potential for resistance, it is necessary to correctly assess which species the patient is dealing with. Most recent diagnostics review divides such practices into few different groups. Following table summarizes just a few of them.[34]

Table 1: Examples of commonly used practices in diagnostics. Provides a summary of some of the methods used to differentiate between Candida spp. as well as more universally applicable methods to identify other pathogens from clinical samples.

Methodology group	Name	Short summary
Microbiological and clinical tests	Germ-tube test (GTT)	Phenotypic method, in which identification is done based on the ability to form hyphae and accurately differentiate between *C. albicans* and *C. dubliniensis* from other *Candida* spp.
	API *Candida* system	This rapid identification system uses differences in fungal enzyme apparatus based on carbohydrate metabolism.
	CHROMagar technique	Chromogenic media-based commercial systems, again uses differences in metabolism, causing a colony colour change.
Serological methods	Uses reagents to identify β-glucan, can be also used to track the status of antifungal treatment.	
Molecular methods	Multi-locus enzyme electrophoresis (MLEE)	Non-DNA based, uses the cross-special protein polymorphism and their different electrophoretic migration. Can be also used to identify novel strains.
	Pulsed-field gel electrophoresis (PFGE)	DNA based technique uses digested DNA to identify pathogens by “fingerprinting”. Can be also used to track plasmid transfer in bacteria.
	PCR	Exact DNA-based methods, uses species specific primers to identify pathogens.
Modern methods	MALDI-TOF MS	Uses “protein fingerprints” of the organism.

1.5.2. Antifungal agents or antimycotics

Antimycotics are a group of agents used in treatment of various fungal infections including those caused by *Cryptococcus, Candida, Aspergillus,* and other human fungal pathogens as well as agriculturally used agents, that help alleviate large crop losses. In fact, fungi are responsible for the destruction of over one third of crops annualy.[32] It is important to note that to this day we possess a limited arsenal of antimycotics which combined with unfavourable climate of the pharma industry (rising costs, less drugs being approved each year) and rising fungal resistance, can have detrimental effects globally. Main antimycotics that are currently used can be divided into four groups based on their mechanism – polyenes, flucytosine, azoles and echinocandins.

1.5.2.1. Polyenes

Polyenes were the very first broad-spectrum fungicidal agent of the macrolide group, approved for human use, specifically Amphotericin B. They are a class obtained from *Streptomyces* bacteria and bind to ergosterol, (similar to mammalian cholesterol) but in fungi. This interaction with ergosterol leads to the weakening of the fungal cell membrane by creating pore-like structures, resulting in leaking of ions out of the cell, leading to its death. Mayor drawback of this group is their nephrotoxicity, putting other antimycotics to the front. Examples include amphotericin B, nystatin or candicidin.[32]

1.5.2.2. Flucytosine

Flucytosine is a pyrimidine derivative and a prodrug, first proposed as an anti-tumour agent in the 1957. It inhibits the synthesis of nucleic acids by incorporating itself into the RNA as a metabolized 5-fluorouracil. The major drawback of flucytosine is the easily acquired resistance to it but is still often used with other antimycotics (e.g. amphotericin B). Nowadays it is most prominently used to treat cryptococcal meningitis.[32]

1.5.2.3. Azoles

Azoles offer the riches group of fungistatic agents, that is further subdivided into three groups based on the heterocycle utilized in its mechanism. This antifungal acts on the biosynthetic pathway of ergosterol synthesis, by inhibiting 14-α-demethylase (*ERG11*), enzyme of the CYP450 group. This results in the accumulation of byproducts within the membrane and lack of ergosterol leading to the loss of the membrane integrity. To this day azoles, primarily fluconazole, are the most commonly used group of antimycotics. However, this (over)use has

allowed the development of resistance mechanisms. Examples include fluconazole, voriconazole, ketoconazole, … [32]

1.5.2.4. Echinocandins

Echinocandins are one of the more recent additions to the antifungal arsenal and slightly resemble penicillin antibiotics based on the ability to inhibit the enzyme 1,3-β-glucan synthase. This group presents low toxicity profile, due to lack of cell wall in mammalian cells. Resistance to them is limited but has been observed. Examples include micafungin and anidulafungin.[32]

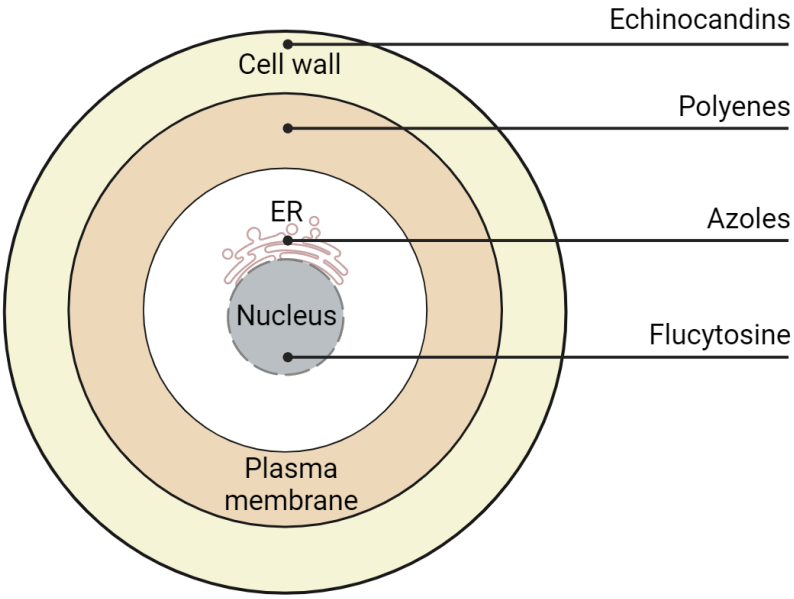

Figure 3: Diagram of a yeast cell showing the target organelles of the selected antifungal agents.

1.6. Selected non-*albicans Candida* species (NAS)

1.6.1. Candida glabrata

Candida glabrata, or formerly known as *Torulopsis glabrata,* is an emerging fungal pathogen phylogenetically more related to *S. cerevisiae* than *C. albicans.* It is a commensal yeast found in a healthy microbiome, as well as the environment. This yeast primarily targets adults in nosocomial infections. *C. glabrata* is haploid yeast that reproduces asexually and does not undergo phenotypic switching. *C. glabrata* closely follows the clinical incidence right after *C. albicans,* however this factor highly depends on the geographical area. *C. glabrata*-related infections are a development of last decades with the rise in the number of immunocompromised patients. *C. glabrata* has a more sophisticated to immunity modulation

since its infections are associated with low cytokine levels and limited tissue damage. *C. glabrata* also has high mortality rates of 40-60%, due to commonly acquired resistance to azoles.[35,36]

1.6.2. *Candida parapsilosis*

C. parapsilosis is also a commensal member of the human microbiome, generally colonizing the skin. Besides immunosuppressed individuals, *C. parapsilosis* also targets low-weight neonates (in contrast to *C. glabrata*) and liquid tumour patients. It is also able to colonize abiotic surfaces, through horizontal transmission and cause nosocomial infections at ICU. Especially dangerous is the capacity to form hydrophobic biofilms on central venous catheters and other implanted devices. Although the mortality rates of *C. parapsilosis* are considerably low, isolates with heightened resistance to echinocandins and azoles have been isolated.[37,38]

1.6.3. *Meyerozyma guilliermondii*

Formerly known as *Candida guilliermondii* is a recently emerging haploid opportunistic pathogen with alarming rise in incidence in China, strongly associated with preterm infants. However, on the global scale, its incidence is on the tail of *Candida* genus. Rise of this pathogen has also been observed in Japan. In addition, the most distressing is the higher innate resistance to antimycotics. Interestingly, *C. guilliermondii* has lower levels of extracellular β-glucans leading to a lower cytokine stimulating effect. What is also important to note in the case of *M. guillemondii,* the literature available is very limited.[39–41]

1.6.4. *Candida auris*

Candida auris presents a fairly new member of the *Candida* species, first report being in 2009. This species has spread to more than 40 countries and has high mortality rates of 30-60%. This haploid yeast possesses high resistance to most antimycotics, can thrive in temperatures above 37°C and resist high osmotic stress. Under physiological conditions, *C. auris* does not rely on phenotypic switching, but under stress can form hyphae. This among many other factors put *C. auris* to the forefront of highly potent fungal pathogens.[42]

1.7. Fungal vacuole

Many scientists tend to compare vacuoles to lysosome, due to their role in cellular degradation, but its other roles are commonly downplayed. Fungal vacuole acts as a hub facilitating cellular trafficking, homeostasis, storage of ions as well as playing crucial roles in virulence and cell death. Mutant strains associated with hampered vacuoles formation have shown that, the formation of at least one vacuole is crucial to cell viability and a prerequisite

for cellular division. Vacuole is a very dynamic organelle, and its composition, volume and other components vary in time. Cells during exponential phase form a cluster of multiple smaller vacuoles, which then enlarge during mid-exponential phase leading to further fusion to one during stationary phase.[43] The morphology of the fungal vacuole is also dependent on the osmotic condition, where high osmolarity leads to vacuole fragmentation, however under hypotonic condition cell contains one large vacuole occupying majority of the cytoplasm.[44] Other interesting point, that arose from deletion mutant studies, is that the size of vacuoles is linked to cell cycle regulation through cell size – larger cells that possess multiple small vacuoles might exhibit behaviours similar to those of smaller cells. The vacuole of oval yeast cell occupies on average 23% of the total cell volume but can increases to 39% [45]

In budding yeast, the vacuole is passed down by budding, where the mother vacuole fragments first, and smaller fragments of the vacuole are then transported to the daughter cell. This budding and transport is facilitated by cytoskeletal proteins myosin and actin. Additional smaller vacuoles are then transported into the daughter cells and fuse together, forming one large vacuole which then expands.[46]

It is well known that lysosome and vacuoles have the lowest pH of organelles. In yeast varying from 6.5 and lower, depending on the environmental conditions. In order to maintain this low pH, organisms use a set of well conserved proton pumps V-ATPases, or the vacuolar H^+-ATPases (related to mitochondrial ATPases). This pump uses the hydrolysis of ATP to pump protons against their gradient into the vacuolar lumen.[44]

Key regulation pathway of vacuolar acidification in yeast is maintained by the assembly of two subunits – membrane and peripheral (V_1 and V_0). This rapid disassembly proceeds in a continuous matter, rather than all-to-none transformation. However, the regulation of this process is still not fully understood.[44]

1.7.1. Roles of vacuole

1.7.1.1.Storage

The wide variety of conditions yeasts can be found in, is closely connected to possession of a vacuole as a storage organelle – the primary elements being amino acids, metal ions and polyphosphate.

In terms of AA, the fungal vacuole comprises mainly of basic and neutral AA and very little acidic ones. In this process the influx and efflux vacuoles use a set of importers and exporters, usually with AA specificity, coupled with proton antiport.[44] Fungal vacuole also has multiple systems for arginine (nitrogen richest AA) sequestration, like arginine-histidine exchange system, suggesting vacuole's importance in nitrogen metabolism. Acidic AA are almost exclusively found within cytosol, implying dedicated system for basic AA internalization.[47] The retention of basic AA is also attributed to the presence of polyphosphate, which might form complexes and prevent their "leaking", making vacuolar membrane virtually impermeable to cations.

Polyphosphate in yeast cells is maintained by a group *VTC* genes (vacuolar transporter chaperone) which play a role in its accumulation. As previously highlighted, polyPi does not only function as a counterion for basic AA and metal ions stored in the vacuole, it also serves as more manageable storage of biogenic phosphate and a cellular buffer.[48]

Calcium cations are actively transported to the vacuole by proton antiporter (Vcx1p) and P-type ATPase (Pmc1p). Antiporter has low affinity but high capacity for calcium cation and is upregulated under stress conditions. On the other hand, the efflux of calcium cation is facilitated by transient receptor potential channel (Yvc1p), in response to hyperosmotic shock, this finding comes from a study of *S. cerevisiae*, but a similar orthologue is present in *C. albicans*.[49] In case of zinc, an important enzyme cofactor, yeast vacuole utilizes a system of importer and exporters (Zrc1p, Zrt3p). Interestingly during excess of zinc, vacuole can internalize large amounts of zinc and sustain reproduction during zinc deprivation.[50] More complex is metabolism of iron, which in itself can cause oxidative stress to the cell, due to its redox activity. This leads to vacuolar internalization using a Ccc1p transporter, where its overexpression increases the luminal concentration of iron.[51]

Subunit deletion of the V-ATPase also leads to impairment in the activity of vacuolar transporters, which in turn disrupts the polyphosphate homeostasis. This network of vacuolar ions, in high concentrations, offers a buffering system, where the pH of the fungal vacuole is highly dependent on the environment, suggesting tight regulation. In contrast to mammalian lysosomes, where the pH remains more constant.[44]

1.7.1.2.Protein degradation

Vacuole and its machinery of proteases is also involved in the maintenance of cellular proteostasis together with ubiquitin proteasome complex (UPC). Vacuolar degradation, also

called autophagy, uses a multitude of hydrolytic enzymes. In *S. cerevisiae* this proteolytic landscape involves proteinase A (Pep4p), carboxypeptidase Y (CPY), proteinase B (Prb1p), carboxypeptidase S (CPS). These proteins are usually synthesized as zymogens, processed in other organelles or/and directly trafficked to the vacuole, which in some cases cause the protein activation, if pH dependent. Deletion studies of Pep4p show, that lack of this protein leads to accumulation of unprocessed precursors (e.g. CPY).[52] Dependent on this type of degradation are also permeases of the plasma membrane (e.g. uracil permease Fur4p), which regulates the uptake of nutrients from the environment in their excess. Interestingly in this case the protein is tagged by ubiquitin.[53]

Under nutrient starvation, vacuoles stand behind the majority of cellular turnover, inducing macroautophagy, leading to degradation of both proteins and whole organelles. However, the consensus, in cases of basal and induced autophagy is that vacuoles are responsible for amino acid turnover, where disruption of this system leads to low levels of amino acids.[54]

Studies of V-ATPase deletion mutants (leading to increased luminal pH) had shown that enzymes with "pH dependent activation", have only been affected moderately. This might suggest that the activation of proteolytic enzymes is not fully dependent on the lower pH.[44]

1.7.1.3.Pathogenesis

As mentioned, vacuole also play a vital role in pathogenesis. When yeast cell is engulfed by macrophages, cells come to a state of nutrient starvation and harsh conditions, in which vacuole-stored molecules are utilized. In addition, morphological changes to vacuole must occur for phenotypic switching to take place, hence being essential in macrophage evasion.[55] This high dependence of pathogenic yeast on vacuole, creates an optimal target for antifungal agents.[56]

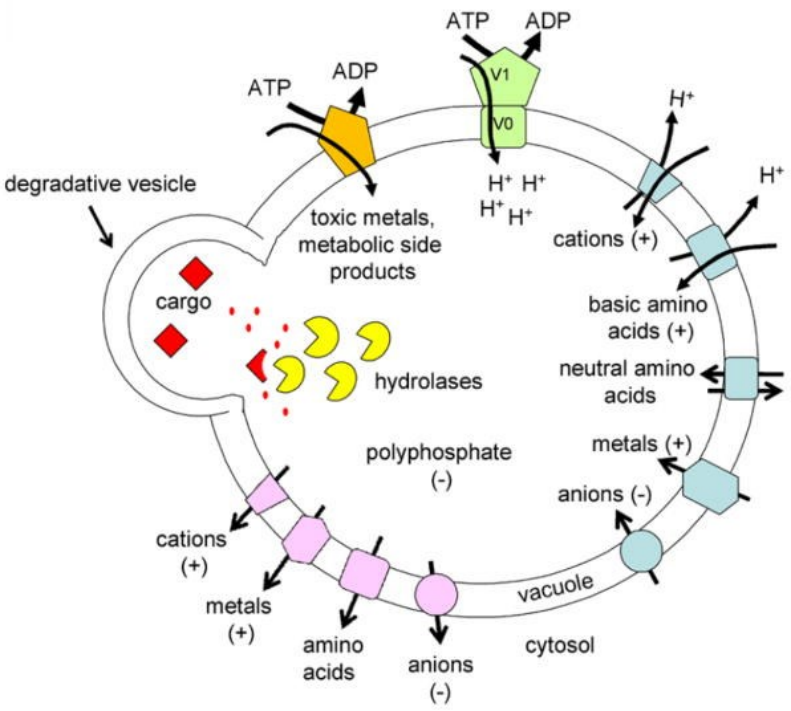

Figure 4: Diagram depicting the functions of a fungal vacuole.[44]

1.8. Aspartic proteases (APs)

Aspartic proteases are a group of ubiquitously present enzymes that use two conserved residues of the aspartic acid, used in a non-covalent acid-base mechanism hydrolysing the peptide bond. They share common characteristics of acidic pH optima and inhibition by pepstatin. They are synthesised as zymogens with an approximately 45 AA propart, which cleaving is necessary for protein maturation, commonly under low pH. The two aspartate residues are commonly labelled based on their placement as Asp32 and Asp215.

1.8.1. Catalytic mechanism of aspartic proteases

Most widely accepted mechanism of aspartic proteases is the acid base mechanism in which water molecule is activated by an aspartate residue by abstracting a proton. This then allows for a nucleophilic attack of the carbonyl carbon of the substrate bond. This action generates a tetrahedral oxyanion intermediate, stabilized by hydrogen bonding of the aspartate residue. Rearrangement of the intermediate then lead to the protonation of the substrate amide, splitting the substrate into two.[57]

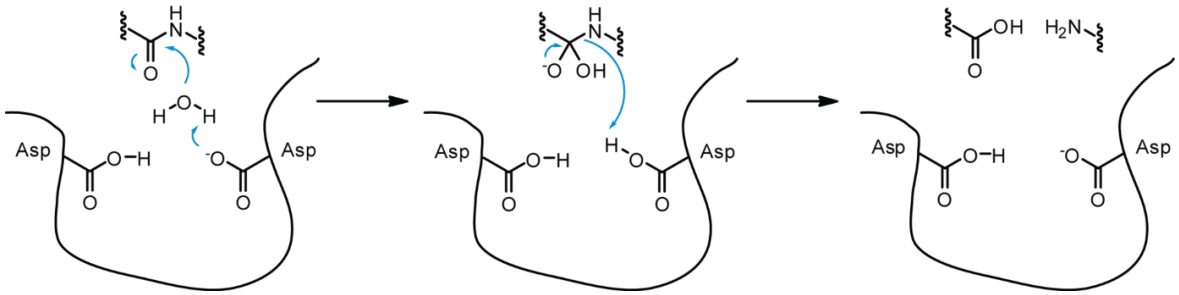

Figure 5: Mechanism of the acid base catalysis of aspartic proteases.[58]

1.8.2. Vacuolar aspartic proteases

1.8.2.1. Aspartic endoprotease Pep4p

As previously discussed, yeast cells possess a multitude of degradative enzymes capable of full amino acid turnover. Enzyme Pep4p, found in *S. cerevisiae*, encoded by the gene *PEP4* belongs to a group of pepsin-like aspartic proteases (PAPs). This means they are similar to human pepsin. Mature Pep4p protein consists of 329 AA, with two N-glycosylation.

This protease is synthesised in a form of preproPep4p, with a size of 52 kDa, containing 405 amino acids. N-terminal sequence (NTS) contains a signal peptide of 22 AA, which tags the protein for processing in the endoplasmic reticulum (ER), in which glycosylation occurs. This generates a proPep4p with molecular weight 48 kDa. Subsequently, the enzymes is translocated to Golgi apparatus (GA), where further glycosylation and processing occurs. This immature enzyme is translocated to the vacuole, where other enzymes and lower pH (e.g. proteinase B) gives rise to mature Pep4p. This mature enzyme has a molecular size of about 42 kDa.

Like most PAP, this enzyme also has autocatalytic potential, under low pH, like that found in the vacuole. The aspartate residues found in the reaction centre (RC) are under physiological conditions protonated, which sterically hinders the interaction of N-terminal peptide of the proenzyme and the RC. This interaction is vital for cleaving and enzyme maturation. Other option of enzyme maturation is through interaction with proteinase B. [59]

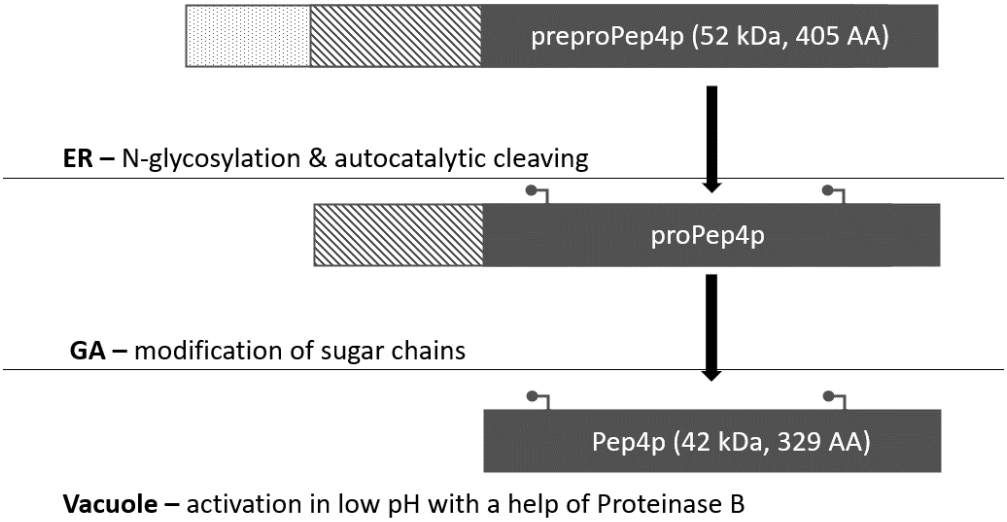

Figure 6: Activation cascade of Pep4p (S. cerevisiae)

1.8.2.1.1. Structure of Pep4p

Aspartic proteases, like cathepsin D or even pepsin, bare minimal resemblance in primary structure of Pep4p, however in terms of tertiary and quaternary structure form a bilobal protein structure resembling scissors, where each lobe possess one aspartic residue. In addition, like most aspartic proteases, Pep4p possesses a β-hairpin loop, sometimes also called "flap", that extends over the RC, possibly playing a role in the catalysis mechanism. The intramolecular structure is also maintained by 268 hydrogen bonds and two disulfide bridges.

1.8.2.1.2. Function of Pep4p

Pep4p vacuolar protease also stands at the start of an activation cascade of other vacuolar enzymes. It is responsible for processing of carboxypeptidase Y (CPY), carboxypeptidase S and Y as well as aminopeptidases I and Y. Besides the maintenance of protein turnover, under peroxide-induced apoptosis, this protein is responsible for nucleoporin degradation, suggesting its presence in the nucleus. Under acetic acid-induced apoptosis, Pep4p is responsible for the degradation of mitochondria, playing a pro-survival role.[60]

1.8.2.1.3. Intrinsic inhibitor IA3

S. cerevisiae possess and an intrinsic inhibitor of Pep4p called IA3 (cytoplasmic proteinase A inhibitor). It is an intrinsically disordered protein (IDP) of 68 AA, which upon contact with the Pep4p forms a hydrophobic α-helix, at the N terminus. This secondary structure actively

blocks the entrance of any substrate into the RC. The cleaving of this substrate is avoided by the stabilization of its conformation and the steric hindrance of aspartate residues.[61]

1.8.2.2. Aspartic endoprotease Apr1p

Although aspartic endoprotease Apr1p found in *C. albicans* carries a high percentage of amino acid identity of 65.8% with Pep4p found in *S. cerevisiae.* Very little is known about this protease. It is known that deletion mutants are still viable, but are unable of phenotypic switching under nitrogen starvation, like that found in macrophages, but not attenuated. The expression of this protein also correlates with vacuolar volume and that under nitrogen starvation Apr1p is upregulated. It is argued that due to different behaviours of orthologue deletion mutants and even WT (e.g. polymorphism), the roles of Pep4p and Apr1p might be different.[62] In addition, there has not been found an intrinsic inhibitor similar to IA3. Overall, besides its importance in the protein degradation, based on its localization and structure, other functions of Apr1p are still largely unknown.

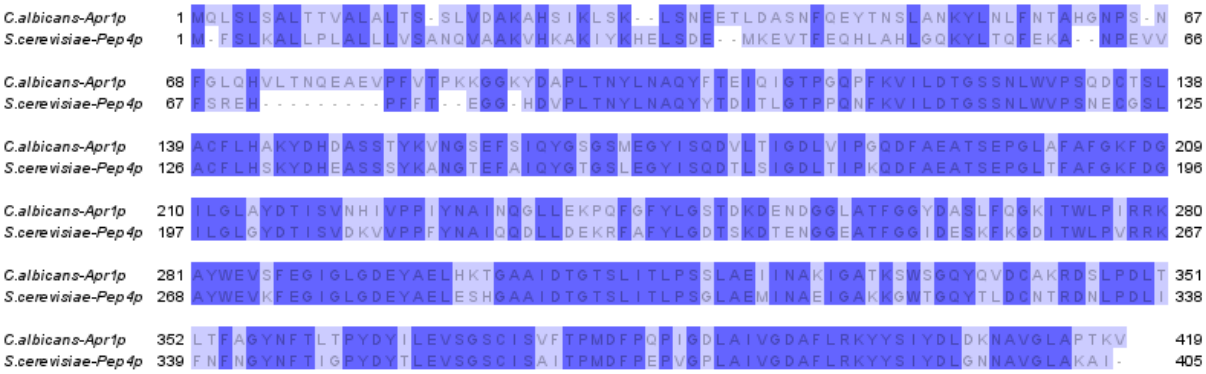

Figure 7: Amino acid sequence of Pep4p (S. cerevisiae) and Apr1p (C. albicans) using JalView.

2. Aims

This work primarily focused on:

1. Production of mature Apr1p: To develop and optimize methods for expressing and purifying active Apr1p using both prokaryotic (*E. coli*) and eukaryotic (*S. cerevisiae*) expression systems.
2. Elucidation of Apr1p's physiological role in *C. albicans*: To investigate the function of Apr1p in *C. albicans* physiology and compare/contrast its role with that of its *S. cerevisiae* orthologue, Pep4p, through phenotypic testing.

3. Material and methods

3.1.Materials and instruments

Materials

0.22 and 0.45 µm syringe filter (VWR)
1 kb DNA Ladder (NEB)
3MM blotting paper (Carl Roth)
Acetic acid (VWR)
Acrylamide (Penta)
Agar (Sigma-Aldrich)
Ammonium sulphate (VWR)
Arginine-HCl (Merck)
Brent Supplement Mix (BSM), - Ura (Formedium)
BSA (Carl Roth)
Calcium chloride (Merck)
Candida albicans (Obtained from CCM)
Citric acid (Merck)
D-(+)-Glucose anhydrous (Merck)
DEAE Sephadex A-50 (Pharmacia)
Dialysis tubing (Mw CO = 12-14 kDa) (Serva)
Dimethyl sulfoxide (Merck)
DNA Marker 155-970 (Top-Bio)
EDTA (P-LAB)
EmeraldAmp GT PCR Master Mix (TaKaRa)
Ethanol 96% p.a. (PENTA s.r.o.)
Extraction solution A (0.2M NaCl (11.6g/l); 20mM EDTA (7.4g/l); 10% SDS (100g/l) (w/w))
Extraction solution B (100 mM Tris-HCl, pH 7.5)
Falcon tubes
Ficoll 400 (Merck)
Final extraction buffer A+B (1:1)
Glass beads, acid-washed (Merck)
Glycerol (Merck)
Glycine (Merck)
Histidine (VWR)
Hydrogen peroxide (VWR)
Imidazole (Merck)
Lactic acid (P-LAB)
LB medium (Thermo-Fisher)
Leucine (VWR)
Lithium acetate (Merck)
Low fat dried milk powder
Lysine (VWR)
Lysozyme
Lyticase (Thermo-Fisher)
MES (Merck)
Methanol (VWR)

NiNTA agarose (Quiagen)
Nitrocellulose membrane (Bio-Rad)
N,N´-methylenbisakrylamid (Sigma-Aldrich)
Phenol:Chloroform:Iso-amyl alcohol (50:50:1) (VWR Chemicals, USA)
Pefabloc SC (Merck)
PEG 3350 (P-LAB)
PIPES (Merck)
Polyphosphate (Sigma-Aldrich)
Potassium chloride
PPP Master Mix (Top-Bio)
Primers (GENERI BIOTECH)
Proline (Sigma-Aldrich)
Sacharomyces cerevisiae (CCM)
Salmon sperm DNA (Thermo-Fisher)
SDS (Merck)
Sephadex G-200 (Pharmacia)
Sodium acetate (Penta)
Sodium azide (Thermo-Fisher)
Sodium chloride (PENTA)
Sorbitol (Merck)
Tris (Merck)
Triton X-100 (Merck)
Tween 20 (Merck)
Uracil (VWR)
Urea (P-LAB)
YNB medium (Thermo-Scientific)
YPD medium (Thermo-Scientific)
YPD medium (Merck)
β-Mercaptoethanol (P-LAB)

Instruments

Analytical scale	Adam®, UK
Autoclave	Panasonic, USA
Centrifuge HERMLE Z383 K	Hermle Labortechnik GmbH, Germany
Centrifuge 5424R	Eppendorf, USA
Shaking incubator ES-60	MIUlab, China
Flow box	Labox, Czechia
Magnetic stirrer	VELP Scientifica, Italy
Microplate reader Multiskan FC	Thermo-Fisher, USA
Microtubes	Eppendorf, USA
Orbital shaking incubator	Gallenkamp, UK
pH meter pHenomenal®, pH 1100L	VWR® Avantor®, USA
Vortex	IKA, Germany
UV-VIS Spectrophotometer Helios Alpha	Thermo Electron Corporation, USA
Nanodrop spectrophotometer DS-11	Denovix, USA
T100 Thermal Cycler	Bio-Rad Laboratories, USA

3.2. Protocols

3.2.1 Cultivation and preservation of yeasts

Long-term stock cultures were stored and preserved in 20 % glycerol solution in -80°C. For short-term use, YPD agar plates were used. Inoculated strain was first cultivated at 37°C overnight and then kept at 4°C. For liquid cultures, Falcon tubes with appropriate volume of YPD medium were inoculated using a wooden toothpick and cultivated in a tabletop orbital shaker at 37°C, 200 RPM for *C. albicans* and 30°C, 230 RPM for *S. cerevisiae*.

3.2.2. DNA isolation

Isolation of DNA was performed according to the protocol of Hoffman and Winston (1987). Liquid culture medium was transferred to screw cap microtubes, centrifuged (7 min, 4.500×g) and the supernatant was discarded. The pellets were resuspended in 0.6 ml of DNA extraction buffer, 0.6 ml of PCI and 0.2 g of acid washed glass beads were added. Screw cap microtubes were placed in a bead beater at the highest setting for 10 min and subsequently centrifuged (5 min, 13,000×g). Water (upper) layer was carefully transferred into second screw cap microtube and the same volume of PCI as water layer was added. Tube was inverted five times and centrifuged (5 min, 13,000×g). Water (upper) layer was transferred to a regular micro tube to which 2.5 volumes of 95% ethanol and 0.1 volumes of 3 M sodium acetate (pH 5.2) were added. Mixture was then precipitated at -20°C for at least 20 min (better overnight) and centrifuged (5 min, 13,000×g). Pellet was washed with 70% ethanol, air dried and dissolved in 50 µl of sterile water. Concentration of DNA was then measured using Denovix DS-11 spectrophotometer.

Solution A: 0.2 M NaCl, 20 mM EDTA, 10 % SDS

Solution B: 100 mM Tris-HCl (pH 7.5)

DNA extraction buffer: Solution A and Solution B mixed 1:1

3.2.3. Optical density (OD) measurement

Optical density of inoculums was measured using UV-VIS spectrometer at 600 nm. Inocula we measured in 10 mm polyethylene cuvette.

3.2.4. Growth curve

Single colony from a YPD plate was inoculated into liquid YPD medium and grown overnight (37°C, 200 RPM). Next day OD_{600} was measured and standardized to OD_{600} = 1.0

and 100 µl was added to 20 ml of YPD media. OD_{600} was measured every hour until stationary phase was achieved.

3.2.4. Competent cells

Desired *E. coli* strain was inoculated into liquid LB medium and cultivated overnight (37°C, 230 RPM). Next day, 200 ml of LB medium was inoculated and cultivated (37°C, 230 RPM) until OD_{600} = 0.3-0.5. Suspension was transferred to sterile centrifugation cuvettes, kept on ice (10 min) and centrifuged (10 min, 1500×g, 4°C). Pellet was resuspended in 5 ml of sterile FCC1 solution (competent cells solution 1). Cell suspension was left on ice (20 min) and centrifuged (10 min, 1500×g). Pellet was resuspended in 2 mi of FCC1 and left on ice (20 min). 100 µl aliquots were transferred into sterile microtubes and immediately frozen (-80°C).

FCC1 solution: 60 mM $CaCl_2$, 15 % glycerol, 10 mM PIPES (pH 7)

3.2.5. *E. coli* transformation

Cell aliquots of 100 µl were thawed on ice and 4 µl of desired plasmid was added to competent cells. Cell culture was then incubated on ice (30 min) and subjected to heat shock using a thermomixer (2 min, 42°C). Afterwards, cells were regenerated using 1 ml of LB medium and incubated at 37°C for at least an hour. 200 µl of cell suspension was then inoculated to LB agar plates, containing antibiotics, according to the plasmid used and incubated overnight at 37°C.

3.2.6. Recombinant protein expression

To LB agar plates, containing transformed cells grown overnight, 1 ml of LB medium was added. Cells were then detached using a Drigalski spatula and transferred to 500 ml of LB medium (containing corresponding antibiotic). Cell suspension was then incubated in an orbital shaker incubator until OD_{550} = 0.6-0.8. To this 2 mM IPTG was added and the cells were incubated for 3h in an orbital shaker incubator (37°C, 230 RPM). Suspension was centrifuged (4600 g, 10 min, 4°C), resuspended in 3 ml of TN buffer (100 mM Tris-HCl, pH 7.0, 150 mM NaCl) and stored at -20°C.

3.2.7. Inclusion bodies isolation

Cells containing recombinant protein were thawed and resuspended in 47 ml of TN buffer. To cell suspension lysozyme was added (1 mg per 1 g of biomass) and the mixture was incubated (30 min, RT). Mixture was sonicated on ice to remove DNA (3×1 min or until mixture turned

significantly less viscous) and centrifuged (9500 g, 15 min, 4°C). Pellets containing inclusion bodies were washed 3 times with 50 ml of TN buffer and centrifuged (9500×g, 15 min, 4°C). Washed inclusion bodies were stored at -20°C for further use.

3.2.8. Solubilization and inclusion bodies dialysis

Inclusion bodies were stirred on a magnetic stirrer and dissolved in a dissolving buffer (~3h, RT). After dissolving, suspension was centrifuged (15 min, 15.000×g, 4°C). Supernatant was then transferred into dialysis tubing (M_w cut-off 12-14 kDa). Dialysis was carried out at conditions mentioned in *Table 7.*

Dissolving buffer: 8M Urea, 20 mM Tris-HCl (pH 7.4), 1 mM β-ME, 150 mM NaCl

3.2.9. SDS-Polyacrylamide gel electrophoresis

Proteins were commonly analysed using 15% separating gels combined with a 5% focusing gel. Samples were commonly mixed 1:1 with denaturing sample buffer and denatured using a boiling water bath for 5 min. Proteins were then separated using constant voltage (180 V) for about 1h (or until methylene blue reaches the bottom of the gel). As an electrolyte Tris-glycine buffer was used. Afterwards gels were stained using Coomassie Brilliant blue stain and destained using destaining solution.

Tris-glycine buffer: 0.25 M Tris, 1.92 M Glycine, 1 % (w/v) SDS, pH 8.3

Destaining solution: 50 % MeOH, 10 % AcOH (in water)

3.2.10. Immobilized metal affinity chromatography

For purification of fusion proteins, affinity chromatography was used – Ni-NTA. 400 µl of Ni-NTA agarose was added into a microtube, centrifuged using a tabletop centrifuge and the supernatant was discarded. Beads were washed using equilibration buffer (5 min, RT), centrifuged and supernatant discarded. 400 µl of sample was added and the mixture was incubated for 0.5-2h (RT). Supernatant was discarded and the beads were washed three times using wash buffer. Protein was then eluted using elution buffer and incubated for at least 30 min. Samples were then analysed using SDS-PAGE.

Equilibration buffer: 50 mM PBS (pH 8), 300 mM NaCl, 10 mM imidazole

Wash buffer: 50 mM PBS (pH 6.5), 300 mM NaCl, 10 mM imidazole

Elution buffer: 300 mM imidazole

3.2.11. Vacuole isolation

On day one, desired yeast strain was inoculated on YPD agar plate and cultivated (37°C, O/N).

On day two, 20 ml of liquid YPD medium was inoculated and cultivated (37°C, 6h, 220 RPM). Afterwards 400 ml of liquid YPD medium was inoculated using 3.5×10^8 cells and incubated (37°C, 14h, 220 RPM).

On day three, cell suspension was centrifuged (4500×g, 5 min) and washed 3× with sterile water. Cells were then transferred to low-nitrogen YNB medium and cultivated for exactly 4h (37°C, 220 RPM). After cultivation powder NaN_3 was added (65 mg/100 ml) and the suspension was centrifuged (3000×g, 8 min, 4°C). Pellet was washed with cold 10 mM NaN_3 and transferred to weighted Falcon tubes. To suspension SPB buffer was added (3 ml/1 g biomass). OD_{600} was measured and lyticase (500 U/200 mg biomass) was added. Cell suspension was then incubated and stirred at RT until $0.1\times OD_{600}$. Spheroplasts were centrifuged (1500×g, 15 min, 4°C) and washed with 1 M Sorbitol (3×). At this point spheroplasts can be stored in the fridge O/N.

Spheroplasts were then resuspended in 6-10× the volume in buffer M, homogenized using Dounce homogenizer (16×) and centrifuged (3500×g, 10 min, 4°C). If necessary, spheroplasts were check under the microscope.

Ultracentrifugation tubes were first layered with buffer M, then topped with supernatant of homogenized cells and ultracentrifuged (100.000×g, 30 min, 4°C). White residue/crust containing vacuoles on top was collected using a Pasteur pipette. Ultracentrifugation tubes were then layered with sample first, then topped with buffer N and ultracentrifuged again (100.000×g, 30 min, 4°C). White residue/crust containing vacuoles from the top was again collected, transfer to -80°C and lyophilize.

Low-nitrogen YNB medium: YNB (no AA, no $(NH_4)_2SO_4$, 2 % glucose, 100 µM proline

SPB buffer: 0.8 M Sorbitol, 50 mM KH_2PO_4, 10 mM NaN_3, 40 mM β-ME

M buffer: 10 mM MES (pH 6.9), 0.1 mM $MgCl_2$, 12 % Ficoll 400

N buffer: 10 mM MES (pH 6.9), 0.5 mM MCl_2, 8 % Ficoll 400

3.2.12. Polymerase chain reaction

Primarily two PCR mixes were used - EmeraldAmp® GT PCR Master Mix and Top-Bio PPP Master Mix. In experiments manufacturer's instructions were followed. Protocols for individual master mixes are listed in *Table 2* and *3*. Primers are listed in *Table 22* and *29*.

Table 2: PCR conditions for Top-Bio PPP MasterMix

Step	Temperature [°C]	Time [s]	Repeats
Initial denaturation	94	60	1
Denaturation	94	15	25-35
Annealing	55-68	15	
Extension	72	60/1kb	
Final extension	72	420	1
Cooling	22	-	-

Table 3: PCR conditions for TaKaRa EmeraldAmp® GT PCR

Step	Temperature [°C]	Time [s]	Repeats
Denaturation	98	10	30
Annealing	60	30	
Extension	72	60/1kb	

3.2.13. Agarose electrophoresis

PCR products obtained using PCR were analysed or purified using a 1.2% agarose gel with TAE buffer. 60 ml of 1× TAE buffer containing 1.2 % agarose was heated up using microwave until dissolved and cooled until safe to touch. To solution was added ethidium bromide (c = 1 µg/ml), mixed and poured into gel mold. PCR mixes already contained components of loading buffer, so no addition of loading buffer was necessary. As a marker Top-Bio DNA marker 155-970 was used. Electrophoresis was carried out at 100 V for 45 min or until samples have reached 2/3 of the gel. Gels were then visualized using Uvitech Alliance Q9 at 365 nm.

50× TAE buffer: 2 M Tris-HCl (pH 8), 0.05 M EDTA, 57.1 ml glacial acetic acid (per 1l)

3.2.14. Size exclusion chromatography

Sephadex G-200 resin was first swelled using swelling buffer for 48h. Swelled resin was then gently added to a 30 ml glass column using a Pasteur pipette to avoid any air bubbles. When the column was packed, 400 µl of cell lyase was applied to the column. Protein was then eluted using elution buffer. After whole column elution, 200 µl of each fraction was then transferred to microtiter plate and absorbance at 280 nm was measured. Fractions with the

highest absorbance, deemed to contain protein of interest, were pooled, and used for kinetic assay and for MS analysis.

Swelling and washing buffer: 0.05 M Tris (pH 7)

Elution buffer: 0.05 M Tris (pH 7), 0.15 M NaCl

3.2.15. Ion exchange purification

Chosen resin was first swelled in a swelling buffer for 48h. Swelled 5 ml of resin was then gently pipetted into a plastic column using a Pasteur pipette. When the column was packed, remaining swelling buffer was drained and 400 µl was added to the top of the resin. After the sample has soaked into the resin, 1 ml of swelling buffer was added to the top of the resin and first 1 ml fraction was collected. Afterwards 3 ml of swelling buffer was added and collected into three 1 ml fractions as a washing step. After this 10 ml of elution buffer was added and again 1 ml fractions were collected. To assess the purity fractions were checked using SDS-PAGE.

3.2.16. Proteolytic activity testing in micro titre plate format

Each reaction consisted of following components and was pipetted into UV microplates:

Buffer solution – 0.05M sodium citrate (pH 5)	100 µl
Peptide (5 mg/ml)	10 µl
Purified cell lysate	10 µl

UV microplates were incubated for 30 min at 30°C and shaken continuously. Absorbance at 300 nm was measured every 1 min using a microplate reader.

Table 4: Peptide library used in our experiments (Ḟ - nitrophenylalanine, Nle – norleucine).

Peptide	Sequence
1	KARQNleḞEANle
2	KPAEFḞAL
3	KPVEFḞRL
4	KPAEFḞHL

3.2.17. Proteolytic activity testing – MS

We used similar approach to micro titre plate format; however, the cleaving was performed over a longer period (1-24 h) and the samples were analysed using mass spectrometry. The analysis was performed by Doc. RNDr. Miroslav Šulc, Ph.D.

3.2.18. Phenotypic testing

Strains of *C. albicans* and *S. cerevisiae* (listed in *Table 28*) were used in a phenotypic testing also called a spot test. All strains were first inoculated onto a YPD agar plate and incubated (O/N, 37°C). Afterwards 20 ml of liquid YPD was inoculated and cultivated (O/N, 37°C). Following day, liquid cultures were centrifuged (4500g, 5 min), washed with sterile water and resuspended in a 0.9% saline solution to $OD_{600} = 1$ (corresponding to 10^7 cells/ml). 100 µl of resuspended cultures were then pipetted into sterile microplates and diluted five times using a dilution factor of 10. Diluted cell suspension was then applied to agar plates using a 6×8 replicator. Media and conditions used in the experiment are listed in *Table 5*. Auxotrophic strains were supplemented with following chemical: 60 mg/l lysine, 40 mg/l histidine, 120 mg/l leucine, 20 mg/l uracil.

Table 5: List of conditions used for phenotypic testing.

Medium - Base	Conditions	Purpose
YPD	-	Control
	1 M NaCl	Osmotic stress
	1 M KCl	
	1.5 M Sorbitol	
	2 mM H2O2	Oxidative stress
	0.04% SDS	Membrane stress
	pH 4	Growth at different pH
	pH 6	
	pH 8	
	pH 10	
YNB (w/o AA, w/o $(NH_4)_2SO_4$)	-	Control
	100 mM (NH4)2SO4	Nitrogen limitation
	100 µM (NH4)2SO4	
	100 mM Proline	
	100 µM Proline	
	100 mM Urea	
	100 µM Urea	
YNB (w/ AA, w/ $(NH_4)_2SO_4$)	-	Control
	2% Glucose	Carbon limitation
	2% Glycerol	
	2% Lactate	
YCB	-	Control
	0.2% BSA	Complex nitrogen source

3.2.19. Expression of Apr1-His-Strep

S. cerevisiae strain containing *APR1*, fused with His-tag and Strep-Tag has been inoculated on an YPD agar plate and cultivated (37°C, O/N). Next day, 30 ml of liquid YPD were inoculated using a single colony. YPD also included 200 µM $CuSO_4$ as an inducer. Culture was then cultivated for 48h at 30°C and 230 RPM in a tabletop orbital shaker.

3.2.20. *S. cerevisiae Apr1-His-Strep* Purification

After cultivation, 1 ml of cell culture was centrifuged (1 min, 13.000×g), washed with water once. and centrifuged again (1 min, 13.000×g). To the pellet 600 µl of 0.05 M citrate buffer (pH 5), 0.2 g glass beads and depending on the use of the cell lysate, inhibitors were added. For IEX and kinetic assays chromatography combination of Pefabloc SC (0.1 mM) and EDTA (5 mM) was added. For IMAC only Pefabloc SC (0.1 mM) was used. Microtubes were then placed in a beat beater for 10 min using the maximum setting and centrifuged (5 min, 13.000 × g). To further remove insoluble particles, 0.45 µm filter was used, to obtain purified cell lysate.

3.2.21. Competent *S. cerevisiae* yeast cells preparation

Selected *S. cerevisiae* strain was inoculated to 25 ml of YPD medium and cultivated overnight (30°C, 230 RPM). OD_{600} was measured and 200 ml of YPD was inoculated with 10^9 cells (OD_{600} = 0.1 ~ 10^6 cells). When OD_{600} reached around 2 (or approximately 2×10^7 cells), liquid medium was centrifuged (3000×g, 5 min) and resuspend two times in sterile distilled water – first in 100 ml and second in 2 ml. Cell suspension was centrifuged last time (3000×g, 5 min) and the cells were resuspended in 2 ml of FFC2 (5%v glycerol, 10%v DMSO). Suspension was then divided into sterile microtubes in 50 µl aliquots. Competent cells were then gradually frozen first in -20°C (inside a polystyrene box) and then transferred to -80°C.

3.2.22. Transformation of *S. cerevisiae* competent yeast cells

Thawed competent cells were centrifuged (14.000×g, 30 s), resuspended in 360 µl of FCC3 including plasmid DNA (summarized below) and mixed well. Cell suspension was then incubated for 20-60 min at 42°C, centrifuged (14.000×g, 30 s) and resuspend again in 1 ml of sterile distilled water (diluted 5-20×, if necessary). Inoculated SC agar plates lacking appropriate selection marker were incubated for 4 days at 30°C.

Table 6: Composition and the volumes of reagents added to the competent S. cerevisiae cells used for transformation.

500 g/l PEG 3350	260 µl
1 M lithium acetate	36 µl
2 mg/ml salmon sperm DNA (ssDNA)	50 µl
Plasmid DNA	0.1-5 µg
Final volume	360 µl

3.2.23 *S. cerevisiae* single colony PCR

After *S. cerevisiae* transformation, individual colonies were tested for successful transformation. Single colony was transferred to 0.1 ml microtube and resuspended in 50 µl of dH_2O. Resuspended colony was then placed in the PCR thermocycler and the cells were disintegrated at 99°C for 7 min. 2 µl of lysed cell suspension was then used during PCR diagnostics.

3.2.24. Western blot (WB)

After running an SDS-PAGE using a 1 mm gel, "transfer sandwich" was prepared (listed below). Blotting paper and nitrocellulose membrane were wetted first in a transfer buffer using a Petri dish.

Cathode
3 sheets of 3MM blotting paper (8×9 cm)
Acrylamide gel
Nitrocellulose membrane
3 sheets of 3MM blotting paper (8×9 cm)
Anode

Bubbles were removed from the "transfer sandwich" using a roller and for transfer Trans-Blot Turbo Transfer System (Bio-Rad) was used (17 min, 2.5 A).

To check for successful transfer, coloured marker was used as well as staining with 0.5% Ponceau S (in 1% AcOH). Membrane was then washed using distilled water to remove Ponceau S staining. Membrane was transferred to a Falcon tube and blocked using a blocking buffer (2h, RT). After incubation, blocking buffer was discard, 5 ml of antibody buffer (including primary antibodies) was added to the Falcon tube, and the mixture was incubated O/N on a rotator in a cold room.

Following day, blocking solution was discarded and the membrane was washed using wash buffer (2×5 min, 1×15 min, RT). Membrane was transferred back to washed Falcon tube and

4 ml of antibody buffer (including secondary antibodies) was added. Mixture was then incubated (2h, RT) and washed in a wash buffer (3×5 min).

For immunodetection, 20 ml of phosphatase buffer with 100 µl of NBT and BCIP each was poured onto a membrane. After first slight colour change, reaction was quenched by transferring the membrane to distilled water. Membrane was then carefully dried between filter papers and photographed.

50× Transfer buffer: 250 mM Tris, 1.92 M glycine, 0.1% SDS

Transfer buffer: 1× Transfer buffer, 20 % MeOH

TBS: 20 mM Tris-HCl (pH 7.5), 150 mM NaCl

Blocking buffer: 1× TBS, 5 % low fat dried milk powder, 0.1 % Triton X-100

Antibody buffer: 1× TBS, 2 % low fat dried milk powder, 0.1 % Triton X-100

Wash buffer: 1× TBS, 0.1 % Triton X-100

Phosphate buffer: 100 mM Tris-HCl (pH 9.5), 100 mM NaCl, 1 mM $MgCl_2$

3.2.25. Rapid dilution refolding (RD)

Inclusion bodies were first dissolved in dissolving buffer and centrifuged (15.000×g, 15 min, 4°C). Soluble protein was the slowly added to the RD buffer to achieve the protein concentration of 1-10 µg/ml. After refolding, the solution was kept at 4°C O/N and analysed the next day using SDS-PAGE.

Dissolving buffer: 8M Urea, 20 mM Tris-HCl (pH 7.4), 1 mM β-ME, 150 mM NaCl

RD buffer: 1 M Urea, 50 mM Tris-HCl (pH 7), 50 mM NaCl, 0.5 M Arg, 5 % Glycerol, 10 mM polyphosphate

4. Overview

For more straightforward navigation in further sections, *Figure 8A* summarises the molecular weights (Mw) of the immature proenzymes (proApr1p, preproPep4p) and their active forms (Apr1p, Pep4p). Figure 1B illustrates the Pep4p activation cascade in *S. cerevisiae*, detailing the post-translational modifications and relevant organelles involved (left). This thesis aims to replicate this activation process in vitro, using conventional recombinant protein refolding methods to convert inactive proApr1p into mature Apr1p (right).

A

Gene	Protein	AA	kDa
APR1 (vector)	proApr1p	429	47
	Apr1p	333	36
PEP4 (native)	preproPep4p	405	45
	Pep4p	329	36

B

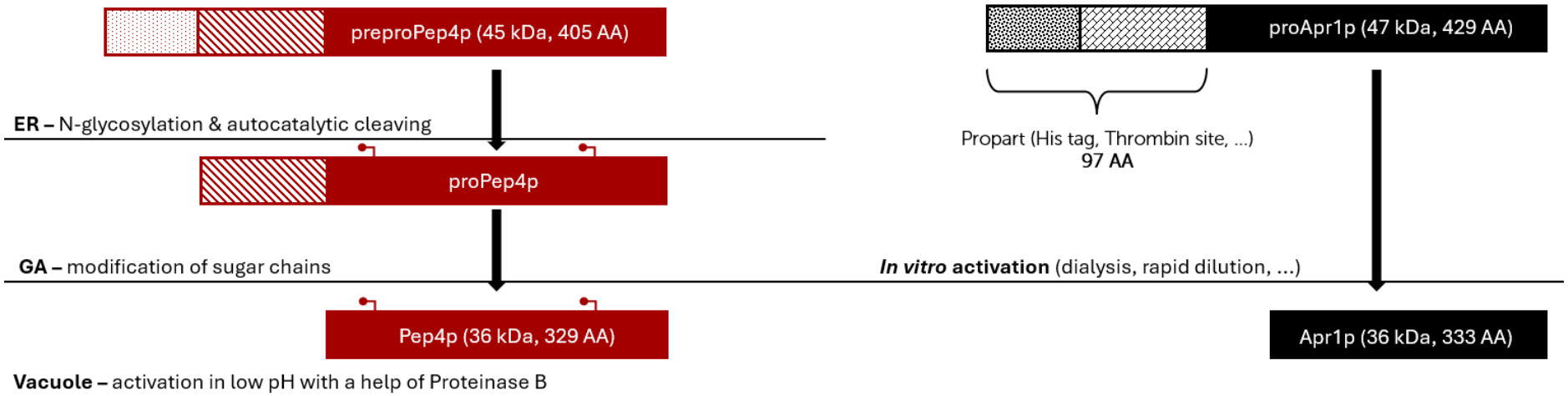

Figure 8: A – Table summarising the Mw and AA lengths of wild-type Pep4p (S. cerevisiae) and recombinant Apr1p. (C. albicans) in their immature (preproPep4, proApr1p) and mature (Pep4p, Apr1p) form. B – Represents the in vivo activation cascade in S. cerevisiae

Table 7: Summary of refolding protocols used in the activation of Apr1p with buffer composition, pH, time and observed level of aggregation (0 = none, 4 = very high).

Conditions under which we have tried to activate recombinant proApr1p																
Protocol	Step	Tris/Citrate	Urea	β-ME	Glycerol	Tween	Arginine	NaCl	Polyphosphate	NaOAc	Vacuoles	*HET1*	pH	Time	Aggregation	Type
A	1	20 mM	4 M	-	0.25%	0.03%	-	-	-	-	-	-	6.3	24/48h	0	Dialysis
	2	20 mM	2 M	-	0.25%	0.03%	-	-	-	-	-	-	6.3	24/48h	1	Dialysis
	3	20 mM	0 M	-	0.25%	0.03%	-	-	-	-	-	-	6.3	24/48h	2	Dialysis
B	1	20 mM	4 M	-	0.25%	0.03%	0.1 M	-	-	-	-	-	6.3	24/48h	0	Dialysis
	2	20 mM	2 M	-	0.25%	0.03%	0.1 M	-	-	-	-	-	6.3	24/48h	1	Dialysis
	3	20 mM	0 M	-	0.25%	0.03%	0.1 M	-	-	-	-	-	6.3	24/48h	2	Dialysis
C	1	20 mM	4 M	-	0.25%	0.03%	-	-	10 mM	-	-	-	6.3	24/48h	1	Dialysis
	2	20 mM	2 M	-	0.25%	0.03%	-	-	10 mM	-	-	-	6.3	24/48h	1	Dialysis
	3	20 mM	0 M	-	0.25%	0.03%	-	-	10 mM	-	-	-	6.3	24/48h	4	Dialysis
D	1	20 mM	4 M	-	0.0025	0.03%	0.1 M	-	10 mM	-	-	-	6.3	24/48h	0	Dialysis
	2	20 mM	2 M	-	0.0025	0.03%	0.1 M	-	10 mM	-	-	-	6.3	24/48h	1	Dialysis
	3	20 mM	0 M	-	0.0025	0.03%	0.1 M	-	10 mM	-	-	-	6.3	24/48h	4	Dialysis
E	1	50 mM	1 M	-	0.005	-	0.5 M	50 mM	10 mM	-	none/native/ Δapr1	-	3/4/5	-	0	Rapid dilution
F	1	25 mM	4 M	1 mM	-	-	0.4 M	150 mM	-	-	-	-	7.5	3h	0	Dialysis
	2	25 mM	2 M	1 mM	-	-	0.4 M	150 mM	-	-	-	-	7.5	3h	0	Dialysis
	3	25 mM	-	1 mM	-	-	0.4 M	150 mM	-	-	-	-	7.5	O/N	1	Dialysis
	4	25 mM	-	1 mM	-	-	-	150 mM	-	-	-	-	7.5	3h	2	Dialysis
	5	-	-	-	-	-	-	-	-	0.1 M	-	-	4	3h (37°C)	3	Dialysis
G	1	25 mM	4 M	1 mM	-	-	0.4 M	150 mM	10 mM	-	-	-	7.5	3h	0	Dialysis
	2	25 mM	2 M	1 mM	-	-	0.4 M	150 mM	10 mM	-	-	-	7.5	3h	0	Dialysis
	3	25 mM	-	1 mM	-	-	0.4 M	150 mM	10 mM	-	-	-	7.5	O/N	1	Dialysis
	4	25 mM	-	1 mM	-	-	-	150 mM	10 mM	-	-	-	7.5	3h	2	Dialysis
	5	-	-	-	-	-	-	-	-	0.1 M	-	-	4	3h (37°C)	4	Dialysis
H	1	20 mM	4 M	-	0.25%	0.03%	0.1 M	-	-	-	Native	-	7.5	24/48h	0	Dialysis
	2	20 mM	2 M	-	0.25%	0.03%	0.1 M	-	-	-	Native	-	7.5	24/48h	0	Dialysis
	3	20 mM	0 M	-	0.25%	0.03%	0.1 M	-	-	-	Native	-	7.5	24/48h	2	Dialysis
	1	20 mM	4 M	-	0.25%	0.03%	0.1 M	-	-	-	*Δapr1*	-	7.5	24/48h	0	Dialysis
	2	20 mM	2 M	-	0.25%	0.03%	0.1 M	-	-	-	*Δapr1*	-	7.5	24/48h	0	Dialysis
	3	20 mM	0 M	-	0.25%	0.03%	0.1 M	-	-	-	*Δapr1*	-	7.5	24/48h	2	Dialysis
I	1	20 mM	4 M	-	0.25%	0.03%	0.1 M	-	10 mM	-	Native	-	7.5	24/48h	0	Dialysis
	2	20 mM	2 M	-	0.25%	0.03%	0.1 M	-	10 mM	-	Native	-	7.5	24/48h	2	Dialysis
	3	20 mM	0 M	-	0.25%	0.03%	0.1 M	-	10 mM	-	Native	-	7.5	24/48h	3	Dialysis
	1	20 mM	4 M	-	0.25%	0.03%	0.1 M	-	10 mM	-	*Δapr1*	-	7.5	24/48h	0	Dialysis
	2	20 mM	2 M	-	0.25%	0.03%	0.1 M	-	10 mM	-	*Δapr1*	-	7.5	24/48h	2	Dialysis
	3	20 mM	0 M	-	0.25%	0.03%	0.1 M	-	10 mM	-	*Δapr1*	-	7.5	24/48h	3	Dialysis
J	1	20 mM	4 M	-	0.25%	0.03%	-	-	-	-	-	-	4	24/48h	0	Dialysis
	2	20 mM	2 M	-	0.25%	0.03%	-	-	-	-	-	-	4	24/48h	2	Dialysis
	3	20 mM	0 M	-	0.25%	0.03%	-	-	-	-	-	-	4	24/48h	3	Dialysis
K	1	20 mM	4 M	-	0.25%	0.03%	-	-	-	-	-	-	3	24/48h	0	Dialysis
	2	20 mM	2 M	-	0.25%	0.03%	-	-	-	-	-	-	3	24/48h	2	Dialysis
	3	20 mM	0 M	-	0.25%	0.03%	-	-	-	-	-	-	3	24/48h	4	Dialysis
J	1	20 mM	4 M	-	0.25%	0.03%	-	-	-	-	-	WO/ALL	6.3	24/48h	0	Dialysis
	2	20 mM	2 M	-	0.25%	0.03%	-	-	-	-	-	WO/ALL	6.3	24/48h	0	Dialysis
	3	20 mM	0 M	-	0.25%	0.03%	-	-	-	-	-	WO/ALL	6.3	24/48h	1	Dialysis

5. Results

5.1. Heterologous Apr1p expression

5.1.1. Prokaryotic expression

5.1.1.1. Selection of *E. coli* strain

To determine the optimal E. coli strain for recombinant Apr1p production, we compared the protein expression capabilities of BL21(DE3)(*Figure 9*), a widely used laboratory strain, and LOBSTR(*Figure 10*), a derivative strain engineered to minimise background contamination during purification. To determine optimal induction conditions, we assessed Apr1p expression levels before and after induction with IPTG at various time points (1h, 2h, 3h, and 4.5h). Doc. RNDr. Olga Heidingsfeld, CSc, kindly provided the expression vector utilised in this study.

Our protocol yielded high-quality inclusion bodies (IBs) with minimal contamination from both *E. coli* strains tested. However, *E. coli* BL21(DE3) exhibited slightly higher contaminant levels than *E. coli* LOBSTR. Consequently, we selected the LOBSTR strain for subsequent recombinant protein expression. Additionally, we observed negligible differences in protein expression levels between 3 and 4.5 hours of induction. Therefore, we opted for a shorter induction period of 3 hours to optimise efficiency.

Table 8: Loading of the 15% SDS-PAGE gel in Figures 9 and 10 of recombinant protein expression (including description and corresponding numbers).

#	Description
M	Marker
1	Pre-induction cell suspension
2	1h post-induction
3	2h post-induction
4	3h post-induction
5	4.5h post-induction
6	Lysed cells (post-sonication)
7	Inclusion bodies

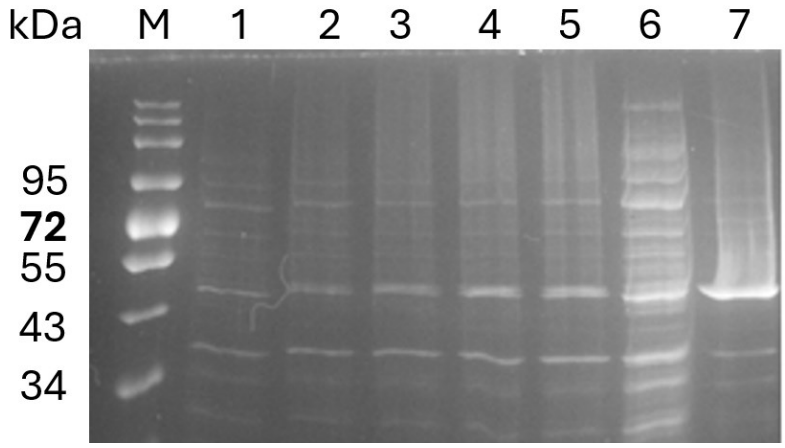

Figure 9: 15% SDS-PAGE gel of proApr1p expression in E. coli BL21(DE3) during 4.5 h of induction. Protein proApr1p has a molecular weight of 47 kDa.

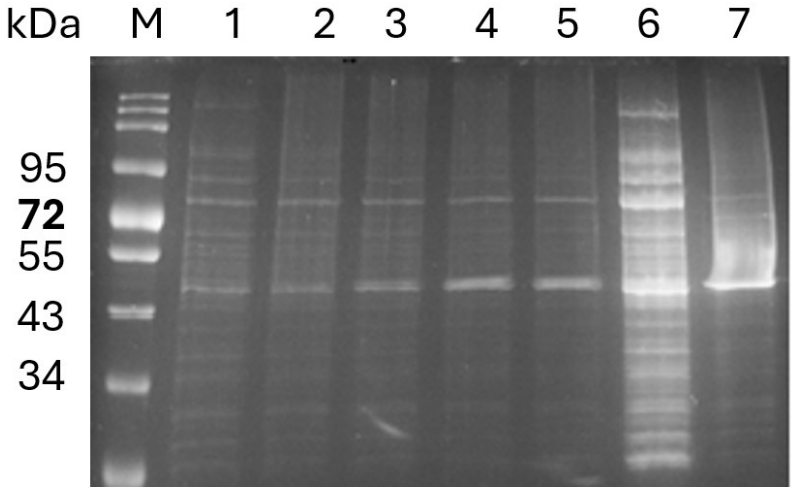

Figure 10: 15% SDS-PAGE gel of proApr1p expression in E. coli LOBSTR during 4.5 h of induction. Protein proApr1p has a molecular weight of 47 kDa.

5.1.1.2. Immobilised metal affinity chromatography (IMAC)

Given the presence of a 6xHis-tag at the N-terminus of proApr1p, we employed Ni-NTA affinity chromatography (IMAC) to purify the protein. While IMAC (*Figures 11, 12*) yielded similarly purified proApr1p from both tested *E. coli* strains and reduced the contamination associated with BL21(DE3), a substantial amount of proApr1p was lost during the process. Due to the high purity of inclusion bodies obtained directly from *E. coli* LOBSTR (*Figure 10*), and considering the cost of the resin, protein loss, and additional processing time, further purification of proApr1p was deemed unnecessary.

Table 9: Loading of the 15% SDS-PAGE gels of IMAC (Figures 11 and 12) (including description and corresponding number).

#	Description
M	Marker
1	Sample pre-purification
2	Flowthrough
3	Wash 1
4	Wash 2
5	Wash 3
6	Eluate
7	Beads

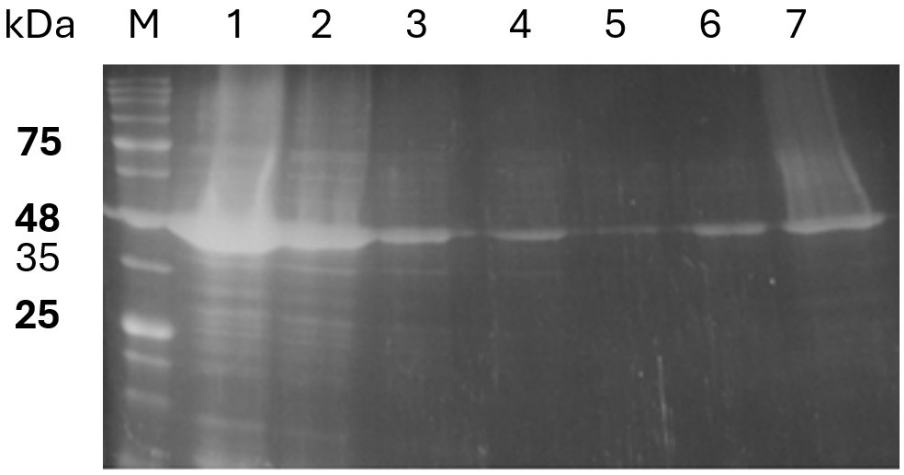

Figure 11: 15% SDS-PAGE gel of Ni-NTA IMAC using inclusion bodies obtained from E. coli BL21(DE3).

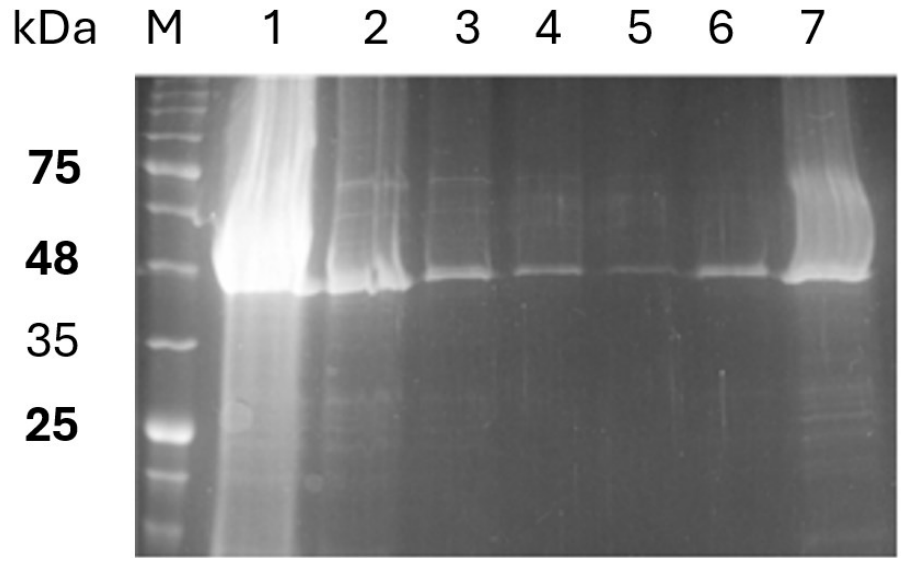

Figure 12: 15% SDS-PAGE gel of Ni-NTA IMAC using inclusion bodies obtained from E. coli LOBSTR.

5.1.1.2. Solubilisation of inclusion bodies

Due to the propensity of proApr1p to aggregate, we screened multiple solubilisation buffers (*Table 10*), to maximise soluble protein yield. While each buffer offered different advantages, we identified buffer B as the most effective. For each solubilisation, 20 ml of buffer was used per 1 g of inclusion bodies.

Table 10: Composition of solubilisation buffer with corresponding concentrations of each component, including a subjective description of approximate time it takes to solubilise the IBs and the resulting solubilities.

Buffer	Urea [M]	Tris [mM]	β-ME [mM]	NaCl [mM]	EDTA [mM]	pH	Solubilisation time	Insolubilities
A	10	20	-	150	-	7.4	>1h	High
B	8	50	100	-	1	7.5	<1h	Very low
C	8	20	1	150	-	7.4	>1h	Low

5.1.1.3. Refolding and activation of proApr1p

To obtain mature Apr1p from inclusion bodies, refolding and activation protocols were necessary. To do so, we built upon work of previous collaborators who proposed the use of protocol A. Since we were not able to obtain mature Apr1p using this protocol and mostly proApr1p was observed, we extended this "library" to 12 refolding protocols with different composition, techniques, lengths, and approaches. Protocols with which we attempted to activate recombinant proApr1p are listed and summarised in the *Table 7.* The following sections will detail the effects of each modification on immature proApr1p derived from *E. coli* LOBSTR inclusion bodies.

5.1.1.3.1. Protocols A, B, C and D – Addition of polyphosphate and arginine

Protocol A, designed by Jakub Papík and Oge Artagan, was unsuccessful in activating proApr1p and served as the foundation for further protocol development in this work. Building upon protocol A, protocol B, C and D were devised for proApr1p activation. Protocol B used the addition of arginine as an aggregation suppressor. Protocol C used the addition of polyphosphate (polyPi), as it is present in the vacuole and may act as a chaperone, potentially aiding in the refolding process. Protocol D combined the addition of polyPi and arginine.

The addition of arginine to the refolding buffer did not reduce protein aggregation compared to the baseline Protocol A. Conversely, the inclusion of polyphosphate resulted in increased

protein aggregation (*Figure 13, Sample 5*). Post-dialysis, samples were evaluated for proteolytic activity using a BSA cleavage assay (*Figure 14*).

Table 11: Loading of 15% SDS-PAGE gel in Figure 13.

#	Description	
M	Marker	
1	Dissolved inclusion bodies	
2	Protocol B	proApr1p post-dialysis (supernatant)
3		proApr1p post-dialysis (aggregate)
4	Protocol C	proApr1p post-dialysis (supernatant) + PolyPi
5		proApr1p post-dialysis (aggregate) + PolyPi

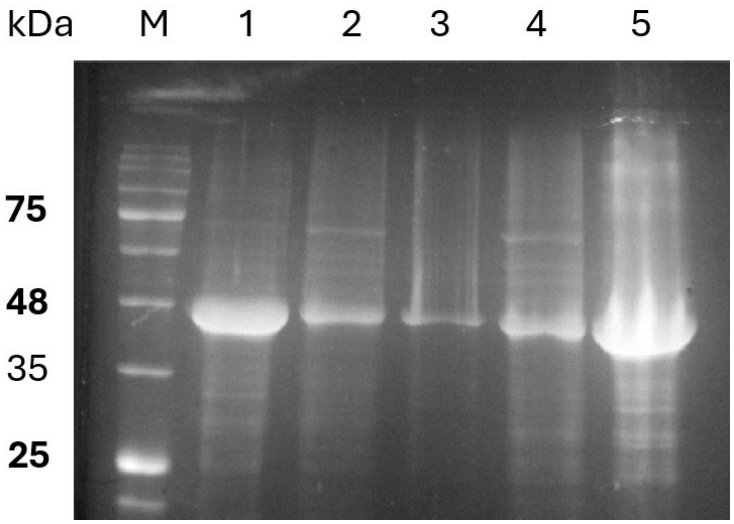

Figure 13: 15% SDS-PAGE gel of refolding protocols B and C. Results of protocol A not shown, due to similar results as protocol B.

Figure 14 demonstrated that lower pH negatively impacted BSA, leading to degradation and cleavage into smaller protein fragments with reduced molecular weights (*Samples 2, 4, 6*). Additionally, minimal differences were observed among *Samples 3, 5,* and *7,* which were expected to contain mature Apr1p post-dialysis. The absence of a change in molecular weight compared to proApr1p (approximately 48 kDa) and the unaltered protein band patterns suggested the presence of predominantly immature proApr1p lacking proteolytic activity.

Table 12: Loading of 15% SDS-PAGE gel presented in Figure 14.

#	Description	
M	Marker	
1	proApr1p + BSA (t = 0)	
2	pH 4, 37°C, O/N	BSA
3		Protocol B – proApr1p + BSA
4		BSA
5		Protocol C – proApr1p + BSA
6		BSA
7		Protocol D – proApr1p + BSA

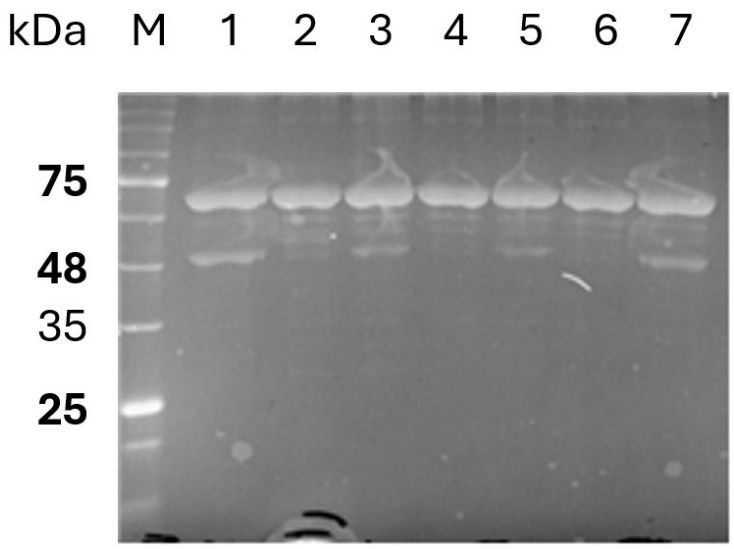

Figure 14: 15% SDS-PAGE gel of a BSA cleaving assay after using protocol A, B and C for dialysis. Cleaving was performed at pH 4 to mimic the condition of a vacuoles.

5.1.1.3.2 Protocol E – Rapid dilution (RD)

Protocol E used a different approach of protein folding utilising rapid dilution, instead of dialysis. We performed rapid dilution at three different pH (3, 4 and 5) to simulate the conditions of a vacuole, which should have favoured proApr1p activation. Additionally, considering the potential of other vacuolar enzymes in proApr1p activation, we incorporated isolated vacuoles into this experiment. We isolated two types of vacuoles, WT (wild type) vacuoles (potentially containing all vacuolar enzymes) and *Δapr1* vacuoles (isolated from *C. albicans Δapr1* strain).

The initial concentration of dissolved IBs was 10 mg/ml, which was then diluted using a dilution buffer by a factor of 1000×, resulting in a final concentration of 0.01 mg/ml. This approach, although sometimes successful, seemed the least intuitive.[63] In our case, the chosen dilution factor may have been too high, as evidenced by the absence of protein bands around

48 kDa in *Figure 15*, which would typically represent proApr1p. Additionally, no cleavage of BSA was observed across any of the samples in *Figure 15*. Like previous BSA samples, the presence of protein bands with lower molecular weight than BSA (66 kDa) can likely be attributed to hydrolysis under acidic conditions.

Table 13: Loading of SDS-PAGE gel in Figure 15. Each trial included 3 different pH, with or without dissolved vacuoles.

#	Description	
M	Marker	
1	No vacuoles added	pH 3
2		pH 4
3		pH 5
4	Wild type vacuoles	pH 3
5		pH 4
6		pH 5
7	*Δapr1* vacuoles	pH 3
8		pH 4
9		pH 5

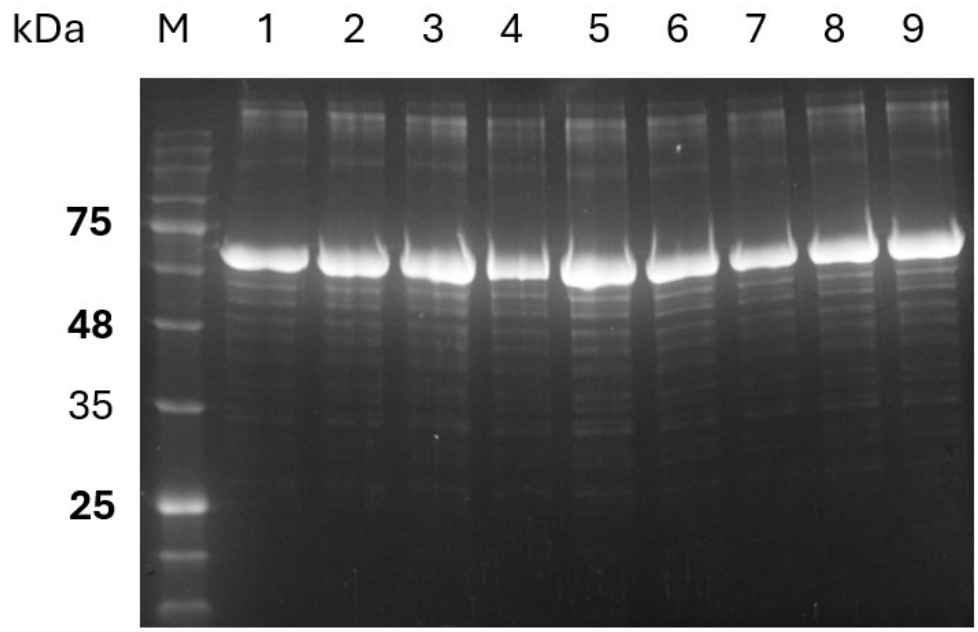

Figure 15: 15% SDS-PAGE gel of rapid dilution protocol, combined with BSA cleaving assay.

5.1.1.3.3. Protocol H and I – Addition of vacuoles

Due to the lack of success in activating proApr1p and its homology to Pep4p, we further hypothesised that other vacuolar enzymes might be necessary for Apr1p maturation (protocols H and I). To test this, we isolated wild-type vacuoles from *C. albicans* HE169 (containing Apr1p) and *Δapr1* vacuoles from *C. albicans* KC281 (a deletion mutant lacking Apr1p). We then incubated the isolated vacuoles with recombinant proApr1p to assess if mature Apr1p would be generated (*Figure 16).*

Surprisingly, in *Figure 16*, *Samples 1* and *2* (dissolved vacuoles) show no protein bands, while *Samples 3, 4,* and *5* predominantly contain proApr1p. Initially, we hypothesised that the high concentration of Ficoll 400, from the lyophilised vacuoles might affect protein electrophoretic properties. However, subsequent testing with BSA revealed no effect of Ficoll 400 on protein electromigration. Despite multiple attempts and approaches, vacuoles proved difficult to solubilise. Notably, a protein band around 25 kDa (*Figure 16, Sample 3*) appeared to be specific to native vacuole fractions, as it is also present in other vacuole-related SDS-PAGE gels (*Figures 18 and 19*).

Table 14: Loading of a 15% SDS-PAGE gel in Figure 16, which utilises isolated vacuoles as a means for proApr1p activation.

#	Description
M	Marker
1	Dissolved vacuoles (*C. albicans* HE169)
2	Dissolved vacuoles (*C. albicans* KC281 (*Δapr1*))
3	proApr1p dialysis (WT vacuoles)
4	proApr1p dialysis (*Δapr1* vacuoles)
5	proApr1p dialysis (no vacuoles)

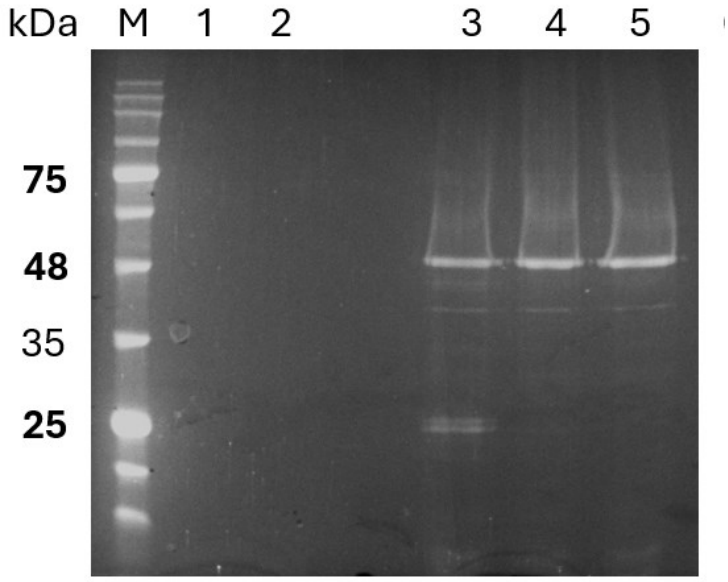

Figure 16: 15% SDS-PAGE gel of activation of proApr1p using protocols H and I where WT and Δapr1 vacuoles were included.

To investigate the inherent proteolytic activity of the vacuoles, we resuspended them in water and assessed their activity using a BSA cleavage assay at pH 4 (*Figure 17*). The absence of protein bands in *Samples 2* and *4* (*Figure 17*) suggested a lack of any proteins in these samples, which would explain the absence of proteolytic activity. This outcome likely stemmed from difficulties in vacuoles solubilisation.

Table 15: Loading of a 15% SDS-PAGE gel in Figure 17, testing for proteolytic activity of dissolved vacuoles.

#	Description
M	Marker
1	BSA – 5 mg/ml
2	*Δapr1* vacuoles (66 mg/ml)
3	BSA + *Δapr1* vacuoles
4	WT vacuoles (52 mg/ml)
5	BSA + WT vacuoles

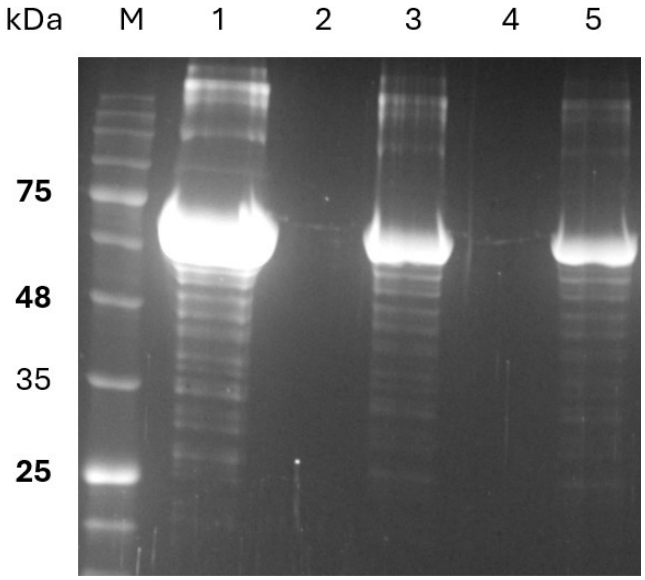

Figure 17: 15% SDS-PAGE gel of resuspended vacuoles only and a BSA cleavage assay of vacuoles (only).

In Protocol I, the presence of additional non-proApr1p protein bands (*Figure 18*) suggested that we successfully solubilised the vacuoles. This indicated that solubilisation in water alone was insufficient (*Samples 4 and 8*). However, when vacuoles were introduced at the beginning of dialysis of proApr1p, the high urea concentration likely aided in solubilisation, resulting in the observed protein bands. Notably, the addition of vacuoles to dialysis appeared to decrease protein aggregation. Furthermore, a prominent band around 25 kDa was observed again, suggesting it is a vacuole associated protein.

Table 16: Loading of 15% SDS-PAGE gel in Figure 18, which analyses samples obtained through protocol I, which again uses vacuoles to active proApr1p.

#	Description	
M	Marker	
1	WT vacuoles	proApr1p – dissolved IB
2		proApr1p – post-dialysis
3		proApr1p – aggregates
4		Dissolved vacuoles
5	*Δapr1* vacuoles	proApr1p – dissolved IB
6		proApr1p – post-dialysis
7		proApr1p – aggregates
8		Dissolved vacuoles

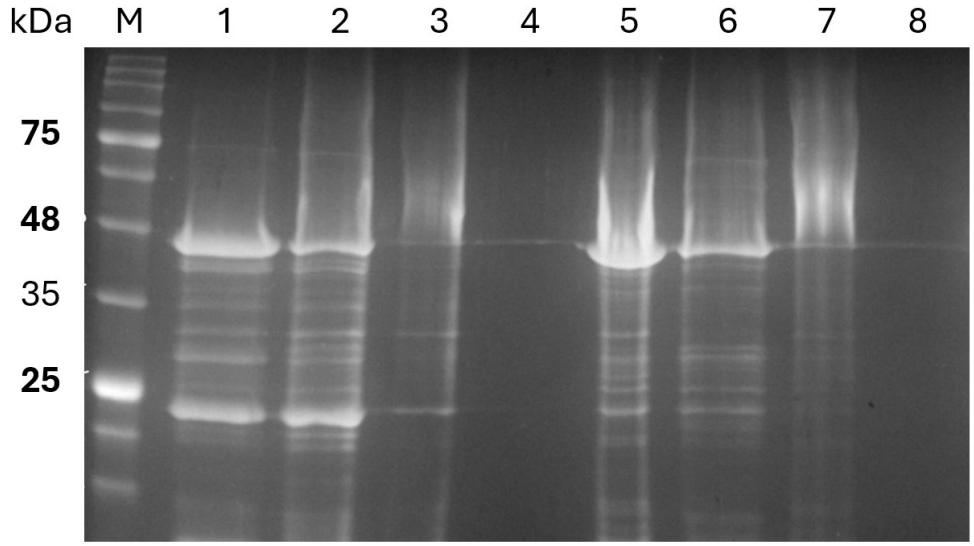

Figure 18: 15% SDS-PAGE gel of protocol I, where polyphosphate and vacuoles were added to proApr1p.

Simultaneously, proApr1p was also dialysed using the same protocol I (*Table 7*), but without the addition of any vacuoles. After dialysis these samples were subsequently used in a BSA cleavage assay (*Figure 19*). *Figure 13* showed similar pattern as those of previous experiments, where variance in pH and the addition of vacuoles had very little effect on proApr1p activation. Although these outcomes might suggest that Apr1p is not activated using vacuolar enzymes, more research is needed into vacuole solubilisation and how they interact with proApr1p.

Table 17: Loading of 15% SDS-PAGE gel analysing the samples from protocol I (Figure 19), which used vacuole assisted dialysis.

#	Description	
M	Marker	
1	proApr1p only (no vacuoles added)	pH 3
2		pH 4
3		pH 5
4	WT vacuoles	pH 3
5		pH 4
6		pH 5
7	*Δapr1* vacuoles	pH 3
8		pH 4
9		pH 5

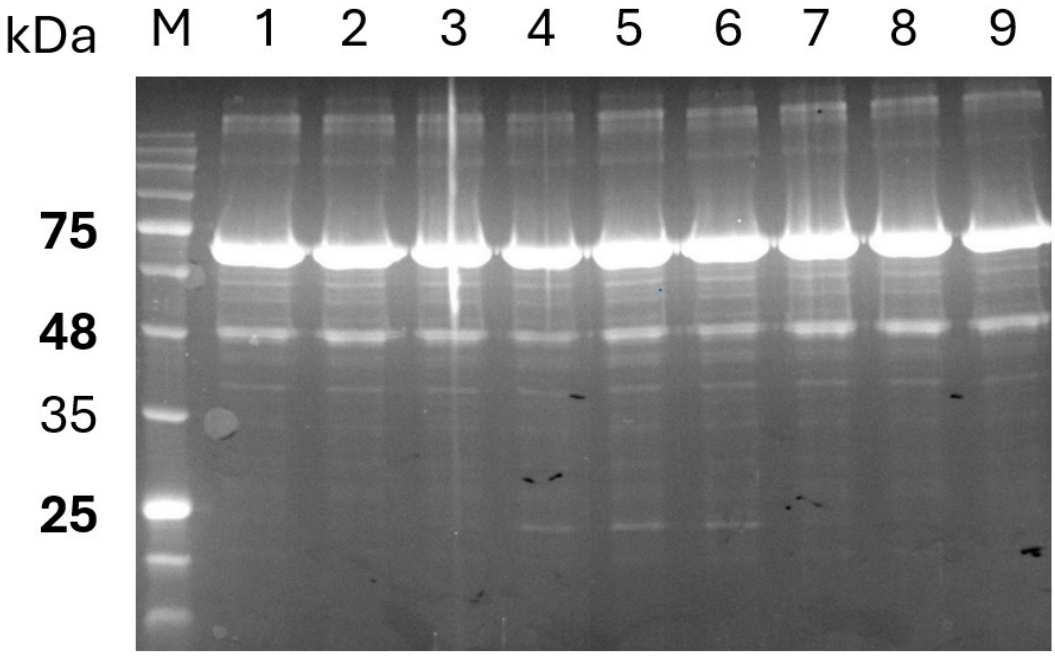

Figure 19: 15% SDS-PAGE gel of a BSA cleaving assay. Attempted activation of proApr1p was carried out with or without the addition of vacuoles at three different pH (3, 4, 5), to further simulate the native conditions of a vacuole.

5.1.1.3.4. Protocol F & G – Cathepsin D – Sojka et al. (2012)

Given the high homology between Apr1p and cathepsin proteases, we tested a refolding protocol published by Sojka et al. (2012), initially designed for pro-cathepsin activation. This protocol incorporated shorter dialysis times and the addition of β-mercaptoethanol (β-ME) and sodium chloride to the dialysis buffers, deviating from our earlier approaches. However, these modifications did not improve refolding and instead increased proApr1p aggregation.

Despite the limited sequence similarity (11.7% identity, 18.2% similarity) between Apr1p and the target of Sojka et al. (2012), Cathepsin D from *Ixodes ricinus*, we investigated their protocol (Protocol F) due to its inclusion of shorter dialysis and an activation step at 37°C and

pH 4. However, this protocol resulted in moderate precipitation during dialysis and significant precipitation during the final activation step, leading to full protein loss (*Figure 20, Sample 5*). We also observed that soluble proApr1p degrades when exposed to 37°C overnight (*Figure 20, Sample 2*). Furthermore, incorporating arginine as a potential folding aid had minimal effect on protein stability or activation, consistent with observations in Protocol B.

Table 18: Loading of 15% SDS-PAGE gel in Figure 20, which used protocol F (Sojka et al. 2012) for proApr1p activation.

#	Description
M	Marker
1	proApr1p pre-dialysis
2	proApr1p pre-dialysis (37°C, O/N)
3	proApr1p post-dialysis
4	proApr1p post-dialysis (37°C, O/N)
5	proApr1p post-activation
6	proApr1p post-activation (37°C, O/N)
7	BSA + Sample post-activation (37°C, O/N)
8	BSA + Sample post-activation (37°C, O/N)
9	BSA (37°C, O/N)

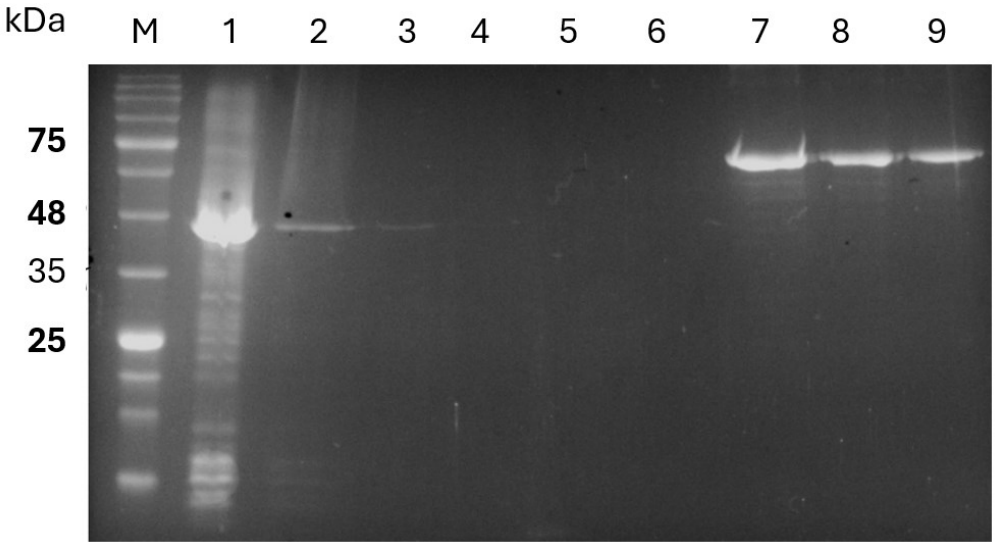

Figure 20: 15% SDS-PAGE gel of Cathepsin D activation protocol F according to Sojka et al. (2012).

To simulate vacuolar conditions better, we reintroduced polyphosphate, despite its previous association with increased protein aggregation (Protocol C, *Figure 6*). Following the dialysis (*Figure 21, Sample 2*), a significant loss of protein was observed. Similarly, the activation step (*Figure 21, Sample 3*), lead to full protein aggregation. Furthermore, *Sample 2* (*Figure 21*) appeared to contain primarily proApr1p based on molecular weight, and no BSA cleavage activity was observed in Sample 5.

Table 19: Loading of 15% SDS-PAGE gel in Figure 21, a re-run of Sojka et al. (2012) protocol with the addition of polyphosphate (Protocol G).

#	Description
M	Marker
1	proApr1p – dissolved IBs
2	proApr1p post-dialysis (with aggregates)
3	proApr1p post-activation
4	proApr1p post-activation – aggregate
5	proApr1p post-activation + BSA

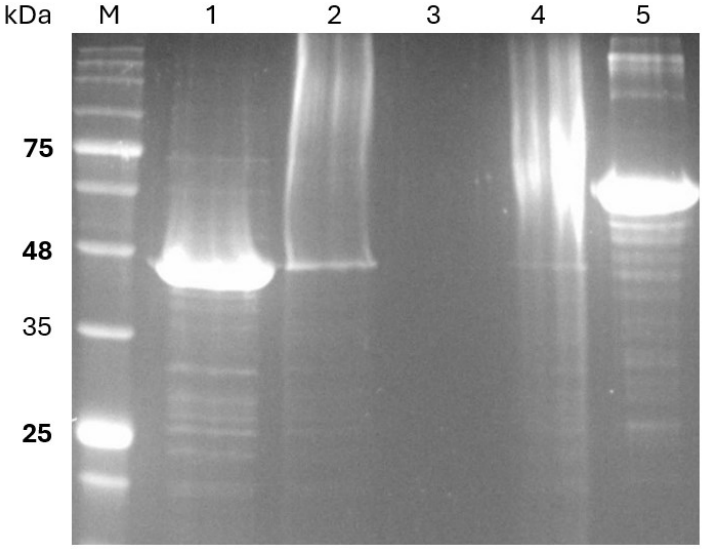

Figure 21: Another run of Sojka et al. (2012) of Cathepsin D activation (protocol G), with the addition of polyphosphate.

5.1.1.3.5. Protocols J and K – Effects of pH on proApr1p activation

While most of our protocols utilised a pH of around 7 to provide mild folding conditions, we also explored lower pH values (3 and 4) to mimic the acidic environment of the vacuole. However, these acidic conditions resulted in substantial protein aggregation.

5.1.1.3.6. Cell lysate as a catalyst

Based on the homology to Pep4p in *S. cerevisiae* and its activation cascade involving multiple steps, it is reasonable to hypothesise that proApr1p also requires other enzymes for its activation. To investigate this, we utilised cell lysates of two deletion mutant strains – *S. cerevisiae* Y12098 (*Δpep4*) and *C. albicans* KC281 (Δapr1). These strains lack the proteolytic activity of their respective orthologs, Pep4p and Apr1p, allowing us to assess the potential involvement of other enzymes in Apr1p precursor activation. To test this hypothesis, we employed protocol D, which included polyPi and Arg.

Figure 22 shows that only a small amount of proApr1p was present within the inclusion bodies (*Sample 1*), with most remaining in the insoluble fraction even after dissolving the IBs

(*Figure 22, Sample 2*). Working with cell lysate as a catalyst is challenging due to the presence of numerous other enzymes that can both exhibit catalytic activity and potentially mask or substitute the proteolytic activity of Apr1p. This makes it difficult to assess if activation occurred, therefore the use of cell lysate may not be optimal. While we inhibited serine and metalloproteases in other experiments, we omitted enzyme inhibition in this experiment in case proApr1p requires serine or metalloproteases for its activity. Notably, Pep4p requires Proteinase B, a serine protease, in its final step of activation.

Table 20: Loading of 15% SDS-PAGE gel in Figure 22, using cell lysates as proApr1p activation catalyst.

#	Description
M	Marker
1	proApr1p (dissolved inclusion bodies) - soluble
2	proApr1p (dissolved inclusion bodies) – insolubilities after centrifugation
3	proApr1p precipitate post-dialysis – proApr1p
4	proApr1p supernatant post-dialysis – proApr1p
5	proApr1p supernatant post-dialysis + cell lysate (*C. albicans* KC 281 (*Δapr1*))
6	proApr1p supernatant post-dialysis + cell lysate (*S. cerevisiae* Y12098 (*Δpep4*))

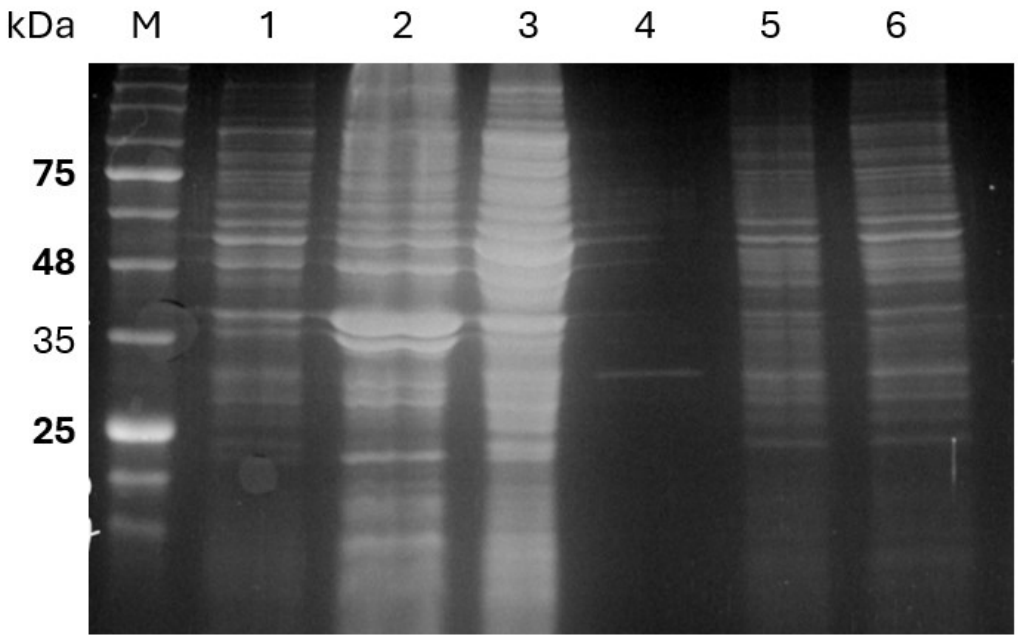

Figure 22: 15% SDS-PAGE gel of proApr1p activation using cell lysates from C. albicans KC281 (Δapr1) and S. cerevisiae Y12098 (Δpep4) as a medium for proApr1p activation. In this experiment we used protocol D.

5.1.1.3.7. Time dependency

Most of our protocols have been carried out multiple times and with various lengths of dialysis – from instant rapid dilution protocol which yielded no success, through shorter ones, where each step took 3-4h, to the common dialysis methods where 24h is allowed for buffer

exchange. We have also attempted to prolong the dialysis steps to 48h, however this approach commonly yielded in higher precipitation of protein samples, when compared to 24 h. Therefore, we think that 24h offers appropriate conditions for buffer exchange while preventing the propagation of precipitation.

5.1.1.3.8. Protocol J – Potential sphingolipid transferase as a proApr1p processing aid

Our previous collaborator, Václava Baureová, suggested that *Candida albicans* might possess an endogenous Apr1p inhibitor analogous to Ia3p, a Pep4p inhibitor found in *S. cerevisiae*. Ia3p is an intrinsically disordered protein that, upon binding to the Pep4p active site, forms a helix, sterically inhibiting the enzyme. In *C. albicans*, we identified Het1p, a putative sphingolipid transferase containing an intrinsically disordered region similar to Ia3p, as a potential Apr1p inhibitor.

To investigate this interaction, we generated two Het1p constructs: Het1p (ALL), which includes the disordered region and could potentially act as an inhibitor, and Het1p (WO), lacking the disordered region and therefore not expected to interact with Apr1p. In a broader study of this potential interaction, we attempted to co-refold both Het1p constructs with Apr1p using protocol D. We also included cell lysate to potentially facilitate proApr1p maturation. This approach aimed to not only investigate the potential inhibitory interaction but also to leverage the potential of inhibitors to stabilise protein structure, which would be beneficial for our studies.[64]

Despite relatively pure inclusion bodies containing proApr1p, the addition of Het1p (*Figure 23*) and cell lysate increased the complexity of the protein mixture, making it difficult to determine if cleavage and formation of mature Apr1p occurred in *Samples 3, 4, 7,* and *8*.

Table 21: Loading of 15% SDS-PAGE gel in Figure 23, where interaction of Het1p and proApr1p was investigated as well as the influence of cell lysates on proApr1p activation.

#	Description	
M	Marker	
1	*C. albicans* KC281 (*Δapr1*)	Cell lysate (only)
2		proApr1p (dissolved inclusion bodies)
3		proApr1p + Het1p (ALL)
4		proApr1p + Het1p (WO)
5	*S. cerevisiae* Y12098 (*Δpep4*)	Cell lysate (only)
6		proApr1p (dissolved inclusion bodies)
7		proApr1p + Het1p (ALL)
8		proApr1p + Het1p (WO)

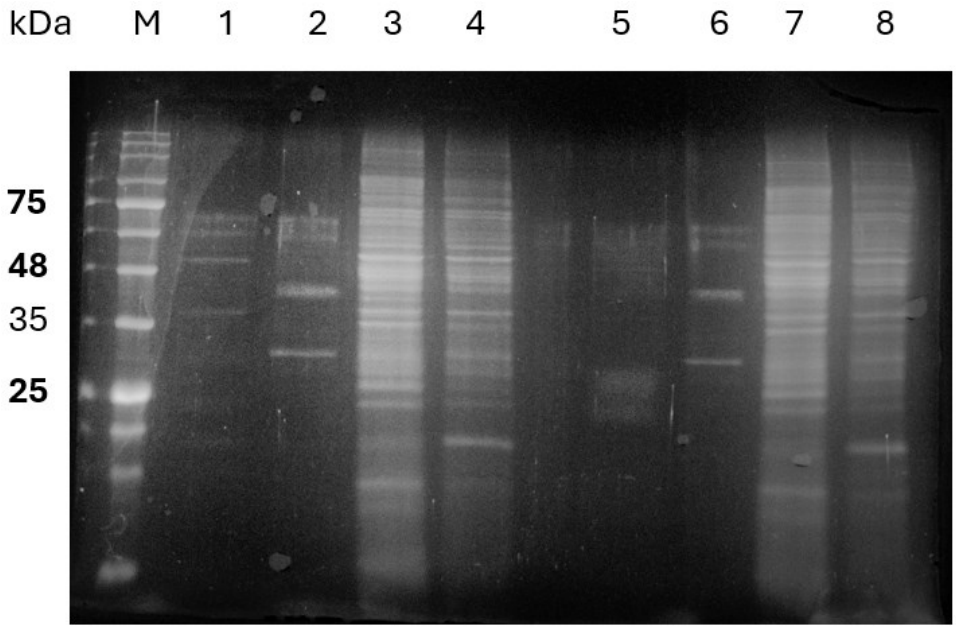

Figure 23: 15% SDS-PAGE gel of a co-dialysis of proApr1p with Het1p and its activation with cell lysates. Dialysis was carried out at pH 4 (Protocol D).

In *Figure 23*, a band between 25 and 35 kDa in *Sample 2* was analysed using Edman degradation. The resulting amino acid sequence suggested cleavage at the site highlighted in red (*Figure 24*). However, the size of this fragment did not correspond to mature Apr1p (*Figure 8*).

RIILFTLRRRYTMGSSHHHHHHSSGLVPRGSHKAHSIKLSKLSNEETLDASNFQEYTNSLAN
KYLNLFNTAHGNPSNFGLQHVLTNQEAEIPFVTPKKGGKYDAPLTNYLNAQYFTEIQIGTPG
QPFKVILDTGSSNLWVPSQDCTSLACFLHAKYDHDASSTYKVNGSEFSIQYGSGSMEGYISQ
DVLTIGDLVIPGQDFAEATSEPGLAFAFGKFDGILGLAYDTISVNHIVPPIYNAINQGLLEK
PQFGFYLGSTDKDENDGGLATFGGYDASLFQGKITWLPIRRKAYWEVLFEGIGLGDEYAELH
KTGAAIDTGTSLITLPSSLAEIINAKIGATKSWSGQYQVDCAKRDSLPDLTLTFAGYNFTLT
PYDYILEVSGSCISVFTPMDFPQPIGDLAIVGDAFLRKYYSIYDLDKNAVGLAPSKV

Figure 24: AA sequence of proApr1p. Probable amino acid residues found during Edman degradation highlighted red. Sequence highlighted in yellow represent N-terminal sequence of mature Apr1p.[43]

5.1.2. Eukaryotic recombinant protein production

Given our challenges in obtaining active Apr1p in *E. coli* and considering the potential importance of eukaryotic post-translational modifications, we shifted to expressing Apr1p in *S. cerevisiae*. We chose the *S. cerevisiae* Y12098 (*Δpep4*) strain, which lacks the Pep4p protease, to avoid interference from the endogenous enzyme. This strain was transformed with the episomal pYEXTHS-BN plasmid (prepared by Jakub Papík), containing the *APR1* gene under the control of the *CUP1* promoter. This construct incorporates both a 6xHis tag at the N-terminus and a Strep tag at the C-terminus for protein purification.

5.1.2.1. Verification of *S. cerevisiae* APR1-His-Strep

To test for successful transformation of *S. cerevisiae* with the episomal plasmid pYEXTHS-BN-*APR1* and to confirm the presence of the *APR1* gene insert, we used PCR and a set of diagnostic *APR1* primers (*Table 22*). *Figure 25* shows the amplified segment of the *APR1* gene (*Lane 1*), confirming the successful transformation of *S. cerevisiae* with the pYEXTHS-BN-*APR1* plasmid. This strain is also referred to as *S. cerevisiae-APR1*-His-Strep and was subsequently used for eukaryotic recombinant protein expression.

Table 22: Summarising APR1 diagnostic primers used to verify plasmid insertion and transformation of S. cerevisiae - Y12098 strain.

Name	5'-3' sequence	Length [bp]	Annealing temp. [°C]	Product size [bp]
APR-diag-F-1	ATGTCTCATCACCATCACCATCAC	24	55.7	825
APR-diag-R-2	GGAGGCATCGTAACCACCAA	20	53.8	

Table 23: Loading of a DNA agarose electrophoresis in Figure 25.

#	Description
M	Marker
1	Amplified segment of *APR1* (PCR product)
PC	Positive control
NC	Negative control

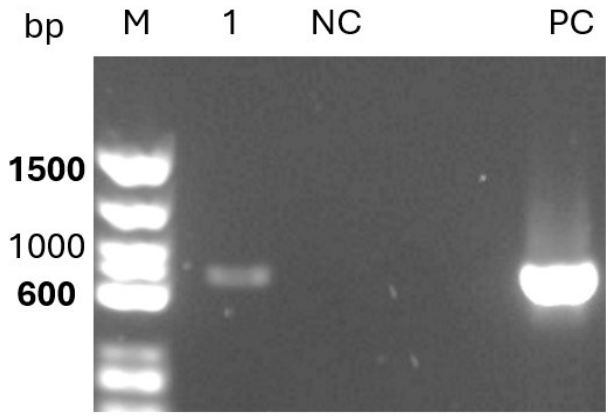

Figure 25: 1.2% agarose gel of an amplified segment of APR1 from S. cerevisiae containing APR1 gene, inserted using pYEXTHS-BN-APR1.Tthe size of amplicon is 825 bp.

5.1.2.2. Growth curve of *S. cerevisiae – APR1*-His-Strep

Growth curve (*Figure 26*) of *S. cerevisiae – APR1*-His-Strep was measured to see growth under induced protein expression with 200 µM $CuSO_4$. This strain reached exponential phase after 13 h and after 48h it had reached OD_{600} of 16.

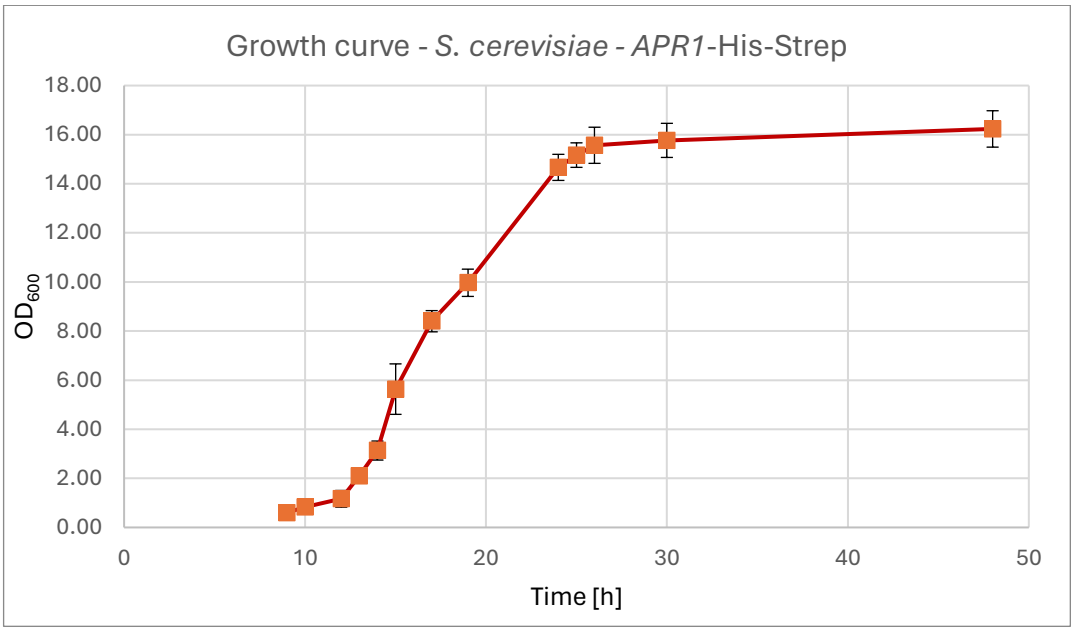

Figure 26: Growth cure of S. cerevisiae - APR1-His-Strep. OD_{600} was measured in a triplicate and the expression of our protein was induced using 200 µM $CuSO_4$.

5.1.2.3. *S. cerevisiae* – Apr1p purification

5.1.2.3.1. Ni-NTA IMAC

To purify our Apr1p-His-Strep we wanted to take advantage of 6× His-tag present at the N-terminal of Apr1p and used Ni-NTA affinity chromatography. Since no binding to Ni-NTA beads was observed (*Figure 27*), it was either possible no Apr1p-His-Strep was expressed or cleaving at the N-terminus occurred, suggesting Apr1p activation. Protein band above 35 kDa also suggested that protease activation might have occurred. This motivated us to proceed with protein purification. Considering the previous problems of protein degradation and precipitation, we opted for a milder protein purification method – size exclusion chromatography.

Table 24: Loading of 15% SDS-PAGE gel in Figure 27, showing IMAC protein purification.

#	Description
M	Marker
1	Sample (cell lysate)
2	Flowthrough
3	Wash 1
4	Wash 2
5	Wash 3
6	Eluate
7	Beads

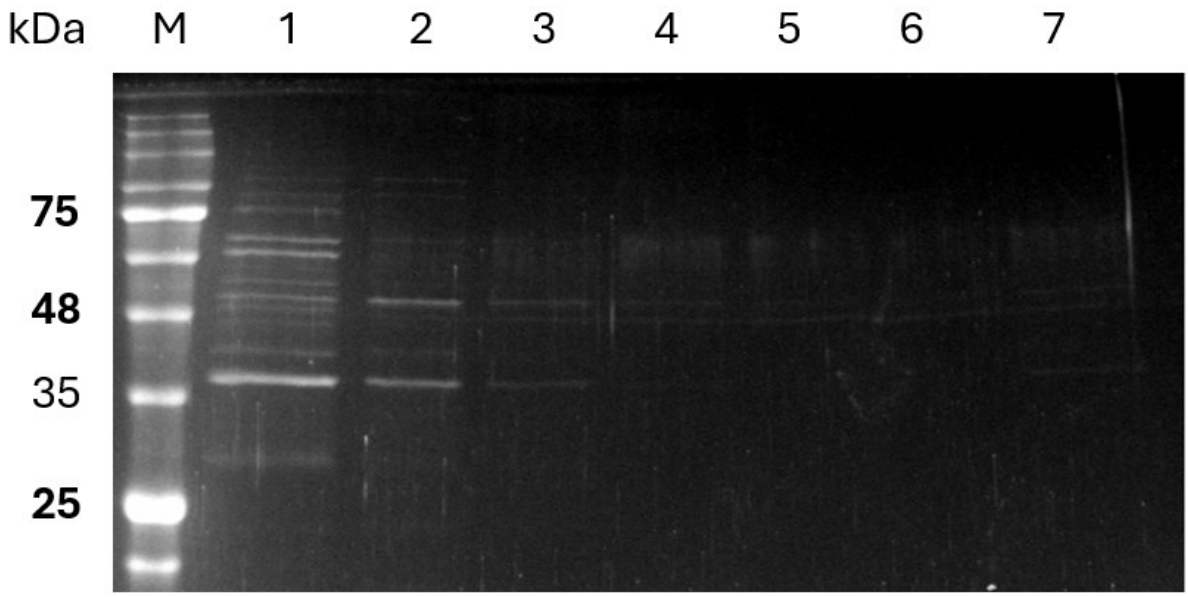

Figure 27: 15% SDS-PAGE gel of Ni-NTA purification of Apr1p-His-Strep.

5.1.2.3.2. Size exclusion chromatography (SEC)

Since our attempts at IMAC purification of cell lysate were unsuccessful, we opted to use SEC as the first option, due to its mild conditions that could potentially preserve the active form of Apr1p. After SEC was performed, fractions collected at 98, 138, and 178 minutes (*Figure 28*) were tested for proteolytic activity and analysed using mass spectrometry. However, no proteolytic activity was detected in any of these fractions. (MS analysis performed by Doc. Šulc)

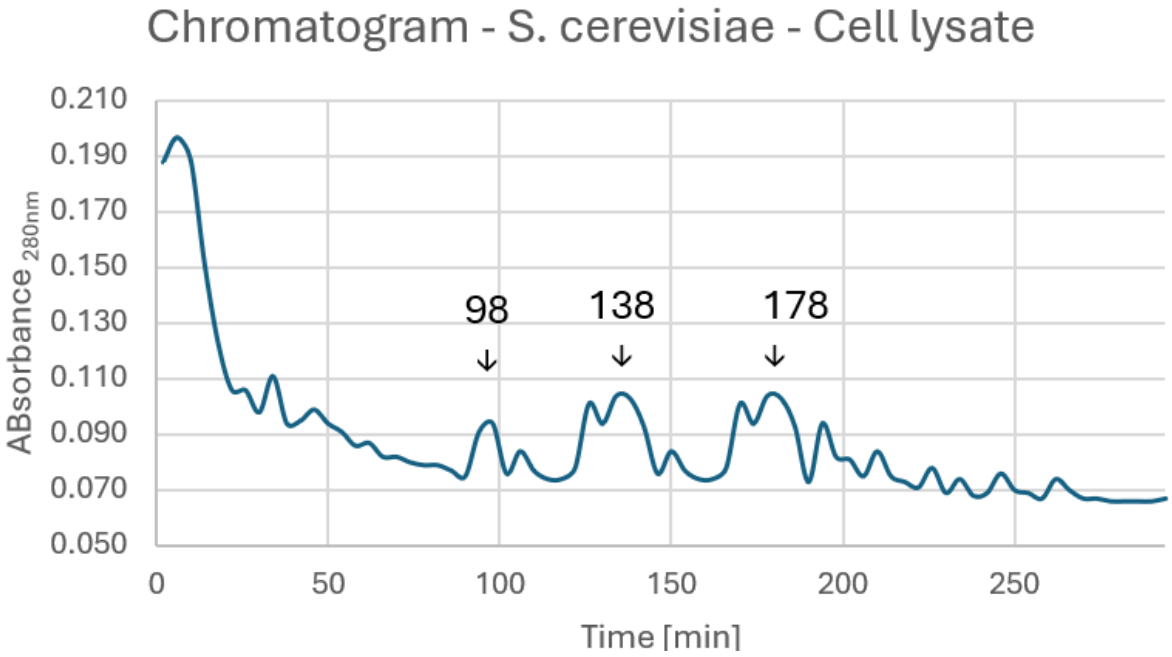

Figure 28: Chromatogram of SEC (Resin: Sephadex G-100, Elution buffer: 0.05 M citrate,.0.15 M NaCl, Column volume: 50 ml). Noted are fractions at which minute the fractions were used for proteolytic cleaving.

5.1.2.3.3. Ion exchange chromatography (IEC)

To optimise Apr1p purification from cell lysates, we screened five different ion exchange resins at four pH levels (3, 4, 5, and 7). The most promising results were obtained using DEAE Sephadex A-50 at pH 5 (*Figure 29*), yielding a purified protein band around 35 kDa. This purification protocol involved applying 500 µl of cell lysate to a 5 ml DEAE Sephadex A-50 column, followed by three washes with 1 ml of 0.05 M citrate buffer (pH 5). Elution was achieved using a salt gradient of 0.05 M citrate buffer (pH 5) containing 1 M NaCl. We chose pH 5 to maintain Apr1p activity, as it closely resembles the vacuolar environment. Mass spectrometry analysis of the purified protein was generously conducted by Doc. RNDr. Miroslav Šulc, Ph.D. and revealed that the purified protein was not Apr1p, but rather

glyceraldehyde-3-phosphate dehydrogenase (GAPDH), a glycolytic enzyme with a similar molecular weight (approximately 36 kDa).

Table 25: Loading of 15% SDS-PAGE gel of DEAE Sephadex A-50 purification (Figure 29).

#	Description
M	Marker
1-3	Washing steps
4-14	Elution fractions

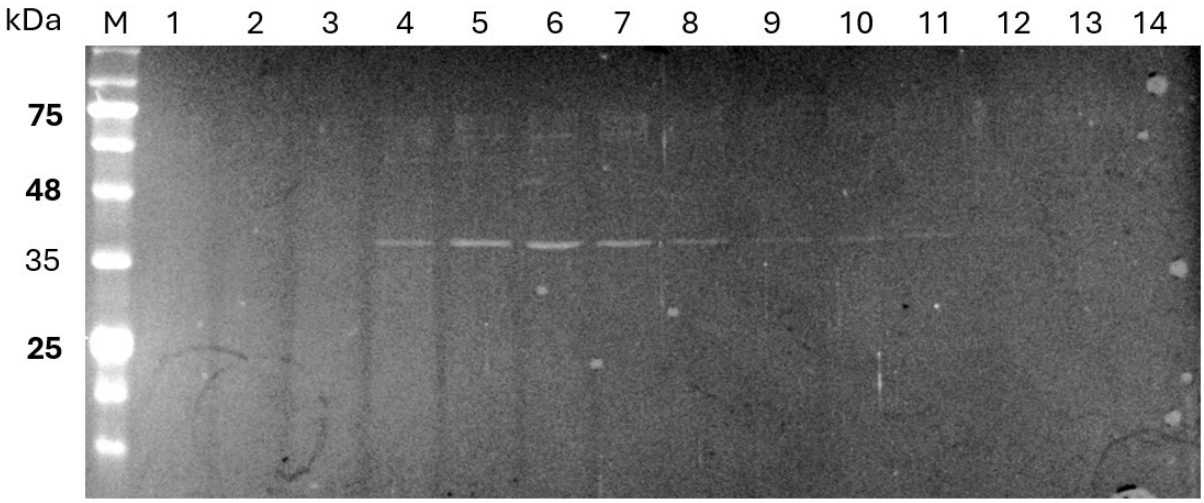

Figure 29: 15% SDS-PAGE gel of DEAE Sephadex A-50 purification.

5.1.2.4. Cleaving activity of Apr1p obtained from *S. cerevisiae*-Apr1p-His-Strep

To investigate the proteolytic activity of Apr1p isolated from the *S. cerevisiae*-APR1-His-Strep strain, we employed a multifaceted approach. For rapid analysis, a microtiter plate cleavage assay was utilised, employing substrates (*Table 4*) containing a nitryl moiety attached to phenylalanine. This modification allowed us to monitor proteolytic activity by detecting the decrease in absorbance at 300 nm, caused by the delocalisation of π-electrons within the aromatic rings upon hydrolysis at the adjacent site (*Figure 30*).

Furthermore, Doc. RNDr. Miroslav Šulc, Ph.D., generously assisted us in specifically analysing peptide cleavage products using mass spectrometry (*Figure 32*).

5.1.2.4.1. Proteolytic activity testing in micro titre plate format

Figure 30 demonstrates the expected trend of gradually decreasing A300, suggesting cleavage of Peptide 2 (*Table 4*). Notably, this experiment employed crude cell lysate with serine and metalloprotease inhibitors at pH 5. This combination should limit most proteases except aspartic ones, suggesting the observed cleavage may be attributed to Apr1p. However, further investigation is needed to definitively confirm this hypothesis.

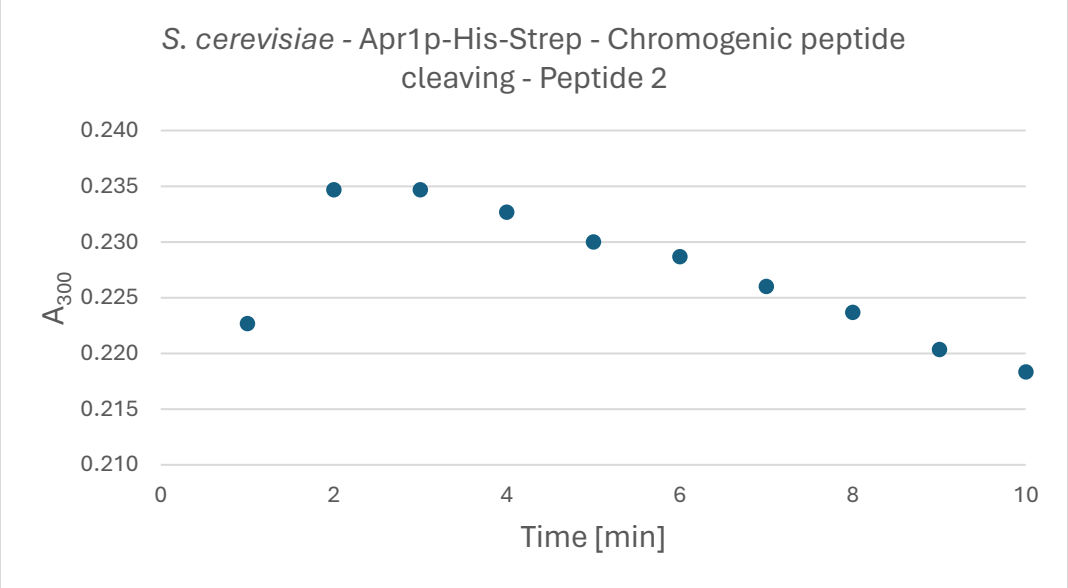

Figure 30: Graph of a microtitration peptide cleaving assay. Peptide 2 was used.

5.1.2.4.2. Proteolytic activity testing using mass spectrometry

To confirm the specificity of peptide cleavage observed in the microtiter plate assay, we conducted mass spectrometry (MS) analysis with the generous help of Doc. Šulc. Results from this experiment clearly demonstrated that the peptide was hydrolysed at the expected site, between phenylalanine residues, in the same conditions used for the microtiter assay. The increasing concentration of cleavage products over a 24-hour period (*Figure 32*) further supports the presence of an active aspartic protease in the crude cell lysate (maintained at low pH with specific protease inhibitors).

Table 26: m/z of peptide 2 and the corresponding cleaving product.

Peptide	m/z
KPAEFḞAL	996.480
KPAEF	591.313

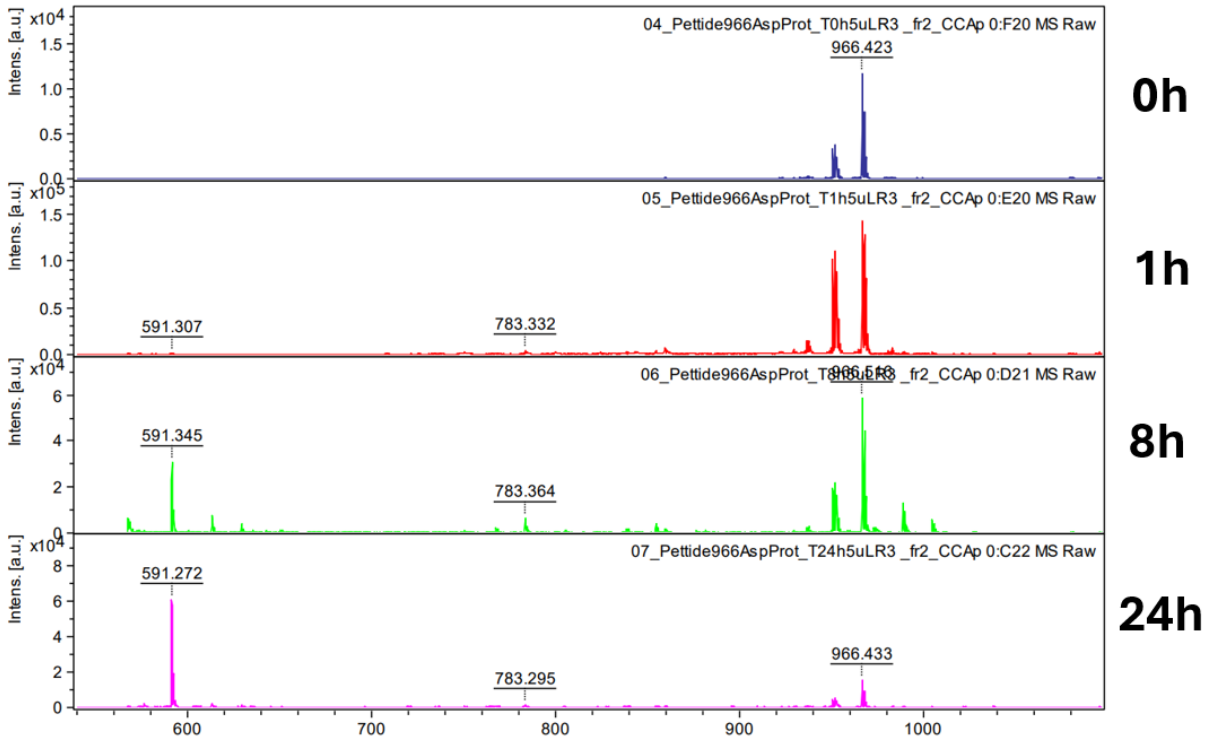

Figure 31: MS spectra showing how peptide 2 is cleaved at 0 h, 1 h, 8 h, 24 h. m/z of peptide 2 and its cleaving product are in Table 26

5.1.2.5. Western blots

We also tested for the presence of our aspartic protease Apr1p using hen polyclonal antibodies designed by Václava Bauerová and prepared by Hena Ltd., which targeted residues 231-243 of Apr1p (*Figure 33*). Following IEC separation, specific fractions indicated the potential presence of Apr1p. Based on molecular weight *Sample 4* might contained immature proApr1p, while *Sample 8* may contain two distinct processed forms of Apr1p.

In *Figure 34* we can see that non-induced *S. cerevisiae – APR1*-His-Strep did not contain any Apr1p (*Sample 1*), whereas IB produced in *E. coli* LOBSTR contained certain form of Apr1p (*Sample 2-5*). However, due to presence of bands higher molecular weight than expected, these antibodies might be of limited specificity.

Table 27: Loading of samples in Figure 33.

#	Description	
M	Marker	Fraction
1	pH 5	5
2		9
3		10
4		11
5		19
6		20
7	pH 7	8
8		13
9		20

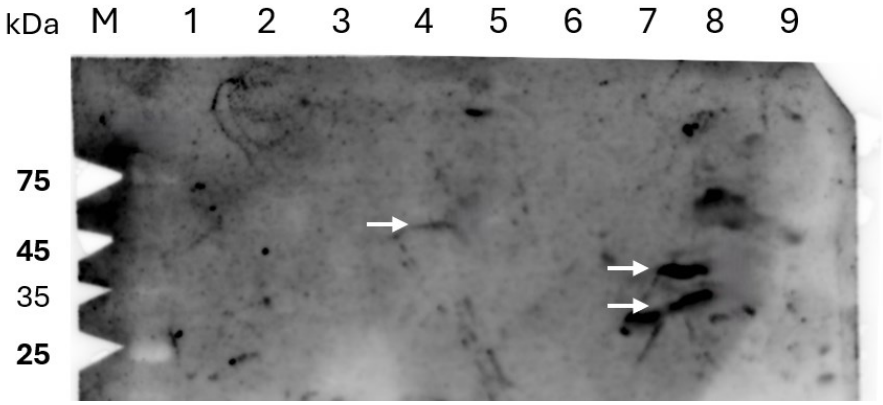

Figure 32: WB of a selected fraction of Apr1p-His-Apr purification. For purification DEAE Sephadex A-50 was used at two different pH 5 and 7. Signals are highlighted using an arrow.

#	Description
M	Marker
1	*S. cerevisiae – APR1*-His-Strep (cell lysate) - preinduction
2	proApr1p (dissolved inclusion bodies) - A
3	proApr1p + Het1 (WO)
4	proApr1p + Het1 (ALL)
5	proApr1p (dissolved inclusion bodies) - B
6	*S. cerevisiae – APR1*-His-Strep (cell lysate) – 48h post-induction

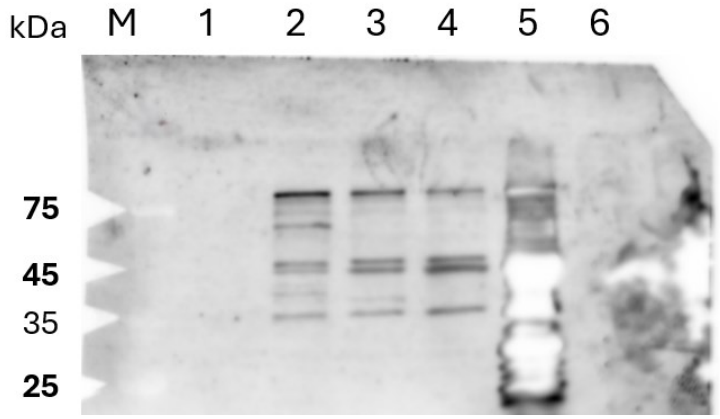

Figure 33: WB of selected samples containing Apr1p obtained either through prokaryotic or eukaryotic expression.

5.2. Phenotyping of gene-swapped strains

Phenotypic characterisation is essential for understanding the functional consequences of genetic manipulations. This chapter assessed the impact of swapping the orthologous aspartic protease genes, *PEP4* and *APR1*, between *Saccharomyces cerevisiae* and *Candida albicans*. By evaluating growth and stress tolerance under various environmental conditions, we aimed to elucidate the specific roles of these proteases in cellular physiology and adaptation. This comparative analysis provided insights into their functional conservation and potential divergence in cellular processes. Additionally, we examined growth on different carbon and nitrogen sources to understand how the protease swap impacted nutrient utilisation and metabolism. *Table 28* summarises the genotypes of deletion mutants used and the prepared new strains.

Table 28: Summary of the strains used in the gene-swap experiment.

Deletion and gene swap mutants			
Yeast	**Strain name**	**Genotype**	**Description**
S. cerevisiae	Y12098	BY4742; MATa; *ura3Δ0; leu2Δ0; his3Δ1; lys2Δ0; YPL154::kanMX4*	*Δpep4* strain
	Y12098-*APR1*	BY4742; MATa; *ura3Δ0; leu2Δ0; his3Δ1; lys2Δ0; YPL154::kanMX4*, pYEXTHS-BN-*APR1*	*S. cerevisiae* strain with *APR1* (instead of *PEP4*)
	Y12098-*PEP4*	BY4742; MATa; *ura3Δ0; leu2Δ0; his3Δ1; lys2Δ0; YPL154::kanMX4*, pYEXTHS-BN-*PEP4*	Revertant of *PEP4* gene (PC)
	Y12098-*URA3*	BY4742; MATa; *ura3Δ0; leu2Δ0; his3Δ1; lys2Δ0; YPL154::kanMX4,* pYEXTHS-BN	Negative control – pYEXTHS-BN
C. albicans	KC281	SN78; *APR1::HIS1/APR1::LEU2*	*Δapr1* strain
	KC281-*APR1*	SN78; *APR1::HIS1/APR1::LEU2, PEP4/RPS10, URA3/RSP10* CIp10-*APR1*	Revertant of *APR1* gene (PC)
	KC281-*PEP4*	SN78; *APR1::HIS1/APR1::LEU2, APR1/RPS10, URA3/RSP10* CIp10-PEP4	*C. albicans* strain with *PEP4* (instead of *APR1*)
	KC281-*URA3*	SN78; *APR1::HIS1/APR1::LEU2, URA3/RSP10* CIp10	Negative control – CIP10

5.2.1 Verification of the newly constructed strains – *C. albicans*

To verify the successful gene swap of our strains, we performed PCR analysis using diagnostic primers designed to amplify specific gene segments (*Table 29*). Each primer pair

targeted a region that was modified in the engineered strains. Plasmids used for transformation were prepared by Doc. RNDr. Olga Heidingsfeld, CSc. and Jakub Papík.

Table 29: List of diagnostic primers used in the gene-swap experiment.

Name	5'-3' sequence	Length [bp]	Annealing temp. [°C]	Product size [bp]
APR-diag-F-1	ATGTCTCATCACCATCACCATCAC	24	55.7	825
APR-diag-R-1A	GGAGGCATCGTAACCACCAA	20	53.8	
APR-diag-R-1B	GGTTGACCCGGTGTACCAAT	20	53.8	374
APR-diag-F-2	TAAGGCCCATAGCATCAAA	19	52.4	500
APR-diag-R-2	GGCCAGGAATAACCAAATC	19	54.5	
PEP-diag-F	ACGAATGTGGTTCCTTGGCT	20	57.3	612
PEP-diag-R	ATTGACCGGTCCAACCCTTC	20	59.4	
CA-URA-diag-F	AAATTGGGTCCTTATGTATGC	21	54	452
CA-URA-diag-R	AGCCAATCAAATCCTTCTTC	20	53.2	
SC-URA-diag-F	TTAGTTTTGCTGGCCGCATCTTCT	24	61	804
SC-URA-diag-R	ATGTCGAAAGCTACATATAAGGAACG	26	56	

To investigate the impact of gene replacement on *Candida albicans*, we utilised an *APR1*-deficient strain (*Δapr1*) *C. albicans* KC281. For transformation, we employed the CIp10 plasmid containing *APR1* or *PEP4* with their native promoters. This generated:

- *C. albicans* KC281-*APR1* (a revertant strain with *APR1* reintroduced)
- *C. albicans* KC281-*PEP4*, a gene-swapped mutant where *APR1* was replaced with PEP4
- *C. albicans* KC281-*URA3* served as a negative control, containing an empty vector that only reintroduced the *URA3* gene, which was used as a selection marker in the process

Table 30: Summary of C. albicans strains used during phenotypic testing. (1 - positive, 0 - negative)

Lane	Strain	*URA3*	*APR1*	*PEP4*
1	*C. albicans* – KC281 – *APR1*	1	1	0
4	*C. albicans* – KC281 – *PEP4*	1	0	1
9	*C. albicans* – KC281 – *URA3*	1	0	0

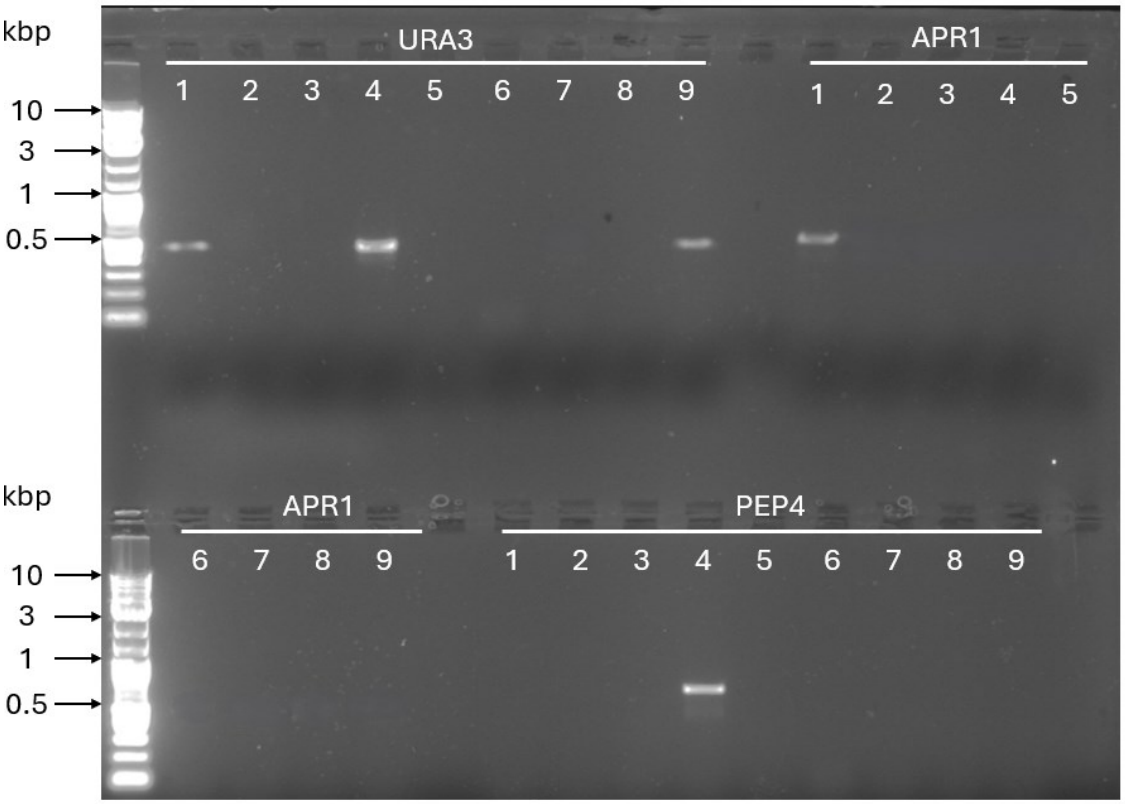

Figure 34: 1.2% agarose gel electrophoresis verification of Candida albicans strains used in phenotypic testing. Primers APR-diag-F-2 and APR-diag-R-2 were used for APR1 amplification. Lanes 1-9 represent different strains containing different plasmids. Genes (URA3, APR1, PEP4) noted above them represent which gene they were diagnosed for the presence of.

In *Figure 35,* using diagnostic primers and PCR allowed us to determine that *Lane 1* represents *C. albicans* – KC281 – APR1. *Lane 4* represents *C. albicans* – KC281 – *PEP4* and *Lane 9* represents *C. albicans* – KC281 – *URA3*.

5.2.2. Verification of newly constructed strains – *S. cerevisiae*

Like *C. albicans* strains, we utilised a *PEP4*-deficient strain (*Δpep4*) *S. cerevisiae* Y12098. For transformation, we again used an episomal plasmid pYEXTHS-BN containing *PEP4* or *APR1* with their native promoters, not *CUP1* promotor. This generated:

- *S. cerevisiae* Y12098-*PEP4* (a revertant strain with *PEP4* reintroduced)
- *S. cerevisiae* Y12098-*APR1*, a gene-swapped mutant where *PEP4* was replaced with *APR1*
- *S. cerevisiae* Y12098-*URA3*, again served as a negative control, containing an empty vector that reintroduced the *URA3* gene

Using protocol by Gietz et al. (2007) yielded high transformation rates, where usually two out of ten colonies were positive.

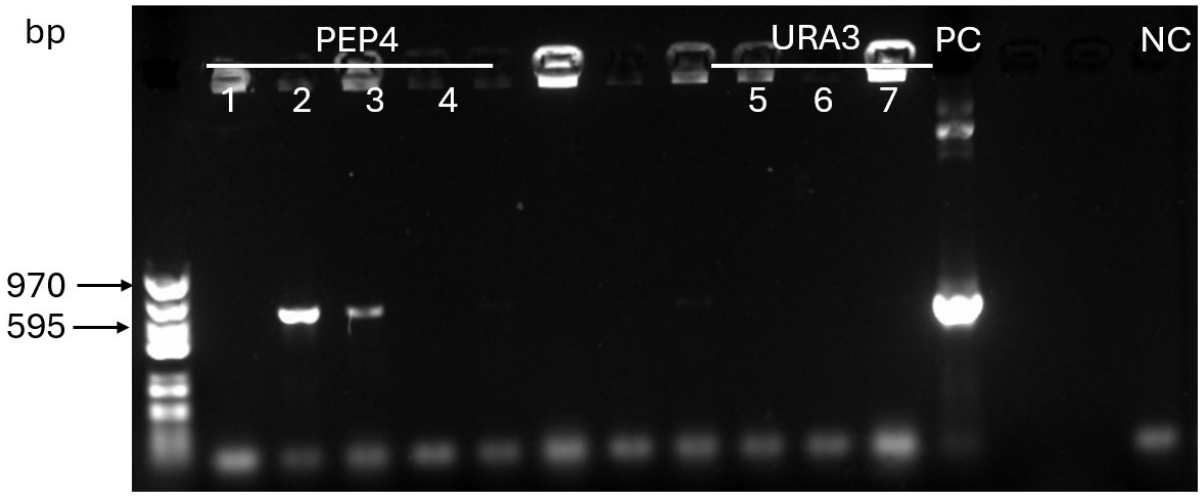

Figure 35: 1.2% agarose gel electrophoresis verification of S. cerevisiae strains used in phenotypic testing. PEP4 diagnostic primers were used to test for PEP4 transformation. Lanes 1-4 represent cells transformed using pYEXTHS-BN-PEP4. Lanes 5-7 represent cells transformed using pYEXTHS-BN-URA3.

Figure 36 demonstrated the successful transformation of *S. cerevisiae* Y12098, as indicated by the positive *PEP4* amplification in *Lanes 2* and *3*, yielding two *S. cerevisiae* Y12098-*PEP4* revertants. The absence of bands in *Lanes 5-7* confirmed the absence of *PEP4* amplification in the pYEXTHS-BN-*URA3* transformants, as expected for the negative control.

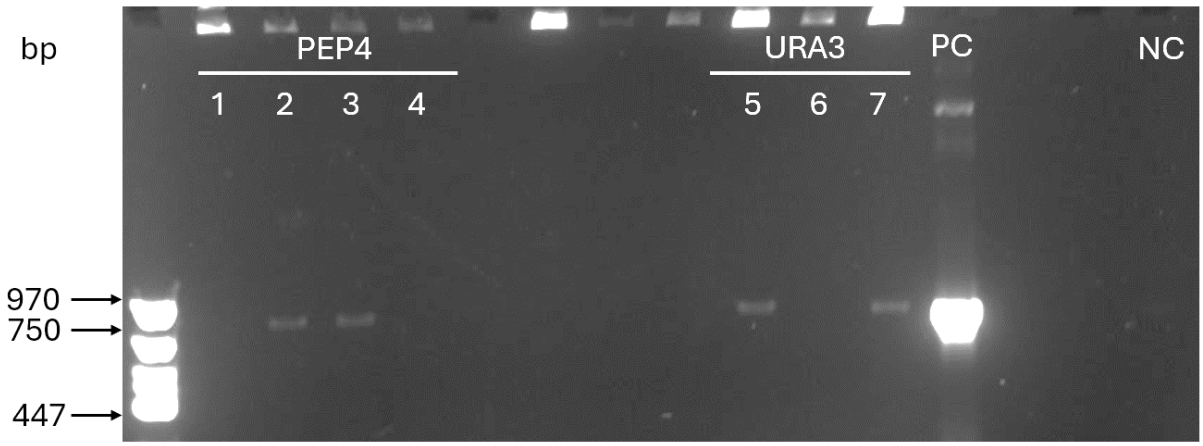

Figure 36: 1.2% agarose gel electrophoresis verification of S. cerevisiae strains used in phenotypic testing. S. cerevisiae URA3 diagnostic primers were used to test for URA3 transformation. Lanes 1-4 represent cells transformed using pYEXTHS-BN-PEP4. Lanes 5-7 represent cells transformed using pYEXTHS-BN-URA3.

Figure 37 confirms the correct transformation of both *PEP4* revertants (*S. cerevisiae* Y12098-*PEP4*) (*Figure 31*) since they also possess *URA3* gene. Additionally, *Figure 37* verifies the preparation of two transformants (*S. cerevisiae* Y12098-*URA3*) (*Lane 5, 7*). The *URA3* and *PEP4* transformations exhibited high success rates, with the first attempt proving successful. However, the same cannot be said for the insertion of APR1, which required three separate transformations to obtain the *S. cerevisiae* Y12098-*APR1* strain.

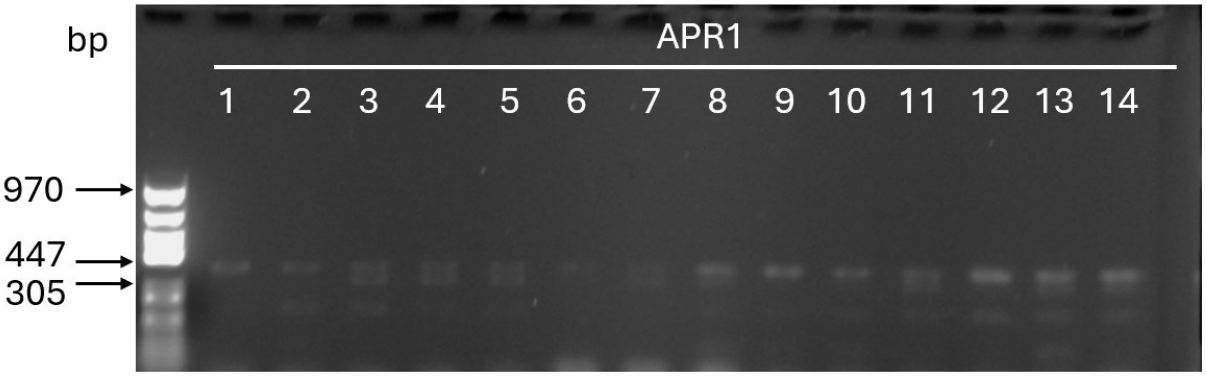

Figure 37: 1.2% agarose gel electrophoresis verification of S. cerevisiae strains used in phenotypic testing. APR1 diagnostic primers were used to test for APR1 transformation. Lanes 1-14 represent colonies tested after being transformed using pYEXTHS-BN-APR1. Negative control not shown, but no bands were observed.

While the high transformation rate was not unexpected (*Figure 38*), the consistent positivity across most lanes raised concerns. Therefore, we only tested a subset of the colonies for the presence of the *URA3* gene (*Figure 39*). Selected colonies (*Figure 39*) with matching numbers were tested using *S. cerevisiae URA3* diagnostic primers. This revealed that only

Lanes 12 and *14* contained the pYEXTHS-BN-*APR1* plasmid, yielding two *S. cerevisiae* Y12098-*APR1* transformants.

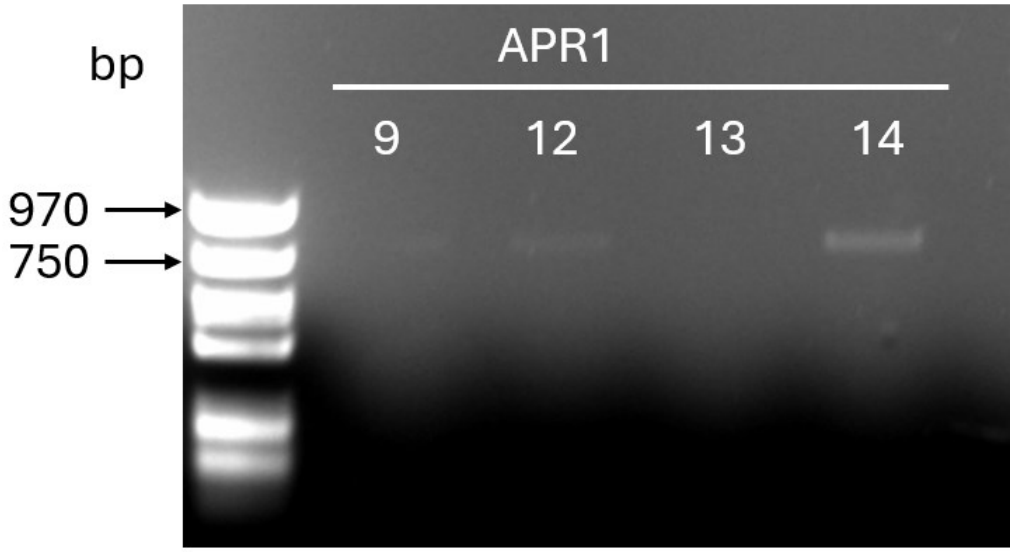

Figure 38: 1.2% agarose gel electrophoresis verification of S. cerevisiae strains used in phenotypic testing. S. cerevisiae URA3 diagnostic primers were used to test for APR1 transformation. Lanes 9, 12, 13, 14 represent the same colonies as in Figure 38. Negative control not shown, but no bands were observed.

Figures 30-34 illustrate the successful transformation of both *S. cerevisiae* and *C. albicans* strains.

5.2.3. Conditions used for phenotypic testing

The newly constructed gene-swapped strains of *S. cerevisiae* and *C. albicans* were subjected to phenotypic testing under various conditions. These included different temperatures, osmotic and oxidative stressors, and the utilisation of both simple and complex nitrogen sources, as well as various carbon sources. The comprehensive list of conditions used in this study is provided in *Table 31*. This approach allowed us to assess the phenotypic impact of replacing *APR1* with *PEP4* on the growth and stress response of these genetically modified strains.

Table 31: Summay of all the condition used for phenotypic testing.

Medium	Conditions	Purpose
YPD	-	Control
	30 °C	Temperature
	37 °C	
	40 °C	
	1 M NaCl	Osmotic stress
	1 M KCl	
	1.5 M Sorbitol	
	2 mM H2O2	Oxidative stress
	0.04% SDS	Membrane stress
	pH 4	Growth at different pH
	pH 6	
	pH 8	
	pH 10	
YNB (w/o AA, $(NH_4)_2SO_4$)	-	Control
	100 mM $(NH_4)_2SO_4$	Nitrogen limitation
	400 µM $(NH_4)_2SO_4$	
	100 mM Proline	
	400 µM Proline	
	100 mM Urea	
	400 µM Urea	
YNB (w/ AA, $(NH_4)_2SO_4$)	-	Control
	2% Glucose	Carbon limitation
	2% Glycerol	
	2% Lactate	
YCB	-	Control
	0.2% BSA	Complex nitrogen source

5.2.4. Phenotypic testing of gene-swapped strains - Photos

Figures 40-47 reveal that swapping the *PEP4* and *APR1* genes did not significantly impact the majority of phenotypic traits tested in *C. albicans* and *S. cerevisiae*. *S. cerevisiae* strains outperformed *C. albicans* under complete nitrogen starvation (*Figure 44*). *C. albicans* also showed reduced tolerance to oxidative and membrane stress induced by peroxide and detergent (*Figure 42*). As expected, each species displayed optimal growth at its respective temperature optimum (*Figure 40*). Notably, both species exhibited similar responses to osmotic stress (*Figure 41*) and varying pH conditions. Interestingly, *C. albicans* demonstrated greater versatility in carbon source utilisation, as *S. cerevisiae* was unable to grow on lactate.

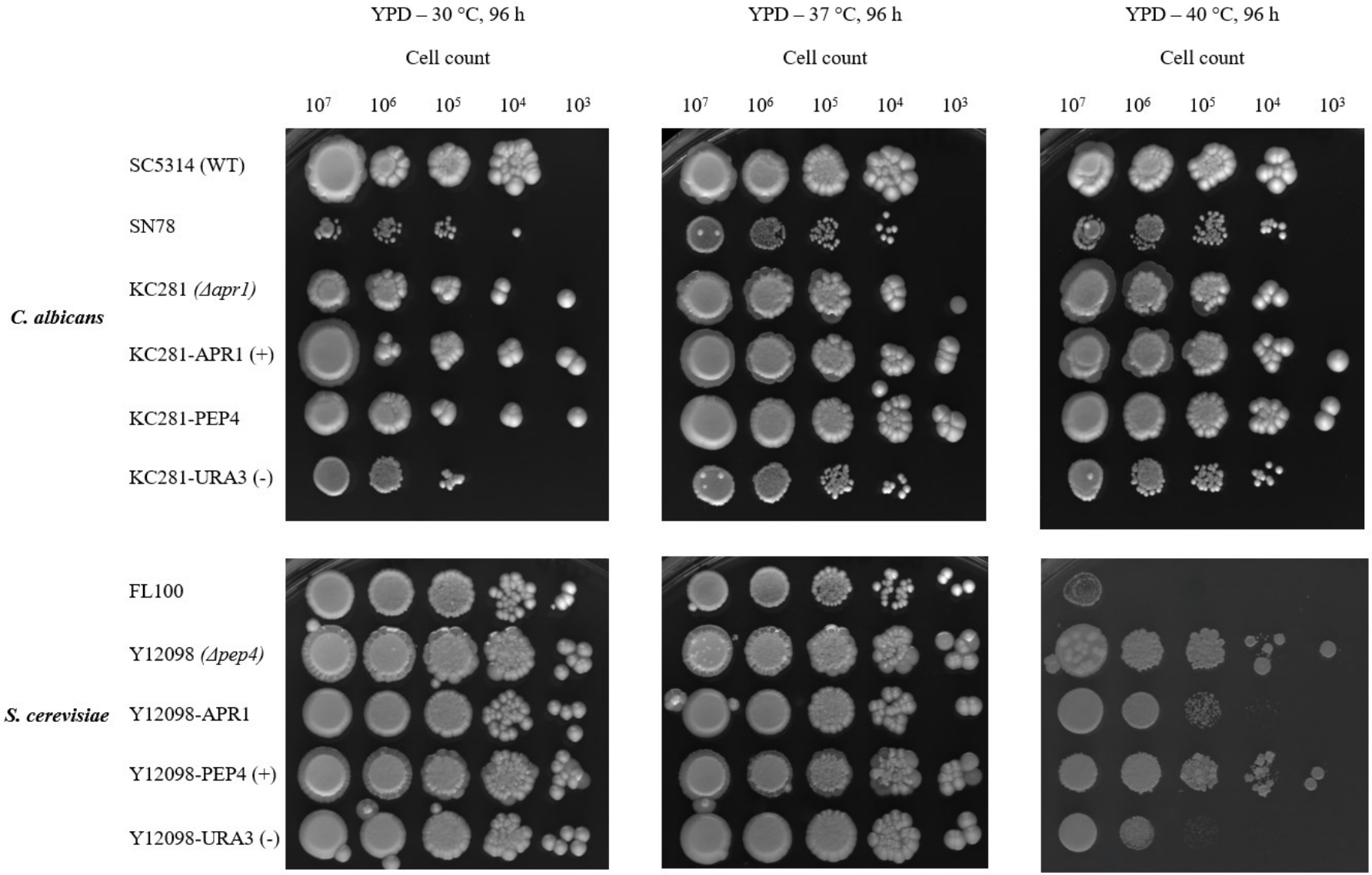

Figure 39: Growth of C. albicans and S. cerevisiae strains at 30 °C, 37 °C and 40 °C on YPD agar plates.

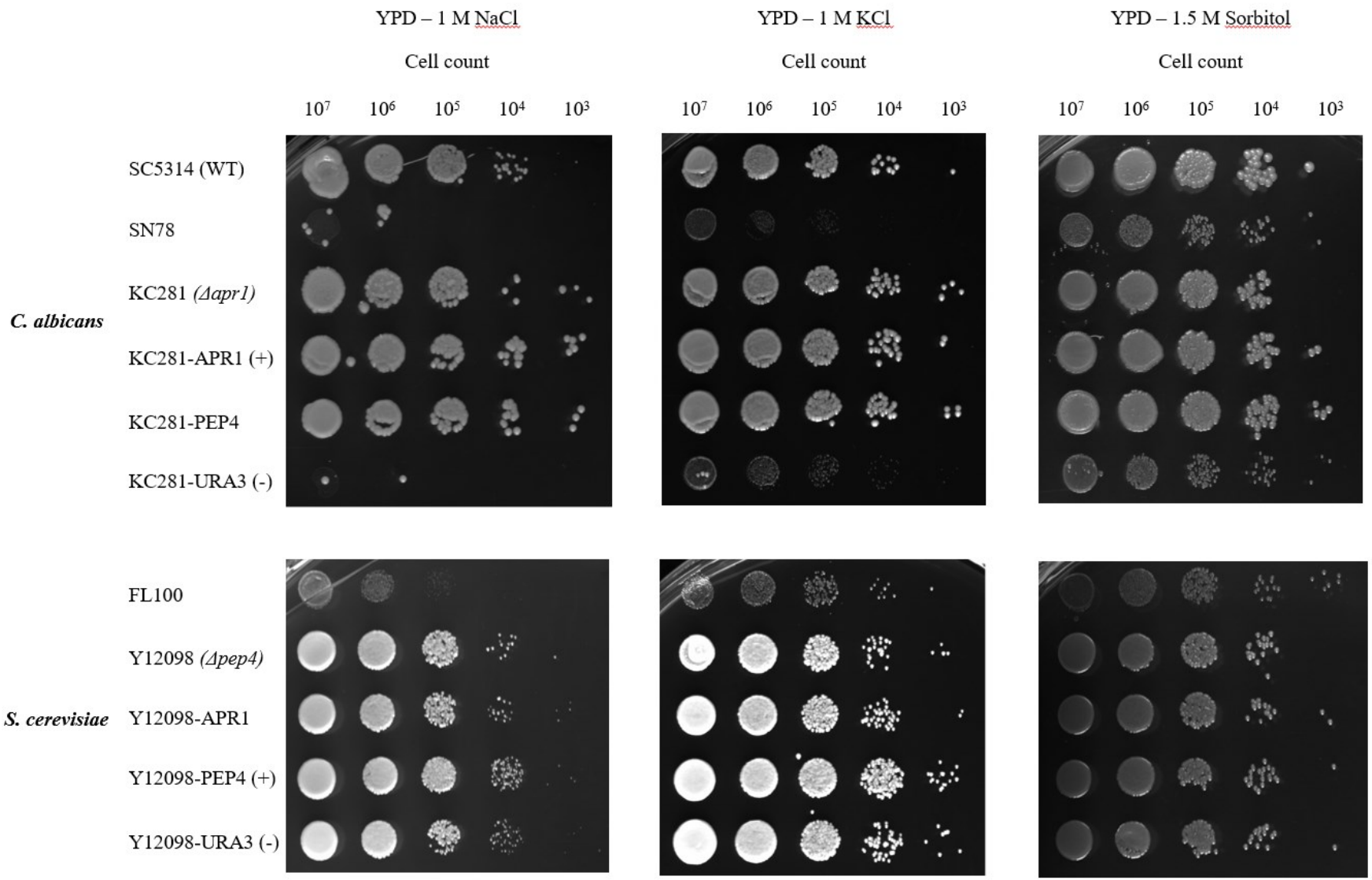

Figure 40: Growth of C. albicans and S. cerevisiae strains at 30 °C on YPD agar plates, where 1 M NaCl, 1 M KCl and 1.5 M Sorbitol simulate osmotic stress.

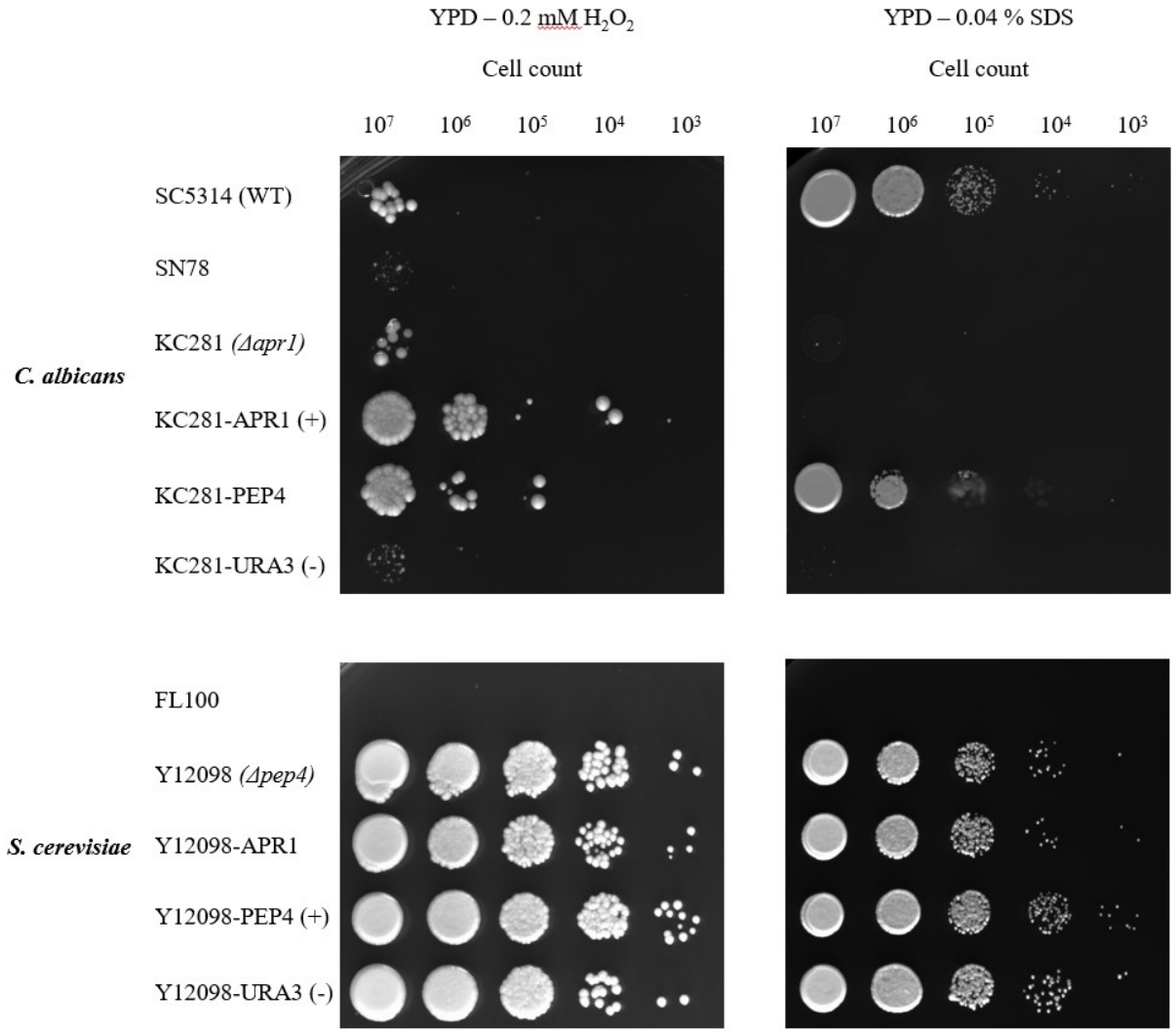

Figure 41: Growth of C. albicans and S. cerevisiae strains at 30 °C on YPD agar plates, where 2 mM H_2O_2 simulates oxidative stress and 0.04 % SDS simulates stress on the plasmatic membrane.

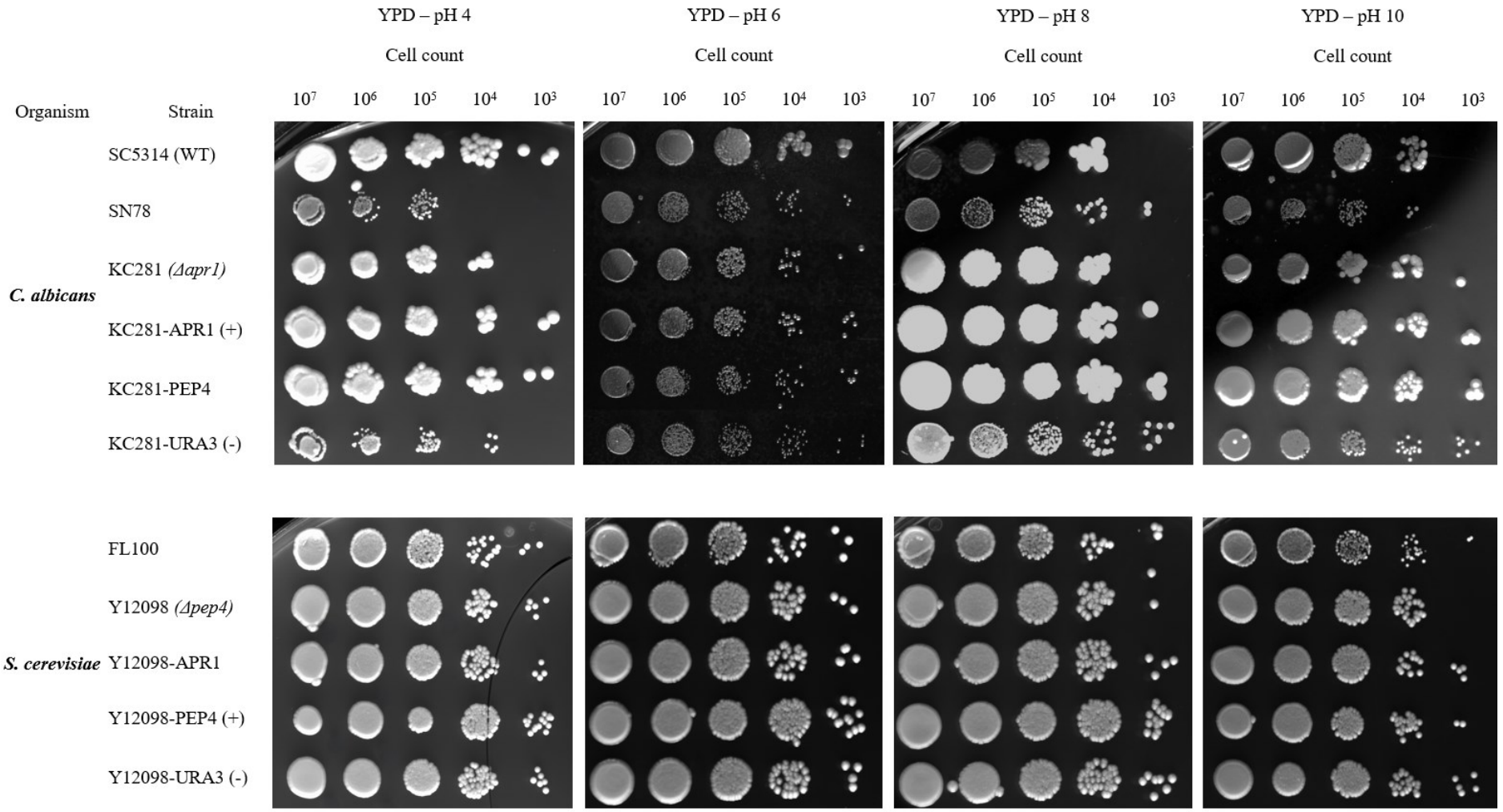

Figure 42: Growth of C. albicans and S. cerevisiae strains at 30 °C on YPD agar plates at different pH.

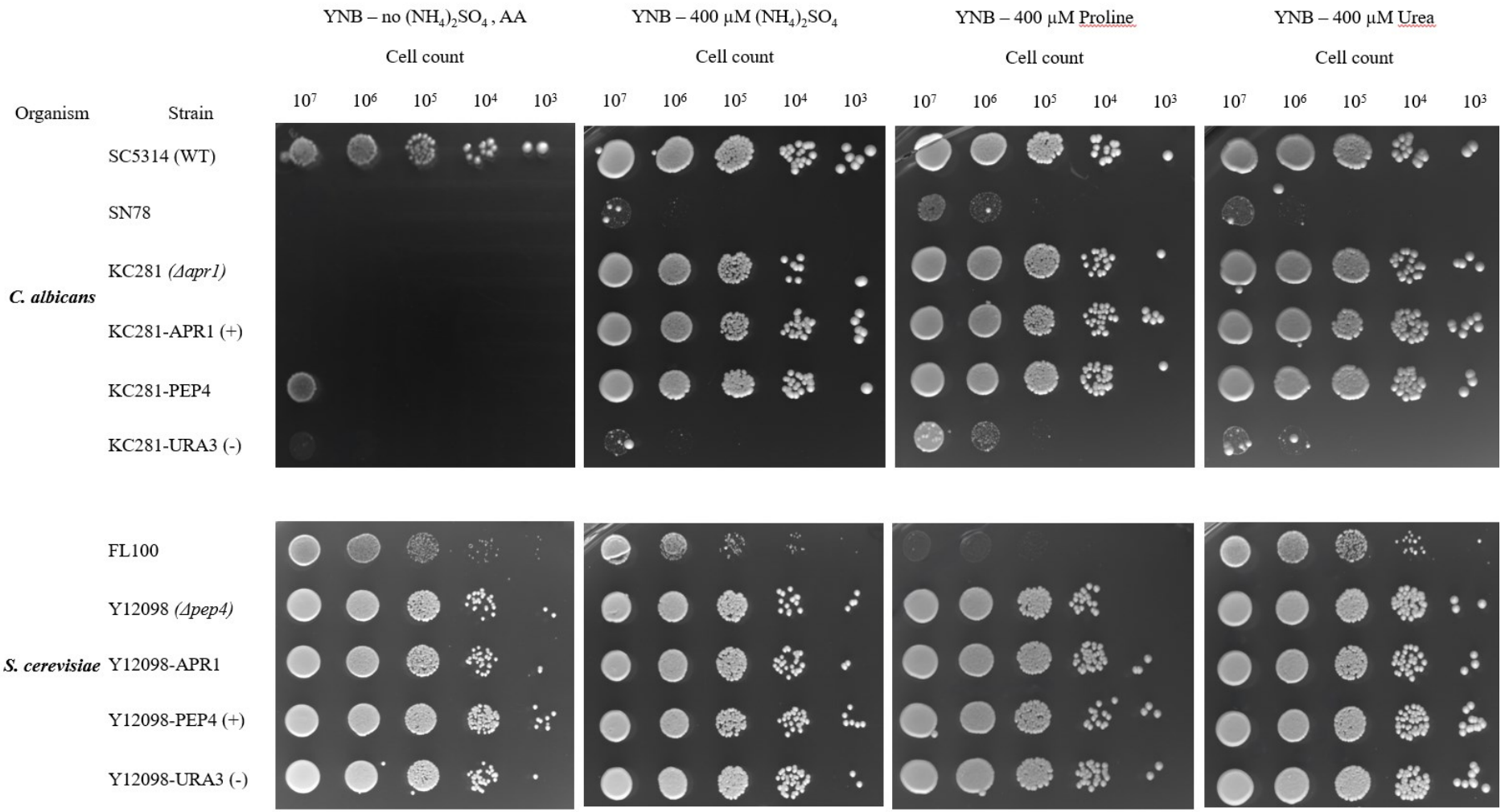

Figure 43: Growth of C. albicans and S. cerevisiae strains at 30 °C on YNB (without $(NH_4)_2SO_4$ and AA (only essential)) agar plates, to test nitrogen source utilisation.

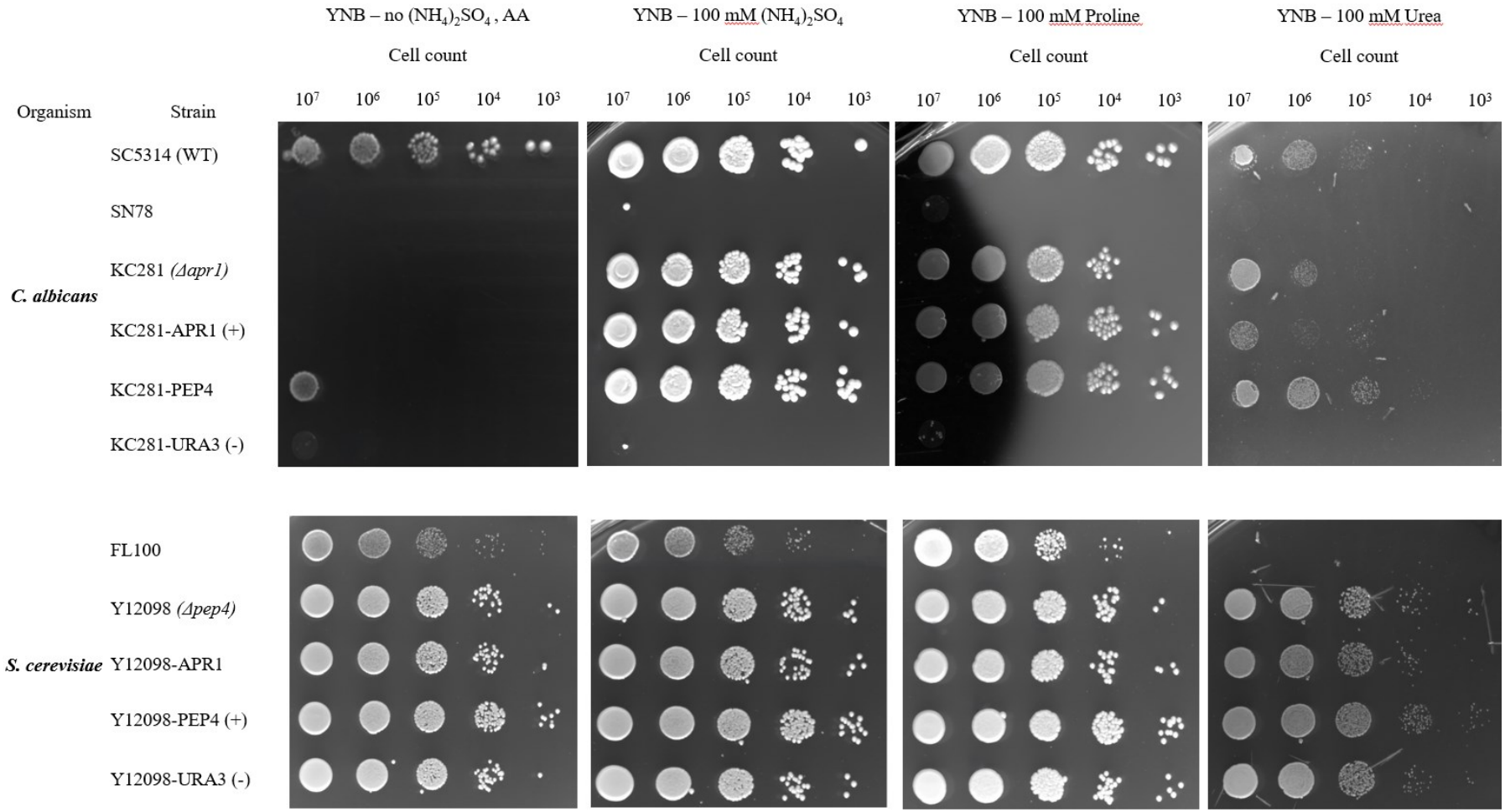

Figure 44:Growth of C. albicans and S. cerevisiae strains at 30 °C on YNB (without $(NH_4)_2SO_4$ and AA (only essential)) agar plates, to test nitrogen source utilisation.

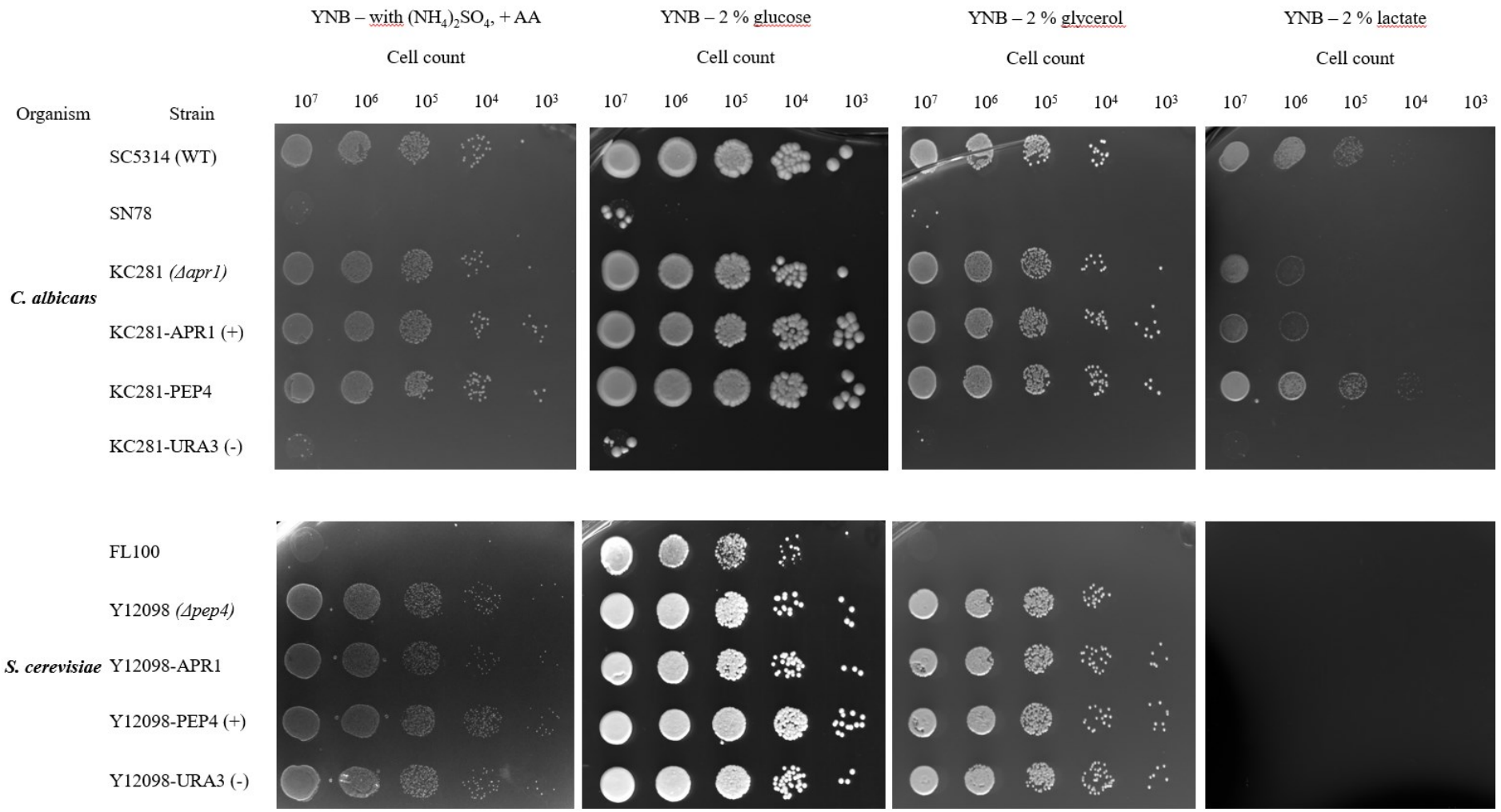

Figure 45: Growth of C. albicans and S. cerevisiae strains at 30 °C on YNB (with $(NH_4)_2SO_4$ and AA) agar plates, to test carbon source utilisation.

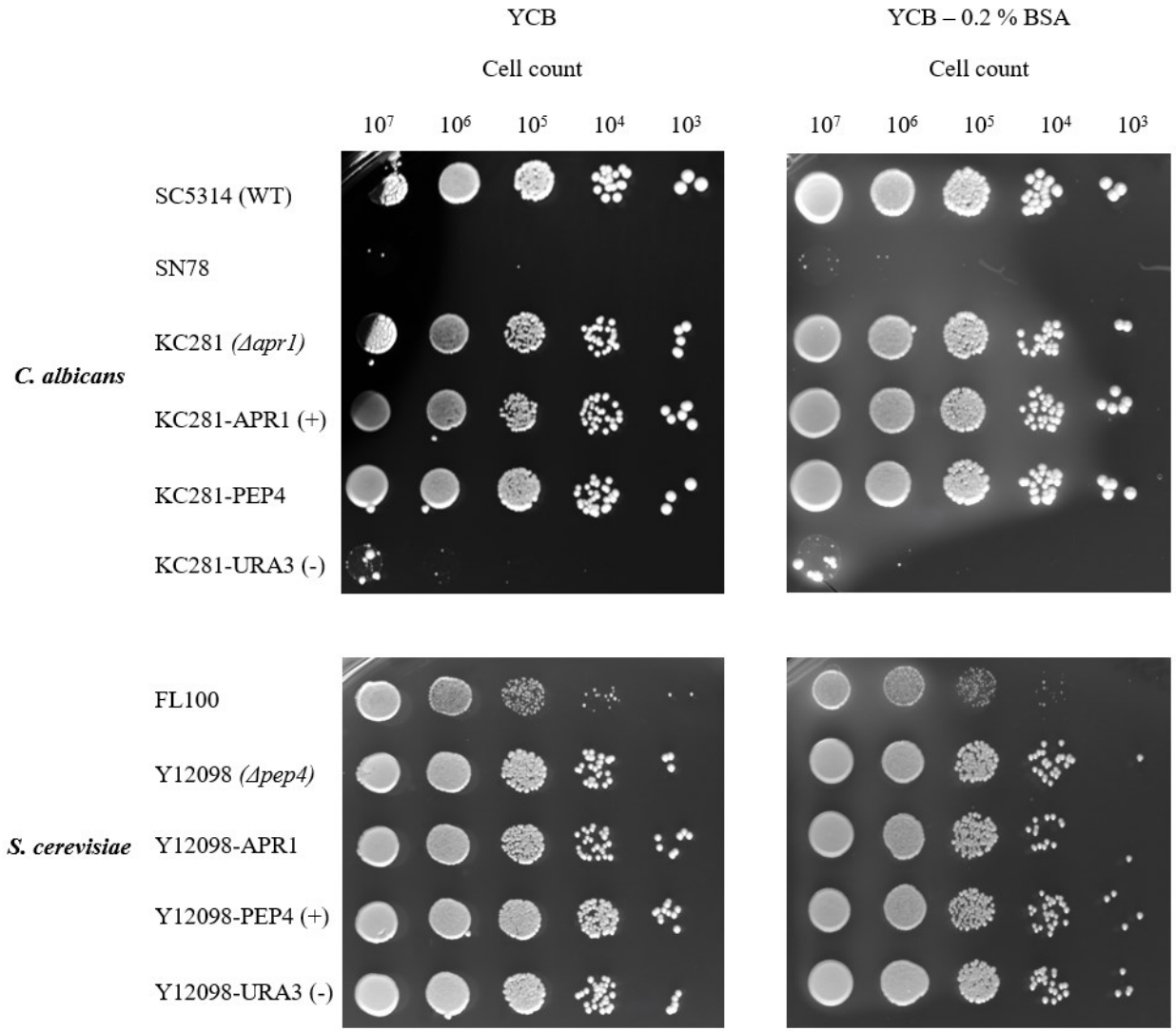

Figure 46: Growth of C. albicans and S. cerevisiae strains at 30 °C on YCB agar plates, to test complex nitrogen source utilisation.

6. Discussion

6.1. proApr1p expression in *E. coli*

6.1.1. *E. coli* – BL21(DE3) x LOBSTR

Prior to any work with Apr1p, we tested two available strains of *E. coli* – BL21(DE3) (*Figure 9*), which is the "golden standard" of recombinant protein production. It offers many advantages, like the lack of Lon and OmpT proteases, minimizing the proteolysis of target protein, and the use of T7 RNA polymerase under the influence of *lac* promoter, which has a high transcription rate, leading to high protein yields[65] *E. coli* LOBSTR (low-background strain) (*Figure 10*) is a derivative of BL21(DE3), engineered to minimize contamination when further purifying the protein using IMAC. LOBSTR strain lacks arnA and slyD, which have a high affinity for Ni-NTA resin, which leads to the minimization of contaminants when purifying a protein using this resin. Although it was not necessary to use the LOBSTR strain, we opted for its use due to minimal contamination of inclusion bodies (IB) as seen in *Figure 3*.[66]

Regarding induction length, we collected cells pre-induction (*Sample 1* in *Figure 9,10*) where some proApr1p expression is evident due to *lac* operon leakiness.[67] We also collected samples at 1, 2, 3 and 4.5 h post-induction, observing a steady increase of proApr1p up to 3 h timepoint, with minimal change afterwards. Therefore, we opted for 3 h of induction period to optimize yield and efficiency.

6.1.2. IMAC – Ni-NTA

While Ni-NTA affinity chromatography is a standard for purifying His-tagged recombinant proteins obtained from *E. coli* cell lysates, it can sometimes be contaminated by other proteins with affinity for metal ions. Due to proApr1p's 6×His Tag, we obtained substantially purified protein (*Figure 11, 12*), where only one band was observed. Although the use of Ni-NTA alleviated the problem with contamination of *E. coli* BL21(DE3) inclusion bodies (*Figure 11*), after considering the purity of IB produced in *E. coli* LOBSTR (*Figure 12*), we deemed this purification step unnecessary due to the high cost of the Ni-NTA resin and added labour. *Figures 11* and *12* illustrate significant protein loss, where much of the protein remained unbound or was bound too firmly to the resin (*Samples 7*). Therefore, we decided to proceed with unpurified IB from *E. coli* LOBSTR.

Our choice to induce the production at 37 °C promoted the formation of inclusion bodies, where target protein is highly concentrated; this reduced the need for extensive purification.

Multiple washing steps in our protocol, including urea in the wash buffer, effectively removed significant contaminants, and resulted in the observed high-purity inclusion bodies (*Figure 10, Sample 7*), which were used without further purification, potentially increasing the concentration of proApr1p in the samples.[68]

6.1.3. Solubilization of inclusion bodies

Solubilization of inclusion bodies is a crucial step for working with recombinant proteins due to their inherent misfolded and insoluble nature. To maximize proApr1p recovery, we investigated the influence of three solubilization buffers (*Table 10*). Standard solubilization buffers typically incorporate chaotropic agents like guanidium or urea as chaotropic agents to facilitate protein unfolding. While guanidinium is considered a more potent chaotropic agent, we used urea due to its affordability and milder denaturing properties.[69]

The presence of β-mercaptoethanol (β-ME) at a high concentration likely accelerated the solubilization process due to the presence of disulfide bridges. Notably, buffer B yielded minimal insoluble material after centrifugation, indicating efficient solubilization of the inclusion bodies, which was typically achieved within 45 minutes. This buffer also included EDTA to chelate metal ions and prevent unwanted protein-ion interaction that might otherwise promote the aggregation. Hence, why we decided to use buffer B for IBs solubilization.

6.1.4. Activation of proApr1p

In our experiment, dialysis was the primary method to obtain soluble Apr1p, a crucial step for its subsequent activation by other proteases or low pH, a common approach for aspartic proteases. Most of the protocols are based on the previously proposed *Protocol A*, to which changes were made. *Table 7* details the protocols, buffer compositions, and subjective observations of aggregation. This section will discuss the rationale behind each component's inclusion and, purpose.

6.1.5. Dialysis

All dialysis buffers contained 20-50 mM of a buffering system. Tris is commonly used due to its suitable pH range but raises concerns about potential interactions with the protein backbone. These interactions are unlikely to significantly disrupt protein folding and may instead promote a gradual folding process. Good's buffers (e.g., MES, HEPES) are generally preferred. When Tris was unsuitable due to pH constraints, citrate buffer was employed,

offering the additional advantage of being a kosmotrope, a molecule known to stabilize protein structures. [70–72]

Insufficient dialysis time can result in protein aggregation due to incomplete removal of the denaturant urea, underscoring the importance of step-wise dialysis, typically involving at least three steps.[73] In our experiments (*Table 7*), a critical urea concentration of approximately 2 M was observed, below which significant protein aggregation occurred across most protocols. While urea, a chaotropic agent, typically unfolds proteins, some proteins may retain activity at higher urea concentrations, although this rarely exceeds 1 M (in the absence of counteracting osmolytes)[74]. Therefore, soluble proApr1p at 2 M urea likely cannot be used in activation efforts. [75]

6.1.5.1. Arginine

As one of the early steps, we decided to include arginine (Arg) as a folding aid. Arginine is known to suppress protein aggregation and enhance protein solubility. While it shares a functional group with guanidine, arginine's carboxylic and amine group lead to weaker interactions with the protein, preventing denaturation and inhibiting aggregation. Arginine can also disrupt the formation of insoluble oligomers driven by hydrophobic interactions.[76] However, adding arginine to our dialysis buffers did not yield any noticeable improvement to the aggregation of proApr1p and did not contribute to its maturation since we primarily observed unchanged proApr1p (47 kDa) (*Figure 13*).

6.1.5.2. Rapid dilution

Rapid dilution, a faster alternative to dialysis for protein refolding, involves diluting the protein 100-1000-fold into a denaturant-free buffer, either in a single step or continuously. This process facilitates protein folding by allowing rapid diffusion of the denaturant away from the protein. To avoid aggregation, the recommended protein concentration for refolding using rapid dilution is 1-10 µg/ml. Despite adhering to this guideline and diluting our protein to 10 µg/ml, the excessive dilution resulted in complete protein loss (*Figure 15*) and unsuccessful proApr1p maturation.[77]

6.1.5.2. Polyphosphate (PolyPi)

The inclusion of polyphosphate was motivated by its presence within the vacuole and its potential role as an inorganic chaperone, facilitating protein folding. However, subsequent literature review revealed conflicting findings, with some studies suggesting polyphosphate can lower the solubility of positively charged proteins and promote aggregation (*Figure 13,*

Samples 4,5). Despite this, the prevailing view considers polyphosphate an aid in protein folding and stress response. Given its potential to neutralize long-distance interactions between positively charged ions, favouring short-range interactions within the protein, and its presence in the vacuole, we decided to incorporate polyphosphate in most of our protocols.[78–80]

6.1.5.3. Glycerol

Our protocols also used glycerol to aid in protein folding of Apr1p. Glycerol is a known cryoprotectant and is also used in protein folding – this is achieved by interaction with hydrophobic regions, limiting their interaction with the aqueous phase and thus limiting aggregation.[81]

6.1.5.4. Tween 20

Tween 20, a non-ionic detergent, can interact with proteins via hydrophobic interactions using its long alkyl chain. While it has some potential to contribute to protein denaturation, this interaction could also potentially assist in the folding process of Apr1p by stabilizing hydrophobic regions.[82]

6.1.5.5. Salts

Salts like, sodium chloride in our case can assist in protein folding through non-specific electrostatic interactions. This promotes the solubility of aggregates with the aqueous phase. However, it is crucial to be mindful of the salting-out effect when using salts like ammonium sulphate, which can again lead to aggregation. In our case, addition of salt did not improve on proApr1p solubility (*Figure 20, 21*).[83]

6.1.5.6. Sodium acetate and pro-cathepsin-like activation

Aspartic proteases, including the Pep4p orthologue, are typically synthesized as inactive zymogens and require activation at their site of action. This activation often involves either the action of other enzymes or exposure to a low pH environment, as exemplified by the final activation of Pep4p within the mildly acidic vacuoles.

Based on this principle, we attempted to activate proApr1p using a sodium acetate solution with a pH of 4 (*Figure 20, 21*) (Protocol F, G). This approach, mimicking the acidic

conditions necessary for aspartic protease activation, is commonly employed in other protocols. We adapted a protocol from Sojka et al. (2012), which utilized similar conditions, but incorporated the use of sodium chloride. We also further modified it with the addition of polyphosphate. [84,85] In addition protocols F and G (*Table 7*), we implemented shorter dialysis steps to minimize aggregate formation. However, this modification resulted in substantial precipitation, potentially due to pH fluctuations, as similar observations were made under lower overall dialysis pH conditions. Additionally, conducting this step at 37 °C may have contributed to protein loss, as evidenced by the extensive degradation of proApr1p observed upon overnight exposure to this temperature (*Sample 2, Figure 20*).

6.1.6. Alternative ways to activate proApr1p

Given the limited success with folding enhancers and aggregation suppressors, we explored an alternative way to obtain a mature Apr1p while investigating its potential for a multi-step activation cascade similar to Pep4p. We pursued two approaches – vacuole isolation and application of cell lysate. Isolated vacuoles would allow us to determine if vacuolar enzymes alone are sufficient for proApr1p maturation while using cell lysates would explore the possibility of obtaining mature Apr1p through the action of other cellular enzymes.

6.1.6.1 Vacuoles

We initially opted for isolated vacuoles as a potential source of both the native protease and the enzymes required for proApr1's activation. However, we have observed that lyophilized vacuoles resuspended in water yielded insoluble organelles, a phenomenon also observed in other proteins after being lyophilized.[86] This was evident in protocols H and I (*Figure 16, 17, 18*). To avoid misinterpretation, vacuoles were also isolated from *C. albicans* KC281 (*Δapr1*). However, this deletion mutant exhibited significantly slower growth and resulted in a poor yield of vacuoles compared to *C. albicans* HE169 (wild type vacuoles).

Figure 18 reveals that co-dialysis of vacuoles with proApr1p resulted in additional bands, indicating that a solubilization step (e.g., inclusion in the dialysis process) is necessary for vacuoles and their enzymes, hinting that simple reconstitution in water yielded non-soluble vacuoles, incapable of activating proApr1p. Samples after co-dialysis were subsequently analysed using BSA cleaving assay (*Figure 19*), but again no proteolytic activity was observed. We hypothesize that urea, while effective in dissolving vacuoles, it also caused their denaturation, thereby eliminating their potential to activate proApr1p. Therefore, the necessity of vacuolar enzymes for Apr1p activation remains unclear.

6.1.6.2. Cell lysate

Crude cell lysates derived from *C. albicans* KC281 (*Δapr1*) and *S. cerevisiae* Y12098 (*Δpep4*) were employed to investigate the potential role of cellular enzymes in proApr1p maturation (*Figure 22, 23*). The use of these specific deletion mutants aimed to mitigate the presence of authentic Apr1p and Pep4p, respectively. In contrast to the cleavage assays, serine and metalloproteases were not inhibited in this experiment, as Pep4p activation involves Proteinase B, a serine protease, and its inhibition could hinder the process. Additionally, each lysate was syringe filtered through a 0.45 μm membrane to reduce potential nucleation sites for aggregation.

Theoretically, cell lysates should contain all the necessary components for successful proApr1p activation. However, this approach did not yield successful cleavage of proApr1p propart, despite the expectation that the lysates would provide the required enzymatic machinery. Addition of cell lysate also introduced extra complexity due to the numerous protein bands observed in *Figure 22* (*Samples 5, 6*). The scarcity of literature on using cell lysates for enzyme activation, with most studies focusing on inhibition, likely stems from the inherent complexity of cell lysates, which hinders analysis.

6.1.7. BSA cleaving in acidic pH

Many of the samples obtained during the proApr1p activation protocol have been subjected to BSA cleaving assay as a simple approach to test for any proteolytic activity. Most of these were carried out at pH ranging from 3 to 5, mimicking the acidic environment of the vacuole. Therefore, we wanted to see if BSA undergoes any intrinsic cleaving when exposed to low pH and increased temperature for a prolonged period. BSA exhibits the highest stability at pH 7, while acidic conditions promote its spontaneous degradation, which would explain bands of smaller molecular weights found in the BSA cleaving samples (e.g. *Figure 19*).[87]

Figure 23 integrated multiple approaches to assess the interaction of Het1p and proApr1p, including the use of cell lysate for protein maturation. Similar to *Figure 22,* addition of Het1p generated a complex protein mixture that hindered the analysis of potential changes in proApr1p's molecular weight (*Sample 3, 4, 7, 8*). *Sample 2* demonstrated that dialysis at a low pH does not always induce full protein aggregation and reveals a novel protein band below 35

kDa. This protein was then analysed using Edman degradation and revealed a potential processing of proApr1p (*Figure 23*). However, the protein band observed in *Figure 23, Sample 2*, did not correspond to the molecular weight of mature Apr1p (36 kDa), suggesting that it was not Apr1p.

We successfully obtained proApr1p but encountered challenges in achieving a soluble form suitable for activation due to a critical urea concentration that could interfered with subsequent steps, such as activation with vacuolar proteins. Our primary objective is to obtain mature Apr1p, lacking the propart. In some aspartic proteases, low pH or other proteins can facilitate this processing. We explored a range of conditions including low pH, inorganic folding aids, and other additives to promote proApr1p maturation, but these approaches did not yield active Apr1p.

Given these limitations, we shifted focus towards utilizing vacuoles or cell lysates to facilitate activation of partially purified proApr1p. Vacuoles and cell lysates represent complex mixtures of proteins and compounds that could potentially contain the necessary components for proApr1p activation, as they are responsible for in vivo activation. Therefore, we believe that our efforts should prioritize these biological approaches over further exploration of inorganic additives to achieve our goal of obtaining mature Apr1p.

6.2. proApr1p expression in *S. cerevisiae*

Given the difficulties encountered in obtaining active proApr1p using *E. coli*, we transitioned to a eukaryotic expression system – *S. cerevisiae* - *APR1*-His-Strep. Recombinant yeast expression offered advantages over prokaryotic expression, including the ability to perform posttranslational modifications like glycosylation and disulfide bond formation, both of which are predicted for Apr1p based on homology to Pep4p and sequence analysis. Furthermore, the high homology between Apr1p and Pep4p, along with their shared vacuolar localization, increased the likelihood of correct processing and activation of Apr1p in the yeast system. This shift in expression strategy aimed to overcome the limitations faced in the *E. coli* system.

Our construct employs the inducible promotor *CUP1*, a metallothionein gene controlling the expression of a gene introduced into the multiple cloning sites between *BamH*I and *Not*I nuclease sites. The main advantage of this vector is the resulting double-tagged protein where

6×His tag is introduced to the N-terminus and StrepII tag, an octapeptide with high streptavidin affinity. The main advantages of a StrepII tag are the reversible binding, mild purifying conditions and the absence of metal ions, which could sometimes be problematic in biological system.[88,89]

6.2.1. Growth curve

Before protein purification, we prepared a growth curve (*Figure 26*) of *S. cerevisiae*-APR1-His-Strep under expression conditions. As discussed, expression is controlled by an inducible promotor, *CUP1*. *S. cerevisiae* Y12098 (*Δpep4*) was not shown due to their overall slow growth.

S. cerevisiae-APR1-His-Strep, reached an early exponential phase after 10 h post-inoculation and induction and reached its stationary phase after 26 h ($OD_{600} \approx 16$). Subsequently, OD_{600} remained relatively constant until cell harvest. This growth closely resembled its parental strain, *S. cerevisiae* – BY4742, which enters the early exponential phase after 9 h and reaches its stationary phase after 24 h. The slight delay in *S. cerevisiae*-APR1-His-Strep might be attributed to induced protein production and potential stress due to 200 µM Cu^{2+}.[90]

6.2.2. Purification of Apr1p-His-Strep

Expression of Apr1p in *S. cerevisiae*-APR1-His-Strep aimed to facilitate purification via Ni--TA IMAC. However, no binding of the target protein to the Ni-NTA beads was observed (*Figure 27*), despite the presence of a 36 kDa protein band in the cell lysate (*Sample 1*), consistent with the molecular weight of mature Apr1p. The lack of affinity to the resin suggested cleaving of the His-tag and the pro-region necessary for Apr1p activation, characteristic of aspartic protease zymogen activation. This however precluded the use of anti-His tag antibodies for proApr1p detection.

Given the unavailability of IMAC, size-exclusion chromatography (SEC) was employed to preserve biological activity. Figure 28 presents a chromatogram from our SEC experiment. Fractions 98, 138, and 178 minutes were collected and assessed for proteolytic activity using MS. However, no cleavage of peptide 2 (*Table 4*) was observed. While purification could be enhanced by using a smaller porosity resin (e.g., Sephadex G-75), the unsuccessful purification was primarily attributed to the small scale of the experiment, leading to dilution-related loss of Apr1p.

For a more controlled and efficient purification, we explored five different ion-exchange resins at various pH levels, maintaining acidic conditions for Apr1p activity and neutral conditions for overall stability. DEAE Sephadex A-50 (*Figure 29*), a weak anion exchanger with a high binding capacity below pH 9, appeared promising for purifying proteins above 30 kDa.[91] *Figure 29* initially suggested successful Apr1p purification based on the molecular weight. This was, however, disproved since MS analysis of this protein revealed that it was a glyceraldehyde-3-phosphate dehydrogenase with a molecular weight of 36 kDa. The abundance of this protein was due to the constitutive expression of glycolytic enzymes and its overexpression in glucose-starved cells during the stationary phase.[92]

Research also suggests that strong induction of recombinant protein production in *S. cerevisiae* represses the expression of its own energy-intensive proteins, potentially involved in the processing of Apr1p itself. This then leads to the formation of protein aggregates within the cell, which are then rapidly degraded by ERAD (ER-associated protein degradation). Consequently, overloading the folding and processing machinery of *S. cerevisiae* leads to increased cellular stress, suggesting potential optimization of Apr1p expression.[93]

Studies show that deleting proteases in *S. cerevisiae* can significantly improve recombinant protein production. *PEP4, PRB1, CPY*, and multiple yapsin proteases are significant contributors to intracellular protein degradation. Yapsin proteins are membrane-bound and have a neutral to basic pH optimum, rendering them inactive at the acidic pH (pH 5 or 4) typically used during protein isolation. Additionally, the removal of cellular debris, including membranes containing yapsins, further reduces their degradative effects.[94–96] Additionally, studies also show that deletion mutants with impaired vacuolar trafficking improve the amount of protein produced and secreted since it does not undergo vacuolar degradation. However, the case of Apr1p is more complex, where trafficking to the vacuole can lead to activation and degradation.[97]

6.2.3. Proteolytic activity assays

Besides BSA, we employed peptides listed in *Table 4*, which are commonly used to study the proteolytic activity of aspartic proteases. The principle involves measuring a decrease in A_{300} caused by the delocalization of π-electrons within aromatic rings as the peptide is cleaved. While some peptides showed the expected trend in A_{300} decrease (*Figures 30*), this approach has significant limitations. Changes in absorbance can be caused by factors other than

proteolysis, such as protein aggregation, impacting the reliability of results. This approach worked well on peptides 1 and 2 but brought very stochastic results without any evident trend in other peptides (not shown). To minimize the confounding effects of other proteases, we conducted assays at low pH and included serine and metalloprotease inhibitors. Additionally, we filtered cell lysates using 0.45 μm syringe filters to reduce potential protein aggregation.

Mass spectrometry (MS) provided more definitive insights into peptide cleavage. MS analysis confirmed that peptide 1 was cleaved at the expected site (between phenylalanines), demonstrating proteolytic activity within the cell lysate. Moreover, the increase in cleavage products over time (*Figure 32*) suggests the involvement of an aspartic protease, consistent with the use of a low pH assay and the inclusion of serine and metalloprotease inhibitors.

6.2.4. Western blots

Immunodetection of cell lysates from *S. cerevisiae*-APR1-His-Strep, fractionated using DEAE Sephadex A-50, was performed with anti-Apr1p antibodies. *Figure 33* shows faint signals, including one consistent with the molecular weight of immature proApr1p in Sample 4, based on molecular weight would represent an immature proApr1p. A signal with a higher molecular weight in *Sample 8* could represent mature Apr1p based on its molecular weight. However, the specificity of these antibodies is still in question. This is also highlighted in *Figure 34,* where *Samples 2-4* contain multiple positive signals even at higher molecular weights. This could be potentially linked to high protein concentration, leading to non-specific binding (as seen in *Sample 5*).

Overall, the expression of Apr1p in *S. cerevisiae* yielded promising results. We observed specific peptide cleavage activity under conditions that favour aspartic proteases while inhibiting most other protease classes. This strongly suggests successful production and activity of Apr1p. We propose that scaling up the expression and purification process is key to obtaining sufficient quantities of active Apr1p for further characterization and investigation.

6.3. Gene-swap

While orthologous genes are often assumed to perform equivalent functions, this does not always have to be true. We investigated this by swapping the *PEP4* and *APR1* orthologues and observed how it affected physiology of the resulting strains. Vectors designed by Jakub Papík contain either of the genes with their own promotor – for *C. albicans,* integrative CIp10

plasmid was used and for *S. cerevisiae* episomal pYEXTHS-BN plasmid. It is essential to talk about the difference between them where pYEXTHS-BN is an episomal plasmid, which means that it does not integrate into the genome and is similar to a bacterial plasmid. However, CIp10 integrates into the genome of *C. albicans* using homologous recombination and is more stable than episomal plasmids. On the other hand, pYEXTHS-BN is based on 2μ plasmids associated with a large number of copies and robust expression of the inserted gene.[98]

S. cerevisiae strain FL100 is haploid with a duplicated 80 kb section of its chromosome III and an absent 45 kb section of its chromosome I, with uracil auxotrophy.[99] *C. albicans* SN78 is a histidine and leucine auxotroph and retains its virulence. Due to their autotrophies and compromised genomes FL100 and SN78, usually performed poorly in the phenotypic testing.

6.3.1. Temperature

We assessed the temperature tolerance of our strains on nutrient-rich YPD media, where they performed similarly when growing at 30 and 37 °C; however, *S. cerevisiae* growth was negatively impacted at 40 °C, reflecting its temperature optimum of 30 °C[100] Surprisingly, the *S. cerevisiae* revertant strain did not demonstrate improved thermotolerance as compared to the deletion mutant, contrary to previous reports.[101] On the other hand, *C. albicans* performed better at 37 and 40 °C and again reflected its higher temperature optimum and relevance to pathogenesis.[102] Research also suggests that *PEP4* is induced by increased temperature; however, both revertant and deletion mutants of *PEP4* performed similarly at 40°C.[103]

6.3.2. Osmotic stress

We assessed the osmotic stress tolerance of our strains using 1 M NaCl, 1 M KCl, and 1.5 M sorbitol. Both *C. albicans* and *S. cerevisiae* rely on the HOG pathway (high-osmolarity glycerol) to respond to osmotic challenges. This pathway triggers adaptation mechanisms like cell cycle arrest and a switch to glycerol synthesis for osmoprotection. In *S. cerevisiae*, HOG signalling has one primary function.[104] In *C. albicans*, it also plays a role in pathogenesis, such as the formation of biofilms or morphological switching, and is expressed under oxidative stress. Deletion mutants of *HOG1* are highly susceptible to oxidative stress. In both organisms, this response is mediated by the MAPK pathway.

Sorbitol, compared to NaCl and KCl, is a weaker osmolyte and other triggers transcription of different genes when compared to NaCl.[105] Notably, both *C. albicans* and *S. cerevisiae* strains displayed similar responses to osmotic stress. However, the reason behind the poorer performance of *C. albicans* KC281-URA3 (strain with inserted plasmid) compared to the control strain (KC281) remains unclear.

6.3.3. Oxidative and membrane stress

Seemingly *C. albicans* performed much poorly when exposed to oxidative and membrane stress. However, the agar plates used for *S. cerevisiae* were used later therefore we suspect that H_2O_2 decomposed and SDS crystalized, potentially affecting the experiment. This is also supported by a genome-wide study showing that 0.03% SDS upregulates nearly 300 genes and downregulates more than 100. These genes are involved in metabolism, cell cycle and other metabolic functions. Moreover, SDS also significantly affected mutants with impaired cellular trafficking (*VMA* genes responsible for vacuolar acidification). Additionally, *VMA* mutants showed severe growth defects under oxidative stress. Due to the well-explored nature of how SDS affects gene expression in *S. cerevisiae,* we can assume our observations to be incorrect since studies also suggest decreased tolerance to oxidative stress.[106,107]

In *C. albicans*, exposure to SDS triggers cell wall remodelling and increased transcription of *CWT1*, a transcription factor also involved in nitrosative stress response. This remodelling consists of a decrease in β-glucans and an increase in mannan levels, leading to increased membrane stress resistance. We hypothesize that low viability under oxidative stress stems from the inability to utilize vacuolar proteases correctly to recycle proteins and produce proteins needed for cell wall remodelling.[108]

6.3.4. pH

Yeast metabolism works with immense amounts of protein-generative processes like fermentation and respiration; therefore, it was also important to look at how the gene-swapped strains perform under different pH conditions. The pH homeostasis is tightly regulated through the interplay of V-type (vacuolar) and P-type ATPases, which are direct orthologues in both organisms. In our case, the V-ATPases should be directly linked to the activation of associated vacuolar enzymes due to their acidification of the vacuolar lumen. Research suggests that both of these ATP-ases are interconnected.[109] However, in our case, it seems that both *C. albicans* and *S. cerevisiae* were not drastically influenced by the extracellular pH, besides the slightly hampered growth at pH 10, which is expected as both organisms are

considered more acidophilic. Additionally, both organisms are excellent at manipulating the pH. In *C. albicans,* this is highlighted by the ability to colonize diverse host environments, and in *S. cerevisiae*, it is exhibited by its adaptability during fermentative processes and tolerance to organic acids.[109–111] However, since these strains were grown on a nutrient-rich YPD, the interplay of vacuolar acidification related to enzyme activation and extracellular pH might not have been highlighted.

6.3.5. Nitrogen acquisition and utilization

As nitrogen is the fundamental building block of all living organisms, its presence is a common limiting factor of growth in any organism. Yeasts are generally very well equipped for the utilization of many sources of nitrogen. We opted to test three nitrogen substrates from the most available form in ammonium sulphate, less preferred nitrogen sources like urea and proline.

The assimilation of ammonium sulphate is facilitated by ammonium permeases (*MEP1,2,3*), but to make it biochemically available, it still has to be transaminated and form glutamate or glutamine through (*GDH1, GDH3, GLN1*)[112]

Since budding yeast lack urease, urea is assimilated using urea carboxylase (*DUR1,2*), an ATP-dependent enzyme with a biotin cofactor. Budding yeast converts urea to allophanate, which is a carboxylate form of urea, which is then hydrolyzed by allophanate hydrolase, forming two molecules of ammonia and carbon dioxide.[112]

Assimilation of proline shares a metabolic pathway with other amino acids like arginine and ornithine. In this pathway, arginine is converted to proline, which undergoes oxidation (*PUT1*) and dehydrogenation (*PUT2*) and is subsequently converted to glutamate. Although this process requires no direct ATP, it still requires three reduction equivalents.[112]

Many enzymes involved in nitrogen assimilation are orthologous; therefore, the gene-swap of proteases, responsible for the degradation of complex nitrogen sources than we used, has minimal effect on these organisms. However, it is interesting that *S. cerevisiae* was able to grow comparably to other nitrogen sources when not supplemented by any nitrogen source. We hypothesize that due to the nature of the plasmids and the large number of its copies containing genes for the selection markers, *S. cerevisiae* is able to metabolize and assimilate the amino acids provided for auxotrophic strains more efficiently. We also hypothesize that pre-incubation on less nutritious media might be necessary, as both organisms were initially

grown on YPD, a nutrient-rich medium. This could have enabled them to store reserves that are utilized under nitrogen starvation conditions.

C. albicans demonstrates reduced viability on urea plates when compared to *S. cerevisiae.* This difference might be linked to other roles of the *DUR1,2* gene in pathogenesis, possibly suggesting a higher energy cost associated with urea metabolism. Interestingly, CO_2 concentration could influence urea metabolism. Since *S. cerevisiae* produces more CO_2 via the Crabtree effect, it might be able to utilize this CO_2 for urea conversion, potentially explaining its growth advantage.[113]

6.3.6. Carbon acquisition and utilization

Together with nitrogen, carbon is another limiting factor for the growth of any organism. We investigated how the gene-swapped strains utilized different carbon sources. As expected, both *C. albicans* and *S. cerevisiae* exhibited optimal growth on glucose, the preferred carbon source. At the same time, both organisms possess the machinery to utilize glycerol (via glycerol dehydrogenase, *GCY1*) by its conversion to DHA.

Lactate highly influences the pH of the media, which can disrupt other metabolic pathways and reduce their viability and carbon utilization. To utilize lactate, both organisms use lactate permease (*JEN1*), which is not expressed when grown on glucose. In *C. albicans,* it is also expressed when phagocytized.

Additionally, both organisms contain orthologous lactate dehydrogenase (*LDH1*). Although they both possess similar machinery to utilize and withstand stress caused by lactate, *C. albicans* (as seen here) is more flexible in its utilization. This is also highlighted during pathogenesis in vulvovaginitis, where lactate is one of the primary carbon sources.[114] Lactate is not an ideal energy source since more energy has to be spent on its conversion to pyruvate conversion, hence the reduced viability. It also seems that these two organisms may sense carbon sources differently, as well as *S. cerevisiae* having a fermentative preference.[115]

6.3.7. Complex nitrogen utilization

We also examined the effect of this gene-swap on the utilization of complex nitrogen sources. We used BSA as a substrate and dextrose as a carbon source. This resulted in the formation of "zones" around the colonies, which might be secreted aspartic proteases (SAPs). Formation of these zones was also observed in mutants with impaired pre-vacuolar protein sorting gene (*VPS4*), where secretion of extracellular proteases and lipases was increased in *Δvps4*

mutants. Therefore, we hypothesize that under nitrogen starvation, *C. albicans* can switch metabolism to secretion of extracellular proteases to survive.[116] It is important to note that yeast grown on nitrogen-rich media may store nitrogen in protein form. This can lead to an error in our observations, potentially explaining why we might observe growth on nitrogen-poor media despite the manufacturer's warning.

6.3.8. Gene-swap conclusion

Our gene-swap experiment investigating the effects of swapping the *PEP4* and *APR1* on yeast physiology yielded several intriguing yet sometimes ambiguous results. Despite expectations of significant differences, both *S. cerevisiae* and *C. albicans* retained resilience to osmotic, thermal and pH stresses, suggesting potentially redundant pathways or other compensatory mechanisms, which might be masking the impact of a single-gene gene swap.

Interestingly, the differences in nitrogen utilization hint at the potential adaptations. *C. albicans'* reduced ability to utilize urea and BSA utilization, raises the possibility of different nitrogen and carbon assimilation pathways influenced by gene-swap.

Although we faced technical limitations, like the degradation of H_2O_2, it provided a foundation for further investigation and highlighted the importance of a multifaceted approach, including proteomic analysis, to better understand the roles of Pep4p and Apr1p in cell physiology.

7. Conclusion

This study partially achieved its first aim by expressing various forms of Apr1p in both prokaryotic (*E. coli*) and eukaryotic (*S. cerevisiae*) systems. While soluble proApr1p was successfully produced in *E. coli*, subsequent activation methods (e.g. low pH or processing *in trans*) failed to yield mature Apr1p. This suggests that proApr1p activation may be dependent on an activation cascade like Pep4p. This warrants further investigation into activation cascade in *C. albicans.*

Conversely, eukaryotic expression in *S. cerevisiae* showed promise for obtaining mature Apr1p. Fractionated cell lysates exhibited targeted substrate cleavage, but further verification is needed to confirm Apr1p as the responsible protease. We also think that upscaling this approach will only benefit the progress of Apr1p characterization.

Regarding the second aim, transgenic strains of *C. albicans* and *S. cerevisiae* were successfully generated and tested under various stress and nutritional conditions. Although minimal phenotypic differences were observed between Apr1p- and Pep4p-expressing strains, suggesting potential functional complementation under the tested conditions, these conditions included preculturing in nutrient-rich medium. Therefore, future experiments should utilize starter cultures prepared in nutritionally limited medium to assess phenotypic differences under more stringent conditions.

8. Bibliography

1. Lin, P., Kook, M. C., Yi, T. H. & Yan, Z. F. Current Fungal Taxonomy and Developments in the Identification System. *Curr Microbiol* **80**, (2023).
2. Taxonomy browser (Candida albicans SC5314). https://www.ncbi.nlm.nih.gov/Taxonomy/Browser/wwwtax.cgi?mode=info&id=237561.
3. Kieliszek, M. *et al.* Biotechnological use of Candida yeasts in the food industry: A review. *Fungal Biol Rev* **31**, 185–198 (2017).
4. Yadav, J. S. S., Bezawada, J., Yan, S., Tyagi, R. D. & Surampalli, R. Y. Candida krusei: biotechnological potentials and concerns about its safety. *Can J Microbiol* **58**, 937–952 (2012).
5. Romo, J. A. & Kumamoto, C. A. On Commensalism of Candida. *Journal of Fungi* **6**, (2020).
6. Siverio, J. ¤ M. Assimilation of nitrate by yeasts. *FEMS Microbiol Rev* **26**, 277–284 (2002).
7. Romo, J. A. & Kumamoto, C. A. On Commensalism of Candida. *Journal of Fungi* **6**, (2020).
8. Chaffin, W. L. Candida albicans Cell Wall Proteins. *Microbiol Mol Biol Rev* **72**, 495 (2008).
9. Hall, R. A. & Gow, N. A. R. Mannosylation in Candida albicans: role in cell wall function and immune recognition. *Mol Microbiol* **90**, 1147 (2013).
10. Brown, G. D., Denning, D. W. & Levitz, S. M. Tackling human fungal infections. *Science* **336**, 647 (2012).
11. Talapko, J. *et al.* Candida albicans- The Virulence Factors and Clinical Manifestations of Infection. *J Fungi (Basel)* **7**, 1–19 (2021).
12. WHO fungal priority pathogens list to guide research, development and public health action. https://www.who.int/publications/i/item/9789240060241.
13. Lockhart, S. R., Chowdhary, A. & Gold, J. A. W. The rapid emergence of antifungal-resistant human-pathogenic fungi. *Nature Reviews Microbiology 2023 21:12* **21**, 818–832 (2023).
14. Lamoth, F., Lockhart, S. R., Berkow, E. L. & Calandra, T. Changes in the epidemiological landscape of invasive candidiasis. *Journal of Antimicrobial Chemotherapy* **73**, i4–i13 (2018).
15. Shao, T. Y. *et al.* Commensal Candida albicans Positively Calibrates Systemic Th17 Immunological Responses. *Cell Host Microbe* **25**, 404-417.e6 (2019).
16. Thomas-Rüddel, D. O., Schlattmann, P., Pletz, M., Kurzai, O. & Bloos, F. Risk Factors for Invasive Candida Infection in Critically Ill Patients: A Systematic Review and Meta-analysis. *Chest* **161**, 345 (2022).

17. Banerjee, M., Lazzell, A. L., Romo, J. A., Lopez-Ribot, J. L. & Kadosh, D. Filamentation Is Associated with Reduced Pathogenicity of Multiple Non- albicans Candida Species. *mSphere* **4**, (2019).

18. Lionakis, M. S., Lim, J. K., Lee, C. C. R. & Murphy, P. M. Organ-specific innate immune responses in a mouse model of invasive candidiasis. *J Innate Immun* **3**, 180–199 (2011).

19. Maza, P. K. *et al.* Candida albicans: The ability to invade epithelial cells and survive under oxidative stress is unlinked to hyphal length. *Front Microbiol* **8**, 1235 (2017).

20. Phan, Q. T. *et al.* Als3 is a Candida albicans invasin that binds to cadherins and induces endocytosis by host cells. *PLoS Biol* **5**, 0543–0557 (2007).

21. Correia, A. *et al.* Limited role of secreted aspartyl proteinases Sap1 to Sap6 in Candida albicans virulence and host immune response in murine hematogenously disseminated candidiasis. *Infect Immun* **78**, 4839–4849 (2010).

22. Rapala-Kozik, M. *et al.* Extracellular proteinases of Candida species pathogenic yeasts. *Mol Oral Microbiol* **33**, 113–124 (2018).

23. Leidich, S. D. *et al.* Cloning and disruption of caPLB1, a phospholipase B gene involved in the pathogenicity of Candida albicans. *J Biol Chem* **273**, 26078–26086 (1998).

24. Lubkin, A. & Lionakis, M. S. Candida lipase packs a punch against IL-17. *Cell Host Microbe* **30**, 1503–1505 (2022).

25. Williams, R. B. & Lorenz, M. C. Multiple Alternative Carbon Pathways Combine To Promote Candida albicans Stress Resistance, Immune Interactions, and Virulence. *mBio* **11**, (2020).

26. Citiulo, F. *et al.* Candida albicans Scavenges Host Zinc via Pra1 during Endothelial Invasion. *PLoS Pathog* **8**, 1002777 (2012).

27. Malavia, D. *et al.* Zinc limitation induces a hyper-adherent Goliath phenotype in Candida albicans. *Front Microbiol* **8**, 300540 (2017).

28. Sherrington, S. L. *et al.* Adaptation of Candida albicans to environmental pH induces cell wall remodelling and enhances innate immune recognition. *PLoS Pathog* **13**, (2017).

29. Danhof, H. A. *et al.* Robust Extracellular pH Modulation by Candida albicans during Growth in Carboxylic Acids. *mBio* **7**, (2016).

30. Wall, G., Montelongo-Jauregui, D., Vidal Bonifacio, B., Lopez-Ribot, J. L. & Uppuluri, P. Candida albicans Biofilm growth and Dispersal: Contributions to Pathogenesis. *Curr Opin Microbiol* **52**, 1 (2019).

31. Eix, E. F. & Nett, J. E. How Biofilm Growth Affects Candida-Host Interactions. *Front Microbiol* **11**, 1437 (2020).

32. Wall, G. & Lopez-Ribot, J. L. Current Antimycotics, New Prospects, and Future Approaches to Antifungal Therapy. *Antibiotics 2020, Vol. 9, Page 445* **9**, 445 (2020).

33. Lu, H., Hong, T., Jiang, Y., Whiteway, M. & Zhang, S. Candidiasis: From cutaneous to systemic, new perspectives of potential targets and therapeutic strategies. *Adv Drug Deliv Rev* **199**, (2023).

34. Arafa, S. H., Khaled Elbanna, ·, Gamal, ·, Osman, E. H. & Abulreesh, H. H. Candida diagnostic techniques: a review. *Journal of Umm Al-Qura University for Applied Sciences 2023 9:3* **9**, 360–377 (2023).

35. Hassan, Y., Chew, S. Y. & Than, L. T. L. Candida glabrata: Pathogenicity and Resistance Mechanisms for Adaptation and Survival. *J Fungi (Basel)* **7**, (2021).

36. Castrejón-Jiménez, N. S., Castillo-Cruz, J., Baltierra-Uribe, S. L., Hernández-González, J. C. & García-Pérez, B. E. Candida glabrata is a successful pathogen: An artist manipulating the immune response. *Microbiol Res* **260**, (2022).

37. Tóth, R. *et al.* Candida parapsilosis: from Genes to the Bedside. *Clin Microbiol Rev* **32**, (2019).

38. Franconi, I., Rizzato, C., Poma, N., Tavanti, A. & Lupetti, A. Candida parapsilosis sensu stricto Antifungal Resistance Mechanisms and Associated Epidemiology. *J Fungi (Basel)* **9**, (2023).

39. Gómez-Gaviria, M., Ramírez-Sotelo, U. & Mora-Montes, H. M. Non- albicans Candida Species: Immune Response, Evasion Mechanisms, and New Plant-Derived Alternative Therapies. *J Fungi (Basel)* **9**, (2022).

40. Pinto, T. N. *et al.* Candida guilliermondii as an agent of postpartum subacute mastitis in Rio de Janeiro, Brazil: Case report. *Front Microbiol* **13**, 964685 (2022).

41. Wu, Z. *et al.* Candidemia: incidence rates, type of species, and risk factors at a tertiary care academic hospital in China. *International Journal of Infectious Diseases* **22**, 4–8 (2014).

42. Chowdhary, A., Jain, K. & Chauhan, N. Candida auris Genetics and Emergence. *https://doi.org/10.1146/annurev-micro-032521-015858* **77**, 583–602 (2023).

43. Bauerová, V., Pichová, I. & Hrušková-Heidingsfeldová, O. Nitrogen source and growth stage of Candida albicans influence expression level of vacuolar aspartic protease Apr1p and carboxypeptidase Cpy1p. *https://doi.org/10.1139/w2012-030* **58**, 678–681 (2012).

44. Li, S. C. & Kane, P. M. The yeast lysosome-like vacuole: endpoint and crossroads. *Biochim Biophys Acta* **1793**, 650–663 (2009).

45. Richards, A., Veses, V. & Gow, N. A. R. Vacuole dynamics in fungi. *Fungal Biol Rev* **24**, 93–105 (2010).

46. Veses, V., Richards, A. & Gow, N. A. Vacuoles and fungal biology. *Curr Opin Microbiol* **11**, 503–510 (2008).

47. Klionsky, D. J., Herman, P. K. & Emr, S. D. The fungal vacuole: composition, function, and biogenesis. *Microbiol Rev* **54**, 266–292 (1990).

48. Parzych, K. R. & Klionsky, D. J. Vacuolar hydrolysis and efflux: current knowledge and unanswered questions. *Autophagy* **15**, 212 (2019).

49. Palmer, C. P. *et al.* A TRP homolog in Saccharomyces cerevisiae forms an intracellular Ca(2+)-permeable channel in the yeast vacuolar membrane. *Proc Natl Acad Sci U S A* **98**, 7801–7805 (2001).

50. Simm, C. *et al.* Saccharomyces cerevisiae vacuole in zinc storage and intracellular zinc distribution. *Eukaryot Cell* **6**, 1166–1177 (2007).

51. Li, L., Chen, O. S., Ward, D. M. V. & Kaplan, J. CCC1 is a transporter that mediates vacuolar iron storage in yeast. *J Biol Chem* **276**, 29515–29519 (2001).

52. Zubenko, G. S., Park, F. J. & Jones, E. W. Mutations in PEP4 locus of Saccharomyces cerevisiae block final step in maturation of two vacuolar hydrolases. *Proc Natl Acad Sci U S A* **80**, 510 (1983).

53. Galan, J. M., Moreau, V., Andre, B., Volland, C. & Haguenauer-Tsapis, R. Ubiquitination mediated by the Npi1p/Rsp5p ubiquitin-protein ligase is required for endocytosis of the yeast uracil permease. *J Biol Chem* **271**, 10946–10952 (1996).

54. Onodera, J. & Ohsumi, Y. Autophagy is required for maintenance of amino acid levels and protein synthesis under nitrogen starvation. *J Biol Chem* **280**, 31582–31586 (2005).

55. Palmer, G. E., Kelly, M. N. & Sturtevant, J. E. The Candida albicans Vacuole Is Required for Differentiation and Efficient Macrophage Killing. *Eukaryot Cell* **4**, 1677 (2005).

56. Palmer, G. E. Vacuolar trafficking and Candida albicans pathogenesis. *Commun Integr Biol* **4**, 240 (2011).

57. Aspartic Protease Inhibitors | Cambridge MedChem Consulting. https://www.cambridgemedchemconsulting.com/resources/hit_identification/aspartic_protease_inhibitors.html.

58. Aspartic protease - Wikipedia. https://en.wikipedia.org/wiki/Aspartic_protease.

59. Parr, C. L., Keates, R. A. B., Bryksa, B. C., Ogawa, M. & Yada, R. Y. The structure and function of Saccharomyces cerevisiae proteinase A. *Yeast* **24**, 467–480 (2007).

60. Kerstens, W. & Van Dijck, P. A Cinderella story: how the vacuolar proteases Pep4 and Prb1 do more than cleaning up the cell's mass degradation processes. *Microbial Cell* **5**, 438 (2018).

61. Phylip, L. H. *et al.* The potency and specificity of the interaction between the IA3 inhibitor and its target aspartic proteinase from Saccharomyces cerevisiae. *Journal of Biological Chemistry* **276**, 2023–2030 (2001).

62. Bauerová, V., Hájek, M., Pichová, I. & Hrušková-Heidingsfeldová, O. Intracellular aspartic proteinase Apr1p of Candida albicans is required for morphological transition under nitrogen-limited conditions but not for macrophage killing. *Folia Microbiol (Praha)* **59**, 485–493 (2014).

63. Ganjave, S. D., O'Niel, R. A. & Wangikar, P. P. Rate of dilution and redox ratio influence the refolding efficiency of recombinant fungal dehydrogenases. *Int J Biol Macromol* **250**, 126163 (2023).

64. Chen, S. Y. & Zacharias, M. What Makes a Good Protein-Protein Interaction Stabilizer: Analysis and Application of the Dual-Binding Mechanism. *ACS Cent Sci* **9**, 969–979 (2023).

65. Studier, F. W. & Moffatt, B. A. Use of bacteriophage T7 RNA polymerase to direct selective high-level expression of cloned genes. *J Mol Biol* **189**, 113–130 (1986).

66. Andersen, K. R., Leksa, N. C. & Schwartz, T. U. Optimized E. coli expression strain LOBSTR eliminates common contaminants from His-tag purification. *Proteins* **81**, 1857–1861 (2013).

67. Penumetcha, P. *et al.* Improving the Lac System for Synthetic Biology. *https://doi.org/10.1893/011.081.0104* **81**, 7–15 (2010).

68. Singh, A., Upadhyay, V., Upadhyay, A. K., Singh, S. M. & Panda, A. K. Protein recovery from inclusion bodies of Escherichia coli using mild solubilization process. *Microb Cell Fact* **14**, 1–10 (2015).

69. Rashid, F., Sharma, S. & Bano, B. Comparison of guanidine hydrochloride (GdnHCl) and urea denaturation on inactivation and unfolding of human placental cystatin (HPC). *Protein J* **24**, 283–292 (2005).

70. Tris for buffer solutions. https://itwreagents.com/italy/en/product/tris-for-buffer-solutions/A1379.

71. Pielak, G. J. Buffers, Especially the Good Kind. *Biochemistry* **60**, 3436–3440 (2021).

72. Zhao, H. *et al.* Effect of kosmotropicity of ionic liquids on the enzyme stability in aqueous solutions. *Bioorg Chem* **34**, 15–25 (2006).

73. March, D., Bianco, V. & Franzese, G. Protein Unfolding and Aggregation near a Hydrophobic Interface. *Polymers (Basel)* **13**, 1–14 (2021).

74. Das, A. & Mukhopadhyay, C. Urea-mediated protein denaturation: A consensus view. *Journal of Physical Chemistry B* **113**, 12816–12824 (2009).

75. Nabiel, A., Yosua, Y., Sriwidodo, S. & Maksum, I. P. Overview of refolding methods on misfolded recombinant proteins from Escherichia coli inclusion bodies. (2023) doi:10.7324/JABB.2023.112204.

76. Chen, J. *et al.* Cooperative effects of urea and L-arginine on protein refolding. *Protein Expr Purif* **66**, 82–90 (2009).

77. Vallejo, L. F. & Rinas, U. Strategies for the recovery of active proteins through refolding of bacterial inclusion body proteins. *Microb Cell Fact* **3**, 11 (2004).

78. Lenton, S. *et al.* Impact of Arginine-Phosphate Interactions on the Reentrant Condensation of Disordered Proteins. *Biomacromolecules* **22**, 1532–1544 (2021).

79. Sasahara, K., Yamaguchi, K., So, M. & Goto, Y. Polyphosphates diminish solubility of a globular protein and thereby promote amyloid aggregation. *J Biol Chem* **294**, 15318–15329 (2019).

80. Xie, L. & Jakob, U. Inorganic polyphosphate, a multifunctional polyanionic protein scaffold. *J Biol Chem* **294**, 2180–2190 (2019).

81. Hirai, M. *et al.* Direct Evidence for the Effect of Glycerol on Protein Hydration and Thermal Structural Transition. *Biophys J* **115**, 313–327 (2018).

82. Saha, D., Ray, D., Kohlbrecher, J. & Aswal, V. K. Unfolding and Refolding of Protein by a Combination of Ionic and Nonionic Surfactants. *ACS Omega* **3**, 8260–8270 (2018).

83. Alibolandi, M. & Mirzahoseini, H. Chemical Assistance in Refolding of Bacterial Inclusion Bodies. *Biochem Res Int* **2011**, (2011).

84. Siripurkpong, P., Yuvaniyama, J., Wilairat, P. & Goldberg, D. E. Active Site Contribution to Specificity of the Aspartic Proteases Plasmepsins I and II. *Journal of Biological Chemistry* **277**, 41009–41013 (2002).

85. Castanheira, P. *et al.* Activation, Proteolytic Processing, and Peptide Specificity of Recombinant Cardosin A. *Journal of Biological Chemistry* **280**, 13047–13054 (2005).

86. Liu, W. R., Langer, R. & Klibanov, A. M. Moisture-induced aggregation of lyophilized proteins in the solid state. *Biotechnol Bioeng* **37**, 177–184 (1991).

87. Estey, T., Kang, J., Schwendeman, S. P. & Carpenter, J. F. BSA degradation under acidic conditions: a model for protein instability during release from PLGA delivery systems. *J Pharm Sci* **95**, 1626–1639 (2006).

88. Holz, C., Hesse, O., Bolotina, N., Stahl, U. & Lang, C. A micro-scale process for high-throughput expression of cDNAs in the yeast Saccharomyces cerevisiae. *Protein Expr Purif* **25**, 372–378 (2002).

89. Schmidt, T. G. M. & Skerra, A. The Strep-tag system for one-step purification and high-affinity detection or capturing of proteins. *Nat Protoc* **2**, 1528–1535 (2007).

90. Gallo, V. *et al.* Proteomic analysis identifies markers of exposure to cadmium sulphide quantum dots (Cds qds). *Nanomaterials* **10**, 1–23 (2020).

91. DEAE Sephadex A-50 | Cytiva. https://www.cytivalifesciences.com/en/us/shop/chromatography/resins/ion-exchange/deae-sephadex-a-50-p-00796.

92. BoucheriÃ©, H., Bataille, N., Fitch, I. T., Perrot, M. & Tuite, M. F. Differential synthesis of glyceraldehyde-3-phosphate dehydrogenase polypeptides in stressed yeast cells. *FEMS Microbiol Lett* **125**, 127–133 (1995).

93. Li, F. *et al.* Improving recombinant protein production by yeast through genome-scale modeling using proteome constraints. doi:10.1038/s41467-022-30689-7.

94. Kang, H. A. *et al.* Proteolytic stability of recombinant human serum albumin secreted in the yeast Saccharomyces cerevisiae. *Appl Microbiol Biotechnol* **53**, 575–582 (2000).

95. Gast, V. *et al.* Engineering Saccharomyces cerevisiae for the production and secretion of Affibody molecules. *Microb Cell Fact* **21**, 1–15 (2022).

96. Gagnon-Arsenault, I., Tremblay, J. & Bourbonnais, Y. Fungal yapsins and cell wall: a unique family of aspartic peptidases for a distinctive cellular function. *FEMS Yeast Res* **6**, 966–978 (2006).

97. Zhao, M., Ma, J., Zhang, L. & Qi, H. Engineering strategies for enhanced heterologous protein production by Saccharomyces cerevisiae. *Microbial Cell Factories 2024 23:1* **23**, 1–16 (2024).

98. Gomes, A. M. V., Carmo, T. S., Carvalho, L. S., Bahia, F. M. & Parachin, N. S. Comparison of Yeasts as Hosts for Recombinant Protein Production. *Microorganisms* **6**, (2018).

99. Casaregola, S. *et al.* A family of laboratory strains of Saccharomyces cerevisiae carry rearrangements involving chromosomes I and III. *Yeast* **14**, 551–564 (1998).

100. Salvadó, Z. *et al.* Temperature Adaptation Markedly Determines Evolution within the Genus Saccharomyces. *Appl Environ Microbiol* **77**, 2292 (2011).

101. Jarolim, S. *et al.* Saccharomyces cerevisiae genes involved in survival of heat shock. *G3: Genes, Genomes, Genetics* **3**, 2321–2333 (2013).

102. Verghese, J., Abrams, J., Wang, Y. & Morano, K. A. Biology of the Heat Shock Response and Protein Chaperones: Budding Yeast (Saccharomyces cerevisiae) as a Model System. *Microbiol Mol Biol Rev* **76**, 115 (2012).

103. Richter, K., Haslbeck, M. & Buchner, J. Molecular Cell Review The Heat Shock Response: Life on the Verge of Death. doi:10.1016/j.molcel.2010.10.006.

104. De Nadal, E. & Posas, F. The HOG pathway and the regulation of osmoadaptive responses in yeast. *FEMS Yeast Res* **22**, 1–7 (2022).

105. Hirasawa, T. *et al.* Comparison of transcriptional responses to osmotic stresses induced by NaCl and sorbitol additions in Saccharomyces cerevisiae using DNA microarray. *J Biosci Bioeng* **102**, 568–571 (2006).

106. Cao, C., Cao, Z., Yu, P. & Zhao, Y. Genome-wide identification for genes involved in sodium dodecyl sulfate toxicity in Saccharomyces cerevisiae. *BMC Microbiol* **20**, 1–11 (2020).

107. Brown, J. A. *et al.* Global analysis of gene function in yeast by quantitative phenotypic profiling. *Mol Syst Biol* **2**, (2006).

108. Moreno, I. *et al.* Characterization of a Candida albicans gene encoding a putative transcriptional factor required for cell wall integrity. *FEMS Microbiol Lett* **226**, 159–167 (2003).

109. Martínez-Muñoz, G. A. & Kane, P. Vacuolar and Plasma Membrane Proton Pumps Collaborate to Achieve Cytosolic pH Homeostasis in Yeast. *J Biol Chem* **283**, 20309 (2008).

110. Peña, A., Sánchez, N. S. ilvia, Álvarez, H., Calahorra, M. & Ramírez, J. Effects of high medium pH on growth, metabolism and transport in Saccharomyces cerevisiae. *FEMS Yeast Res* **15**, 5 (2015).

111. Vacca, I. Acidic pH interferes with Candida persistence. *Nature Reviews Microbiology 2017 15:7* **15**, 382–382 (2017).

112. Linder, T. Nitrogen assimilation pathways in budding yeasts. *Non-conventional Yeasts: from Basic Research to Application* 197–236 (2019) doi:10.1007/978-3-030-21110-3_7.

113. Navarathna, D. H. M. L. P., Harris, S. D., Roberts, D. D. & Nickerson, K. W. Evolutionary aspects of urea utilization by fungi. *FEMS Yeast Res* **10**, 209–213 (2010).

114. O'Hanlon, D. E., Come, R. A. & Moench, T. R. Vaginal pH measured in vivo: lactobacilli determine pH and lactic acid concentration. *BMC Microbiol* **19**, 1–8 (2019).

115. Vieira, N. *et al.* Functional specialization and differential regulation of short-chain carboxylic acid transporters in the pathogen Candida albicans. *Mol Microbiol* **75**, 1337 (2010).

116. Lee, S. A. *et al.* A functional analysis of the Candida albicans homolog of Saccharomyces cerevisiae VPS4. *FEMS Yeast Res* **7**, 973–985 (2007).